Université de Montréal

Étude de l'étoile Wolf-Rayet variable WR 46 dans l'ultraviolet lointain et les rayons X

par

Vincent Hénault-Brunet

Département de physique

Faculté des arts et des sciences

Mémoire présenté à la Faculté des études supérieures

en vue de l'obtention du grade de

Maître ès sciences (M.Sc.)

en physique

Août, 2009

Université de Montréal

Faculté des études supérieures

Ce mémoire intitulé:

Étude de l'étoile Wolf-Rayet variable WR 46 dans l'ultraviolet lointain et les rayons X

présenté par:

Vincent Hénault-Brunet

a été évalué par un jury composé des personnes suivantes:

Pierre Bergeron,	président-rapporteur
Nicole St-Louis,	directrice de recherche
Claude Carignan,	membre du jury

Mémoire accepté le: 11 septembre 2009

«Il me semble que ce qui est requis est un délicat équilibre entre deux tendances : celle qui nous pousse à scruter de manière inlassablement sceptique toutes les hypothèses qui nous sont soumises et celle qui nous invite à garder une grande ouverture aux idées nouvelles.»

- Carl Sagan

Sommaire

L'étoile Wolf-Rayet WR 46 est connue pour sa variabilité complexe sur des échelles de temps relativement courtes de quelques heures et sur des échelles de temps plus longues de plusieurs mois. Des décalages périodiques mais intermittents en vitesse radiale ont déjà été observés dans ses raies d'émission optiques. Plusieurs périodes photométriques ont aussi été mesurées dans le passé. Des pulsations non-radiales, une modulation liée à la rotation rapide, ou encore la présence d'un compagnon de faible masse dont la présence reste à confirmer ont été proposées pour expliquer le comportement de l'étoile sur des échelles de temps de quelques heures. Dans un effort pour dévoiler sa vraie nature, nous avons observé WR 46 avec le satellite *FUSE* sur plusieurs cycles de variabilité à court terme. Nous avons trouvé des variations sur une échelle de temps d'environ 7,5 heures dans le continu ultraviolet lointain, dans l'aile bleue de la composante d'absorption du profil P Cygni du doublet de O VI $\lambda\lambda$1032, 1038, ainsi que dans la composante d'absorption du profil P Cygni de S VI $\lambda\lambda$933, 944. Nous avons également récupéré des données archivées de cette étoile obtenues avec le satellite *XMM-Newton*. La courbe de lumière en rayons X montre des variations sur une échelle de temps similaire aux courbes de lumière du continu ultraviolet et ultraviolet lointain, et le spectre rayons X de WR 46 est très mou avec un pic d'émission à des énergies plus faibles que 1 keV. Nous discutons des différentes contraintes sur la nature de la variabilité de cette étoile que ces nouvelles observations aident à poser. Parmi les scénarios suggérés, nous concluons que celui des pulsations non-radiales est le plus probable, bien que nous soyons encore loin d'une compréhension détaillée de WR 46.

Mots clés: étoiles: Wolf-Rayet: individuelle (WR 46) – étoiles: ultraviolet – étoiles: émission rayons X

Abstract

The Wolf-Rayet star WR 46 is known to exhibit a very complex variability pattern on relatively short timescales of a few hours and also on longer timescales of months. Periodic but intermittent radial velocity shifts of optical lines as well as multiple photometric periods have been found in the past. Nonradial pulsations, rapid rotational modulation or the presence of a yet-to-be-confirmed low-mass companion have been proposed to explain the short-term behaviour. In an effort to unveil its true nature, we observed WR 46 with *FUSE* over several short-term variability cycles. We found significant variations on a timescale of about 7.5 hours in the FUV continuum, in the blue edge of the absorption trough of the O VI $\lambda\lambda$1032, 1038 doublet P Cygni profile, and in the S VI $\lambda\lambda$933, 944 P Cygni absorption profile. We also retrieved archival *XMM-Newton* data of this star. We found the X-ray light-curve to show variations on a timescale similar to the UV and FUV continuum light-curves, and the X-ray spectrum of WR 46 to be very soft with a peak below 1 keV. We discuss the different constraints on the nature of the variability that these new observations help to establish. Among the suggested scenarios, we conclude that non-radial pulsations is the most likely, although we are far from a complete picture.

Subject headings: stars: Wolf-Rayet: individual (WR 46) – stars: ultraviolet — stars: X-ray emission

Table des matières

Liste des figures

Liste des tableaux

Liste des sigles et abréviations

c	Compagnon compact
CalFUSE	*FUSE* calibration pipeline
CBSSs	Close Binary Supersoft X-ray Sources
CIRs	Corotating Interaction Regions
CMFGEN	Code de transfert radiatif à géométrie sphérique dans des atmosphères en expansion
CNO	Cycle carbone-azote-oxygène
DACs	Discrete Absorption Components
EPIC	European Photon Imaging Cameras
ETL	Équilibre Thermodynamique Local
EW	Equivalent Width
FUSE	Far Ultraviolet Spectroscopic Explorer
FUV	Far ultraviolet
HMXRBs	High-Mass X-Ray Binaries
IDF	Intermediate Data Files
IUE	International Ultraviolet Explorer
LiF	Lithium Fluoride
LWRS	*FUSE* low-resolution aperture

MAST	Multimission Archive of the Space Telescope Science Institute
MOST	Satellite Microvariabilité & Oscillations STellaires
MWRS	*FUSE* medium-resolution aperture
OM	*XMM-Newton* Optical Monitor
PSPC	Position Sensitive Proportional Counters
ROSAT	ROentgen SATellite
SB2	Binaire à deux spectres
SiC	Silicon Carbide
TTAG	*FUSE* time-tagged observation mode
TVS	Temporal Variance Spectrum
UT	Universal Time
UV	Ultraviolet
WC	Classe d'étoiles Wolf-Rayet dont le spectre est dominé par le carbone
WN	Classe d'étoiles Wolf-Rayet dont le spectre est dominé par l'azote
WNE	Étoile WN de type précoce
WO	Classe d'étoiles Wolf-Rayet dont le spectre est dominé par l'oxygène
WR	Wolf-Rayet
XMM-Newton	X-ray Multi-Mirror mission - Newton

Remerciements

Je tiens d'abord à remercier ma directrice de recherche, Nicole St-Louis, pour son enthousiasme, son aide, sa confiance et sa grande disponibilité tout au long de ce projet, en particulier dans le dernier droit. Je lui suis également reconnaissant de m'avoir permis de participer à des campagnes d'observation durant lesquelles j'ai pu acquérir une précieuse expérience au télescope. Merci aussi à Jean Dupuis pour son support constant, sa patience, son esprit critique et surtout pour m'avoir offert une première chance de m'initier à la recherche en astronomie qui fut déterminante pour la suite des choses. Salutations à Tony Moffat ainsi qu'à tous ceux et celles qui sont passés par le club des étoiles massives ces deux dernières années pour ces rencontres hebdomadaires toujours instructives, souvent ponctuées d'humour et de gastronomie! Ces échanges informels où l'on peut confronter nos idées et apprendre de nos collègues resteront toujours pertinents. Je salue également les collègues du bureau F-420, Rémi et Amélie, que je remercie pour leur agréable compagnie, et tous les enseignants, professeurs, collègues et amis qui au fil du temps m'ont communiqué et transmis leur passion pour l'astronomie et la science en général. Dans un autre ordre d'idées, je suis reconnaissant au Département de physique, à la Faculté des études supérieures de l'Université de Montréal et au Conseil de recherches en sciences naturelles et en génie du Canada (CRSNG) pour le support financier dont j'ai bénéficié durant ma maîtrise.

En terminant, un grand merci à Maude, unique, resplendissante, attentionnée et d'une rare sensibilité, pour tout le bonheur partagé, ainsi qu'à mes parents, Sylvie et Richard, qui ont toujours encouragé les études, le goût d'apprendre, la curiosité et les passions.

Chapitre 1

Introduction

1.1 Propriétés des étoiles Wolf-Rayet

En 1867, Wolf et Rayet ont découvert trois étoiles de type précoce dans la constellation du Cygne montrant de spectaculaires bandes d'émission anormalement fortes et larges (Wolf & Rayet 1867). Aujourd'hui, nous connaissons dans la Galaxie environ 200 de ces étoiles lumineuses (magnitudes absolues $-4.5 \gtrsim M_{\rm V} \gtrsim -6.5$) et chaudes ($T_{\rm eff} \gtrsim 30\ 000$ K) de type Wolf-Rayet (p. ex. van der Hucht 2001). Elles sont relativement massives, typiquement de 10 à 25 $M_{\odot}$ (Crowther 2007), et possèdent des vents denses et rapides qu'on caractérise par leur vitesse terminale (v_{∞}) et leur taux de perte de masse ($\dot{M}$). Les vitesses terminales des vents des étoiles Wolf-Rayet sont de l'ordre de 1000 à 3000 km s^{-1} et leurs taux de perte de masse autour de 10^{-5} à 10^{-6} $M_{\odot}$/année, soit environ 10 à 100 fois plus importants que ceux de leurs progéniteurs, les étoiles de type O (p. ex. Hamann & Koesterke 1998). Ce sont ces vents denses et rapides qui permettent l'apparition de raies d'émission fortes et larges dans leur spectre. En fait, les vents sont suffisamment denses pour qu'une profondeur optique de $\tau = 1$ dans le continu soit atteinte dans le vent même de l'étoile, voilant ainsi sa surface.

Toutes les étoiles Wolf-Rayet sont riches en hélium et pauvres en hydrogène. Certaines montrent des spectres dominés par l'azote (les WN) alors que d'autres (les WC) montrent des spectres dominés par le carbone. Une troisième classe, plus minoritaire et considérée par certains comme

une extension de la classe WC (Crowther 2007), regroupe celles riches en oxygène (les WO). À cause de ces compositions chimiques particulières suggérant l'apparition successive dans le vent des produits des cycles CNO et triple-α, les étoiles Wolf-Rayet sont maintenant clairement identifiées comme étant une phase évoluée de la vie des étoiles massives (Lamers et al. 1991). Elles sont considérées comme les descendantes des étoiles massives de type O ayant une masse initiale d'au moins 25 $M_{\odot}$ environ (Crowther 2007). La phase Wolf-Rayet compte pour à peu près 10% des quelques millions d'années de la vie de l'étoile (Meynet & Maeder 2005).

Les vents des étoiles de type O et B sont relativement bien décrits (v_{∞} et $\dot{M}$) par la théorie des vents entraînés par la radiation (Castor et al. 1975; Pauldrach et al. 1986). Il est effectivement admis que les photons diffusés dans les nombreuses transitions d'éléments lourds exercent une pression de radiation qui permet l'accélération de ces vents. Pour ce qui est des étoiles Wolf-Rayet, les bases de ce modèle s'appliquent, mais des soins particuliers doivent être apportés. La prise en compte des diffusions multiples des photons semble être l'ingrédient supplémentaire nécessaire pour expliquer l'accélération des vents plus denses des étoiles Wolf-Rayet (Lucy & Abbott 1993; Springmann 1994; Gayley et al. 1995), contrairement aux premiers modèles (p. ex. Castor et al. 1975) où chaque photon n'est jamais diffusé plus d'une fois.

Les vents des étoiles Wolf-Rayet sont denses par rapport à ceux d'autres types d'étoiles, mais demeurent extrêmement ténus en comparaison aux densités typiques des photosphères. Les processus radiatifs dominent ainsi sur les processus collisionnels, et les effets hors équilibre thermodynamique local (hors-ETL) sont importants. Des modèles d'atmosphère en expansion hors-ETL ont été développés (p. ex. Hillier & Miller 1998; Hamann & Koesterke 1998) dans le cadre du «modèle standard», où l'on suppose que les raies d'émission sont formées dans un vent dense, lisse, sphériquement symétrique, photoionisé par le noyau chaud et ne variant pas dans le temps. Ces modèles arrivent à reproduire quantitativement bon nombre de caractéristiques stationnaires des étoiles Wolf-Rayet (températures, luminosités, abondances, flux ionisants, propriétés des vents), mais ils sont incapables de décrire certaines autres caractéristiques, parmi lesquelles on retrouve évidemment celles qui varient dans le temps. Ces modèles ne

peuvent expliquer l'émission en rayons X mous provenant des vents et la saturation complète souvent observée dans les composantes d'absorption des profils P Cygni dans l'ultraviolet. La variabilité stochastique couramment détectée dans les raies d'émission dans l'optique et dans l'aile bleue des composantes d'absorption P Cygni, ainsi que les «composantes d'absorption étroites» (*Discrete Absorption Components*, DACs) observées dans les profils P Cygni sont d'autres exemples de caractéristiques que le modèle standard ne peut expliquer. Ces limitations nous forcent à laisser tomber certaines des suppositions du modèle standard en considérant des phénomènes qui varient dans le temps et qui induisent des structures nous éloignant du cas idéal d'un vent lisse et sphériquement symétrique.

1.2 Variabilité et structure dans le vent des étoiles Wolf-Rayet

On peut diviser la variabilité observée dans les étoiles Wolf-Rayet en deux grandes catégories: la variabilité stochastique associée à des structures à petite échelle et la variabilité cyclique (périodique ou quasi-périodique) associée à des structures à plus grande échelle.

La première catégorie est généralement reliée à l'instabilité radiative intrinsèque aux vents entraînés par la radiation (Owocki et al. 1988; Gayley & Owocki 1995) et se manifeste le plus clairement dans les étoiles Wolf-Rayet par de petites bosses superposées au sommet des raies d'émission et qui se déplacent du centre de la raie vers ses ailes sur des échelles de temps de plusieurs minutes à quelques heures (p. ex. Moffat et al. 1988; Lépine et al. 2000). L'instabilité radiative et les structures qu'elle produit (voir des simulations numériques à la Figure 1.1) semblent aussi pouvoir expliquer l'émission en rayons X des vents (Lucy & White 1980; Lucy 1982; Feldmeier et al. 1997), la saturation complète de l'absorption de certains profils P Cygni (p. ex. Puls et al. 1994) et la variabilité stochastique dans l'aile bleue de l'absorption des profils P Cygni (p. ex. Puls et al. 1993; Marchenko et al. 2006). Fait à noter, de par sa dépendance au carré de la densité électronique, le taux de perte de masse déterminé à partir de raies d'émission dans l'optique ou de l'émission du continu libre-libre est extrêmement sensible à ces surdensités à petite échelle. Le fait de ne pas tenir compte des inhomogénéités causées par

l'instabilité radiative conduit à une surestimation du taux de perte de masse. L'incorporation des effets de la variabilité stochastique est donc nécessaire à une modélisation adéquate de plusieurs caractéristiques des vents des étoiles Wolf-Rayet.

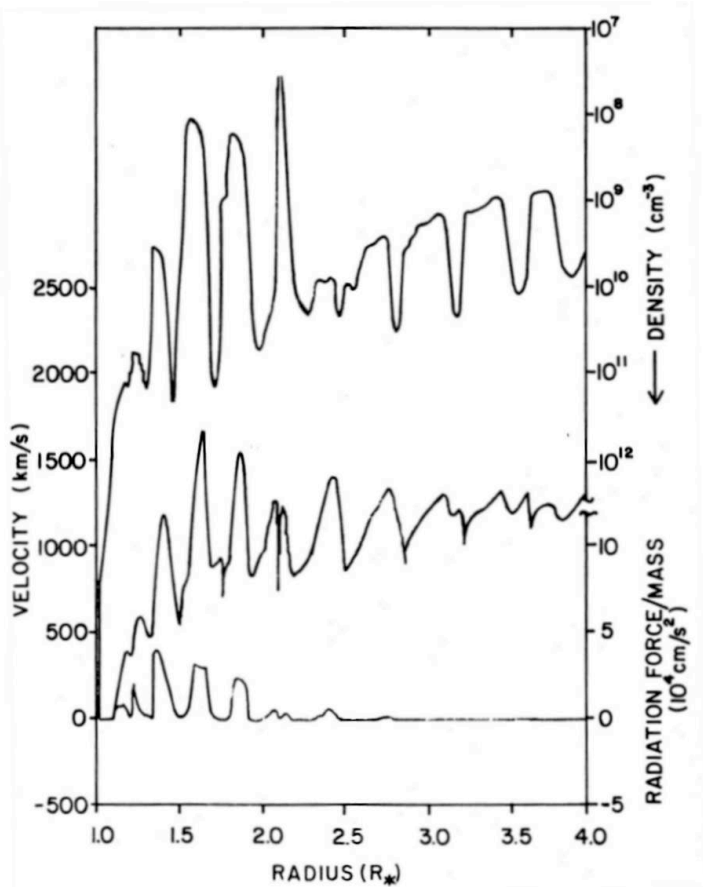

FIG. 1.1 – Exemple de structures en densité (courbe du haut) et en vitesse (courbe du milieu) engendrées par l'instabilité radiative en fonction de la distance radiale dans le vent. Figure tirée de simulations numériques de Owocki et al. (1988).

La deuxième catégorie de variabilité est, quant à elle, reliée à des perturbations périodiques qui ne sont pas intrinsèques aux vents, par exemple des structures à la surface d'une étoile en rotation ou l'effet d'un compagnon en orbite autour de l'étoile Wolf-Rayet. Les manifestations de cette catégorie de variabilité sont multiples: variations photométriques, évidence d'écart à la symétrie sphérique du vent (donc d'une structure à grande échelle) par spectropolarimétrie, variations spectroscopiques dans l'optique et dans l'ultraviolet (p. ex. Antokhin 1996). Au fil du temps, trois principaux scénarios ont été proposés pour interpréter les variations cycliques dans les étoiles Wolf-Rayet: la binarité, la rotation stellaire et les pulsations. Lorsqu'un compagnon brillant ne peut être détecté, il est généralement difficile d'identifier si la variabilité origine

de la rotation de l'étoile, de pulsations, ou encore d'un compagnon beaucoup moins lumineux que l'étoile Wolf-Rayet. Cette difficulté s'explique en partie par le fait que la surface de l'étoile nous soit cachée par le vent opaque. Les diagnostics utilisant, par exemple, l'élargissement des raies photosphériques pour mesurer la vitesse de rotation de l'étoile (plus précisément $v \sin i$) ou encore les variations de vitesse radiale et de profil de ces raies pour identifier des modes de pulsation ou tout simplement un mouvement orbital ne sont alors pas disponibles. Les mécanismes doivent donc être étudiés indirectement à travers les perturbations qu'ils induisent plus loin dans le vent de l'étoile. Malgré le fait que l'interprétation soit souvent complexe, l'étude détaillée de la variabilité cyclique des étoiles Wolf-Rayet est hautement souhaitable. Les retombées de la validation de l'un ou l'autre des trois scénarios, même pour un nombre limité d'étoiles, peuvent s'avérer cruciales pour mieux comprendre la structure et l'évolution des étoiles Wolf-Rayet ou l'évolution des systèmes binaires massifs.

1.3 Variabilité cyclique à court terme des étoiles Wolf-Rayet

Puisque c'est de variabilité cyclique dont il sera question dans l'étude de l'étoile WR 46 présentée au Chapitre 2, nous présentons dans les prochaines sous-sections un survol des différents mécanismes susceptibles d'en être la cause. Nous mettrons l'accent sur la variabilité cyclique à court terme (quelques heures à quelques jours), car ce régime s'applique au cas de WR 46.

1.3.1 Binarité

Quand un compagnon lumineux peut être identifié dans le spectre d'une étoile Wolf-Rayet et que son mouvement en vitesse radiale est en anti-phase par rapport aux raies d'émission de celle-ci, alors sans ambiguïté on peut attribuer la variabilité à la binarité. Même quand la lumière du compagnon est noyée par celle de l'étoile Wolf-Rayet, plus brillante, il est en principe possible de détecter ce compagnon par l'analyse des variations de vitesse radiale des raies formées près de la base du vent. Des systèmes binaires contenant une étoile Wolf-Rayet sont connus depuis bien longtemps, Wilson (1939) ayant découvert la première Wolf-Rayet

binaire spectroscopique. Les compagnons lumineux des étoiles Wolf-Rayet sont généralement des étoiles massives de type O ou B (van der Hucht 2001). Il arrive que la séparation de tels systèmes binaires soient relativement petite et que la variabilité observée montre une courte période (la période orbitale) de l'ordre d'un jour.

La mesure spectroscopique de la masse d'une étoile par le biais de la gravité de surface en utilisant des raies photosphériques n'est évidemment pas possible dans le cas des étoiles Wolf-Rayet. Par contre, pour celles faisant partie d'un système binaire, la troisième loi de Kepler est une méthode robuste pour déterminer les masses stellaires, en particulier dans les binaires à deux spectres (SB2) éclipsantes, où l'inclinaison peut être déterminée. L'inclinaison peut aussi être obtenue dans les systèmes non-éclipsants par des études de la variabilité de la polarisation linéaire (p.ex. St-Louis et al. 1988) ou des éclipses atmosphériques (Lamontagne et al. 1996). Le taux de perte de masse des étoiles Wolf-Rayet peut également être estimé à l'aide de la forme des éclipses atmosphériques ou de l'amplitude des variations polarimétriques. Les éclipses atmosphériques, de même que l'interaction entre le vent des deux étoiles d'un système WR + OB, sont aussi à l'origine de variations spectroscopiques. Des modèles, même simplifiés, de ces variations permettent de poser d'importantes contraintes sur les paramètres des vents et des étoiles elles-mêmes (Antokhin 1996, et référence incluses), mais nous n'en discuterons pas plus en profondeur puisque WR 46 ne semble pas posséder un compagnon lumineux avec un vent dense.

Des étoiles de faible masse sur la séquence principale sont parfois suggérées comme compagnons potentiels aux étoiles Wolf-Rayet, mais ce scénario semble peu probable. Par exemple, en étudiant la fréquence de binaires des étoiles de type O, Garmany et al. (1980) ont conclu que des systèmes binaires massifs rapprochés avec un ratio de masses plus grand que $\sim$3 n'existent probablement pas. Plus récemment, Bonnell (2007) a étudié la formation d'étoiles massives en terme d'accrétion compétitive dans des amas stellaires. Ces travaux suggèrent que les systèmes binaires massifs rapprochés sont formés par l'accrétion sur des systèmes de faible masse plus éloignés. Il a montré que ce mécanisme tend à produire des systèmes où les deux compagnons

ont une masse similaire.

D'un point de vue évolutif, un autre type de compagnon, beaucoup moins lumineux qu'une étoile O ou B et plus probable qu'une étoile de faible masse de la séquence principale, est susceptible de former un système binaire avec une étoile Wolf-Rayet. La théorie générale de l'évolution des systèmes binaires massifs rapprochés prédit en effet la séquence évolutive suivante (van den Heuvel & de Loore 1973):

$$\mathrm{O} + \mathrm{O} \rightarrow \mathrm{WR} + \mathrm{O} \rightarrow \mathrm{c} + \mathrm{O} \rightarrow \mathrm{c} + \mathrm{WR} \rightarrow \mathrm{c} + \mathrm{c}\ ,$$

où «c» signifie un compagnon compact, soit une étoile à neutron ou un trou noir, produit de l'explosion d'une supernova. En réaction à l'explosion de la première supernova menant au système c + O, celui-ci devrait acquérir une grande vitesse systémique. Si elle est assez massive, l'étoile O évoluera à son tour en Wolf-Rayet, et à ce moment le système devrait avoir atteint une latitude galactique élevée pour une étoile de Population I. Une grande vitesse systémique et une haute latitude galactique étaient d'ailleurs parmi les critères de sélection des candidats WR + c lors des premiers efforts pour rechercher de tels systèmes (van den Heuvel 1976; Moffat et al. 1982; Cherepashchuk & Aslanov 1984).

Au début des années 80, une douzaine d'étoiles Wolf-Rayet montrant des variations cycliques à court terme de faible amplitude (photométrie et vitesse radiale des raies optiques) sans qu'un compagnon soit visible ont été identifiées, puis suggérées comme étant des systèmes WR + c (p. ex. Moffat et al. 1982). Un de ces candidats WR + c, WR 148, est assurément un système binaire avec une périodicité stricte de 4,32 jours quoique la nature du compagnon demeure incertaine. D'après Marchenko et al. (1996), ce compagnon serait soit une étoile B2-4 V-III ou un objet compact. Pour plusieurs des autres candidats WR + c, les périodes se sont révélées ne pas être persistantes (p. ex. van Genderen & van der Hucht 1986). De plus, ces candidats ne sont pas des sources intenses d'émission rayons X comme on devrait s'y attendre, par exemple, dans le scénario où une étoile à neutron accrète de la matière en provenance du vent dense de

l'étoile Wolf-Rayet (Stevens & Willis 1988). De fait, les trois plus probables systèmes WR + c maintenant connus sont tous très lumineux en rayons X ($L_{\rm X} \sim 10^{38}$ erg s^{-1}). Un de ceux-là est Cyg X-3, un système galactique bien connu, et les deux autres, IC 10 X-1 et NGC 300 X-1, font partie d'autres galaxies (Bauer & Brandt 2004; Carpano et al. 2007b; Wang et al. 2005). Cyg X-3 a une période de 4,8 h (Parsignault et al. 1972), tandis que IC 10 X-1 et NGC 300 X-1 ont tous les deux une période d'environ 35 h (Prestwich et al. 2007; Carpano et al. 2007a). Il a été suggéré que chacun de ces trois systèmes contient une étoile Wolf-Rayet et un trou noir (van Kerkwijk et al. 1992; Schmutz et al. 1996; Hanson et al. 2000; Silverman & Filippenko 2008; Carpano et al. 2007b), bien que ce scénario ait été contesté dans le cas de Cyg X-3 (p. ex. Mitra 1998).

Le nombre si faible de systèmes WR + c détectés n'est pas vraiment une surprise. La rareté apparente d'étoiles OB «en cavale» possédant un compagnon compact (Kumar et al. 1983; Gies & Bolton 1986; Philp et al. 1996; Sayer et al. 1996) suggère que le nombre de systèmes binaires massifs ayant survécu à la première explosion de supernova est relativement faible. Des modèles de synthèse de population de systèmes binaires massifs suggèrent également que le nombre de WR + c observables dans la Galaxie est faible, soit ≤ 5 (de Donder et al. 1997). D'un autre côté, Moffat (1992) a estimé qu'environ 15 à 20% des étoiles Wolf-Rayet de notre Galaxie devraient posséder un compagnon compact. L'identification d'un seul système WR + c dans la Galaxie tient donc possiblement du fait que trop peu d'étoiles Wolf-Rayet ont été observées de façon intensive.

Certaines signatures observationnelles pourraient permettre d'identifier de nouveaux systèmes WR + c galactiques comme Cyg X-3, bien que l'espoir d'en trouver plusieurs semble bien mince. D'abord, comme nous l'avons mentionné précédemment, on peut s'attendre à ce que la luminosité en rayons X d'un tel système soit élevée s'il y a accrétion sur un compagnon compact. De plus, ces rayons X devraient être relativement durs dans le cas de l'accrétion sur une étoile à neutron (p. ex. Rappaport & Joss 1983). On peut aussi anticiper que le flux de ces rayons X durs varie en fonction de la phase orbitale, soit à cause de la modulation

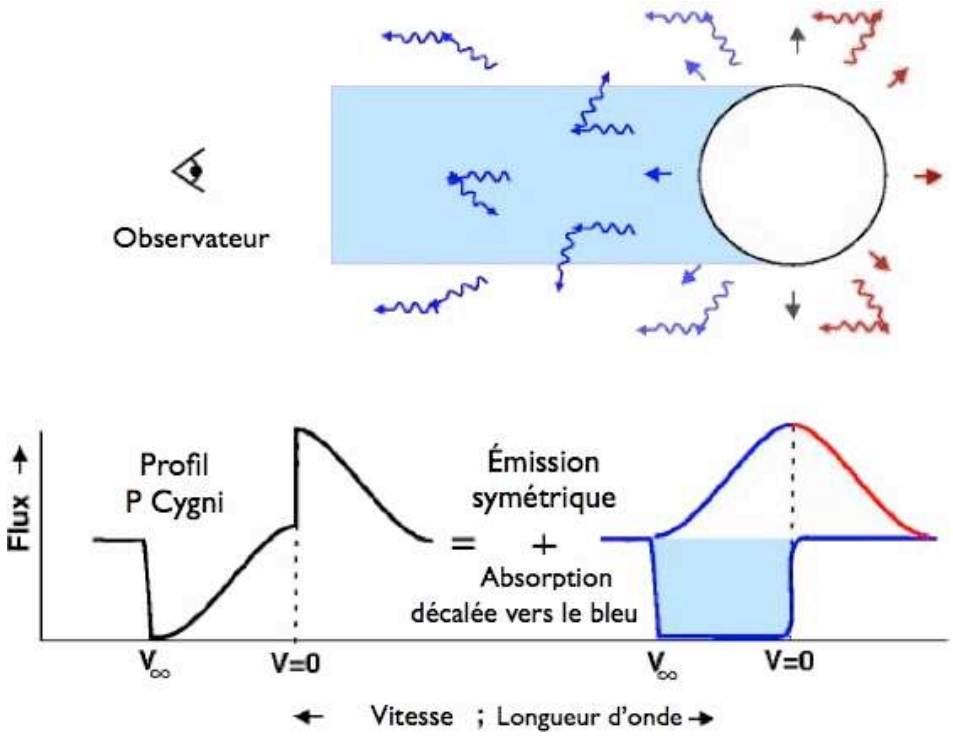

FIG. 1.2 – Description schématique de la formation d'un profil P Cygni, d'après un schéma original de S. Owocki (www.bartol.udel.edu/∼owocki).

de la densité de colonne de gaz qui atténue les rayons X, soit à cause de différences dans les conditions du vent de l'étoile Wolf-Rayet le long de l'orbite du compagnon compact menant à une modulation du taux d'accrétion et donc de la luminosité en rayons X. Une autre signature de la présence d'un compagnon compact dans le vent dense de l'étoile Wolf-Rayet a été suggérée par Hatchett & McCray (1977). Ces auteurs ont proposé que l'émission de rayons X du compagnon compact devrait ioniser le gaz dans son entourage vers des états d'ionisation plus élevés. Cette zone d'ionisation pourrait avoir un effet observable sur les profils P Cygni des raies de résonance que l'on retrouve dans l'ultraviolet. Ces profils, constitués d'une composante d'absorption et d'une composante d'émission, sont formés dans le vent de l'étoile Wolf-Rayet par diffusion résonante des photons vers la ligne de visée et hors de celle-ci (voir Figure 1.2). Si le compagnon se trouve devant l'étoile Wolf-Rayet, le gaz contribuant à l'absorption P Cygni est affecté par la zone d'ionisation et la réduction du nombre de diffuseurs devrait rendre la composante d'absorption moins forte (et inversement si le nombre de diffuseurs augmente). À la phase orbitale opposée, la composante d'absorption devrait plutôt refléter l'état du vent

non-perturbé par la zone d'ionisation. L'effet «Hatchett-McCray» a déjà été observé avec le satellite ultraviolet *IUE (International Ultraviolet Explorer)* dans plusieurs systèmes binaires à rayons X de type O + c (p.ex. van Loon et al. 2001, et références incluses), mais jamais encore dans un système contenant une étoile Wolf-Rayet.

1.3.2 Rotation

Devant les insuccès de l'interprétation de la variabilité cyclique à court terme de certaines étoiles Wolf-Rayet en terme d'un compagnon compact, d'autres explications ont été proposées. Une de ces alternatives est la rotation. Dans ce cas, ce sont des structures à la surface de l'étoile, possiblement reliées à des champs magnétiques ou à des pulsations (Kaper et al. 1997; de Jong et al. 2001), qui sont à l'origine des variations photométriques et des perturbations dans le vent qui occasionnent des changements dans les profils des raies d'émission optiques et dans les profils P Cygni de l'ultraviolet.

EZ CMa (WR 6) est certainement l'exemple le plus concluant d'une étoile Wolf-Rayet pour laquelle la rotation semble être à l'origine de la variabilité observée. Des données photométriques très étendues ont permis de montrer que la variabilité de cette étoile est caractérisée par une seule période indépendante (P=3,766 jours) et que cette période est stable dans le temps (Antokhin et al. 1994), comme on devrait s'y attendre si la rotation de l'étoile est à l'origine de la périodicité. Cette période persiste même si les courbes de lumières et de vitesses radiales changent de forme de façon significative sur des échelles de temps de plus de quelques cycles (Robert et al. 1992). Des observations spectropolarimétriques (Schulte-Ladbeck et al. 1991) suggèrent également que le vent de EZ CMa est aplati, supportant ainsi l'hypothèse de la rotation. Des données *IUE* s'échelonnant sur 16 jours, soit plus de quatre cycles, ont aussi permis de déduire la présence d'une structure qui serait modulée par la rotation (St-Louis et al. 1995). Deux types principaux de profils P Cygni ont été observés dans ces spectres ultraviolets: certains dont l'aile bleue de la composante d'absorption s'étend environ jusqu'à v_∞ et d'autres qui montrent une absorption supplémentaire jusqu'à environ 900 km s^{-1} en excès

de v_∞ accompagnée d'un excès d'émission aux basses vitesses négatives. Ces deux types de profils ont été associés à certains intervalles de phase et leur variabilité reliée à la période de 3,766 jours. Pour expliquer ces observations, un modèle qualitatif a été proposé dans lequel le vent est divisé en pointes de tartes correspondant à des parties plus rapides ou plus lentes de la structure en rotation. Ce modèle ressemble beaucoup à l'idée des régions d'interactions en co-rotation (*Corotating Interaction Regions*, CIRs) proposée pour la première fois par Mullan (1984).

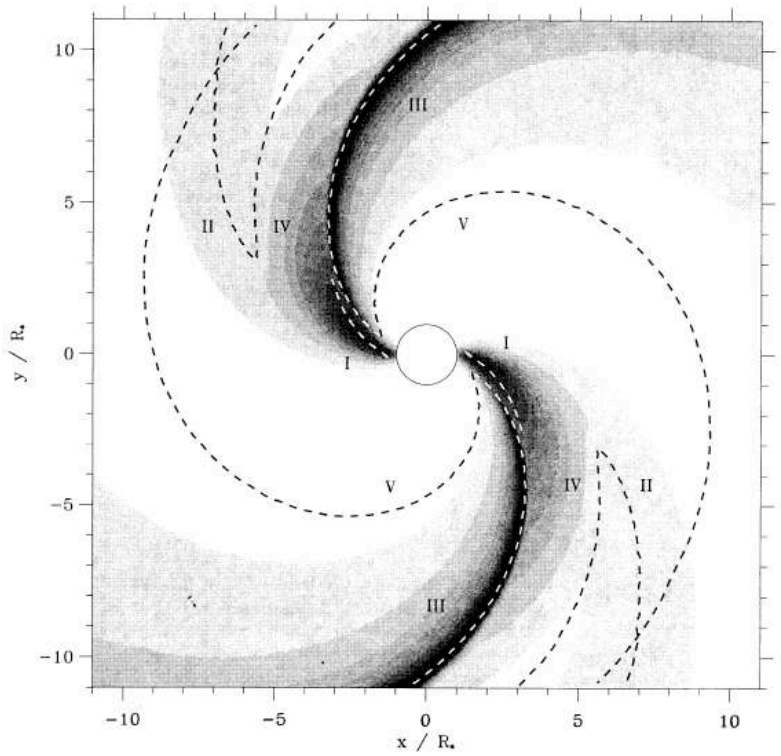

FIG. 1.3 – Simulation hydrodynamique de régions d'interaction en co-rotation (CIRs). Les teintes plus foncées représentent des zones de plus grande densité. La discontinuité dans le gradient de vitesse est dénotée ici par la lettre V et le trait pointillé adjacent. Figure tirée de Cranmer & Owocki (1996).

Les CIRs sont des perturbations à grande échelle de la densité et de la vitesse du vent qui prennent la forme de spirales en co-rotation avec la surface de l'étoile (voir Figure 1.3). Elles originent de modulations à la surface de l'étoile, possiblement des pulsations ou les effets d'un champ magnétique, et s'étendent sur de grandes distances. Des simulations hydrodynamiques détaillées des CIRs ont étés effectuées au cours des dernières années (Cranmer & Owocki 1996; Dessart & Chesneau 2002; Lobel & Blomme 2008). Ces simulations montrent comment des variations azimutales de la brillance de surface d'une étoile en rotation génèrent les fameuses

spirales. Les variations de la brillance (et donc de la force radiative) à la base du vent induisent une structure dans le vent avec des raréfactions rapides qui rencontrent des régions plus denses et lentes. La rencontre de ces régions mène à un choc qui compresse le matériel dans une coquille dense. L'interaction produit aussi un plateau dans le profil radial de vitesse du vent séparé du reste du vent en accélération par une discontinuité dans le gradient de vitesse. Les structures de densité et de vitesse créées traversent la ligne de visée au rythme de la rotation des perturbations à la base et modulent les profils des raies formées dans le vent. La profondeur optique radiale du vent est proportionnelle à la densité et inversement proportionnelle au gradient de vitesse (p. ex. Cranmer & Owocki 1996). Les régions de surdensités ou de gradient de vitesse plus faible sont donc susceptibles d'avoir un plus grand impact sur les variations dans les profils de raies. En fait, les simulations montrent que c'est le plateau de vitesse qui domine la variabilité induite dans les profils de raies.

Couplés à des calculs de profils synthétiques, les modèles montrent que les CIRs peuvent causer des variations périodiques très caractéristiques dans les profils P Cygni de l'ultraviolet (Figure 1.4), notamment sous la forme des DACs, ainsi que dans les raies d'émission optiques (Figure 1.5). La variabilité observée dans les raies d'émission optiques de EZ CMa (Morel et al. 1998) rappelle d'ailleurs l'effet prédit par des CIRs dans ces raies d'émission (Dessart & Chesneau 2002). WR 134 est une autre étoile Wolf-Rayet qui montre ce genre de variabilité dans les raies d'émission optiques (Morel et al. 1999) et pour laquelle le scénario des modulations causées par la rotation a été privilégié pour expliquer sa période de 2,25 jours. Des observations spectropolarimétriques (Schulte-Ladbeck et al. 1992) suggèrent également un vent aplati pour WR 134. Récemment, en recherchant le même genre de variabilité spectroscopique typique des CIRs dans les raies d'émission optiques, Chené & St-Louis (2008) ont pu estimer la vitesse de rotation de quelques étoiles Wolf-Rayet additionnelles (WR 1, WR 67, WR 120). Ces vitesses de rotation se situent entre 10 et 60 km s^{-1}.

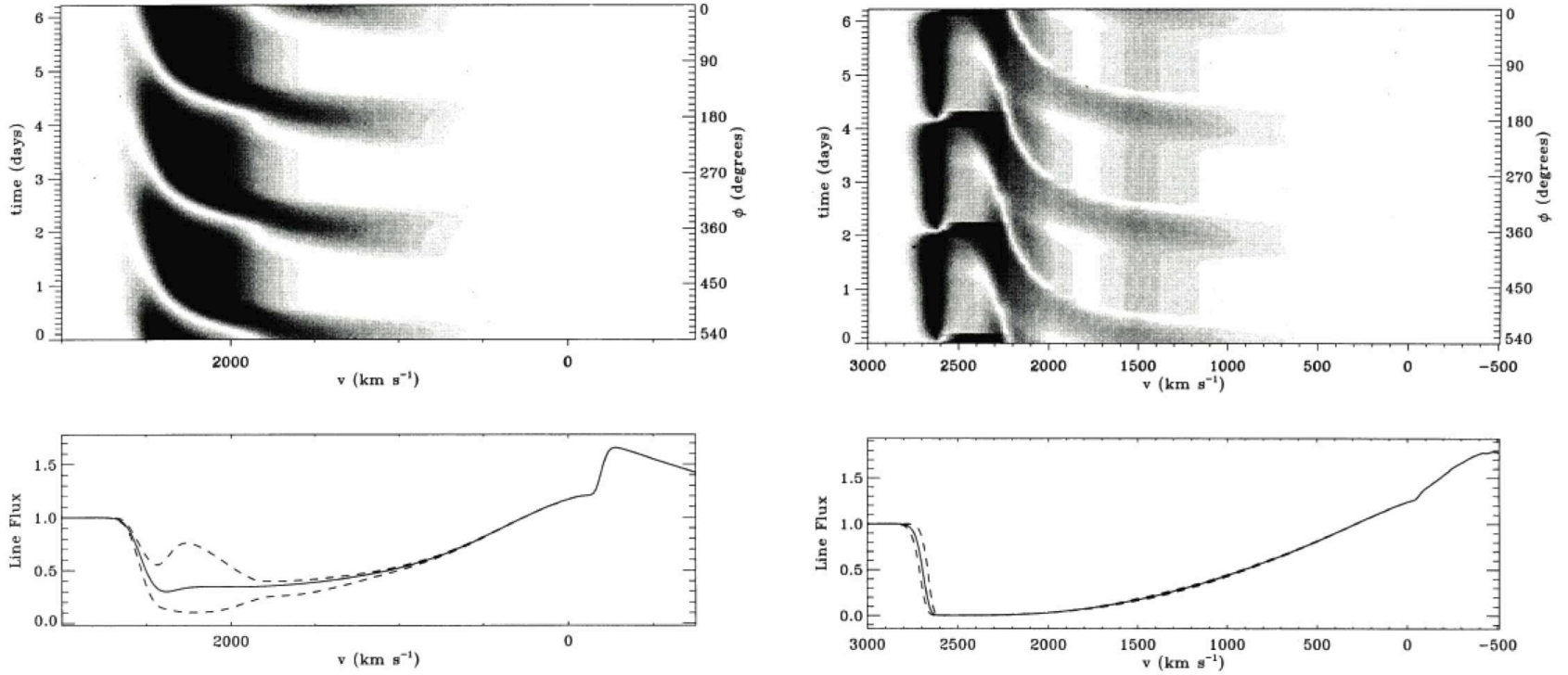

FIG. 1.4 – Exemple de simulation des variations causées par des CIRs dans des profils P Cygni de l'ultraviolet dont la composante d'absorption n'est pas saturée (à gauche) ou saturée (à droite), tiré de Cranmer & Owocki (1996). Le temps augmente verticalement sur les panneaux du haut. L'échelle en teintes de gris sur les panneaux du haut représente le quotient du flux sur le flux maximum à une vitesse donnée, avec le minimum en noir et le maximum en blanc. Le profil moyen est montré en trait continu sur les panneaux du bas. Le fait que les variations de flux ne soient pas exactement zéro dans la partie saturée du profil d'absorption est dû à une limitation du modèle. Les variations dans le profil non-saturé sont caractéristiques des DACs.

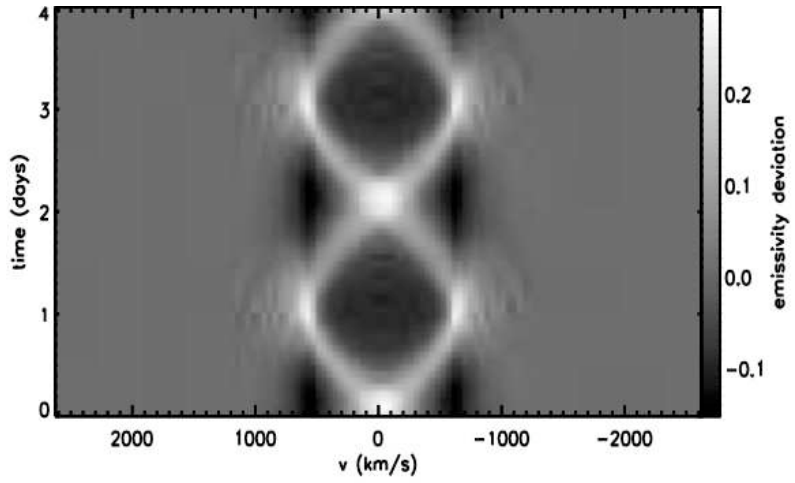

FIG. 1.5 – Exemple de simulation des variations causées par des CIRs dans une raie d'émission optique. Le temps augmente verticalement. Les zones plus pâles (foncées) correspondent à des excès (déficits) d'émission par rapport au profil normal de la raie. Tiré de Dessart & Chesneau (2002).

Bien que fragmentaire pour l'instant, la connaissance des vitesses de rotation des étoiles Wolf-Rayet est importante vu le rôle crucial que joue la rotation dans l'évolution des étoiles massives (p. ex. Meynet & Maeder 2005). Soulignons aussi que l'effondrement d'une étoile Wolf-Rayet en rotation rapide ($\sim$300 km s^{-1} en surface) semble être le scénario le plus probable pour expliquer les sursauts gamma longs (*long-term Gamma Ray Bursters*) (MacFadyen & Woosley 1999). Éventuellement, l'identification d'étoiles Wolf-Rayet en rotation rapide pourrait donc permettre d'étudier la phase précédant ces sursauts gamma longs.

1.3.3 Pulsations

Il pourrait s'avérer difficile de conclure si l'échelle de temps de la variabilité cyclique à court terme d'une étoile Wolf-Rayet est dominée par la rotation de structures à grande échelle générées par des perturbations à la base du vent (p. ex. associées à un champ magnétique ou des pulsations), par la ou les période(s) des pulsations elles-mêmes, ou par une combinaison des deux. En effet, les pulsations, qui sont souvent identifiées comme un mécanisme potentiel pour générer des CIRs (Kaper et al. 1997; de Jong et al. 2001), et la rotation sont deux processus menant à des variations périodiques. Il n'est donc pas évident de savoir quelle période

se manifestera dans les variations observées. Cette dernière dépendra de manière complexe du rapport des périodes. La confusion peut même être amplifiée par le fait qu'une période de plusieurs heures est en théorie possible pour chacun des deux phénomènes. Par contre, dans certaines conditions, on peut exclure un des deux scénarios. Par exemple, pour des périodes qui sont plus longues qu'environ un jour, on peut exclure pour l'instant les pulsations étant donné qu'aucune théorie ne prédit de pulsations avec des périodes aussi longues dans les étoiles Wolf-Rayet. D'autre part, pour des périodes trop courtes (autour de quelques heures), la rotation peut ne plus être une explication valide de la variabilité car la vitesse de rotation ne peut dépasser la vitesse de rotation critique (la vitesse au-delà de laquelle la force centrifuge dépasse la force de gravitation). Une interprétation en fonction de la rotation seulement pourrait également devenir problématique dans le cas où plusieurs périodes seraient présentes simultanément.

Les premières études théoriques de pulsations dans les étoiles Wolf-Rayet ont été effectuées par Maeder (1985) et Maeder & Schaller (1991). Ces auteurs ont conclu que dans les modèles avec brûlage d'hélium dans le noyau, le mécanisme ϵ devrait produire des pulsations radiales avec des périodes de 15 à 60 minutes. Noels & Scuflaire (1986) ont ensuite investigué les pulsations non-radiales et ont montré que le mécanisme ϵ devrait produire de telles pulsations dans le cas d'une étoile Wolf-Rayet avec brûlage d'hydrogène dans une coquille (*shell burning*), mais pas dans le cas du brûlage d'hydrogène ou d'hélium dans le noyau. Les périodes prédites pour ces pulsations non-radiales sont de l'ordre de quelques heures. Par contre, la durée prédite de la phase d'instabilité de ces modes n'est environ que de 5000 ans, ce qui en fait un mécanisme peu probable pour expliquer la variabilité d'un grand nombre d'étoiles Wolf-Rayet. D'autres études se sont intéressées aux modes de pulsations dits étranges (*strange modes*). Par exemple, pour des masses stellaires entre $\sim$4 et 18 $M_{\odot}$, Glatzel et al. (1993) ont déterminé que les périodes de ces modes devraient généralement être inférieures à environ 25 minutes. Finalement, Townsend & MacDonald (2006) ont examiné la stabilité des modes g avec $l = 1$ et $l = 2$ dans des modèles d'étoiles Wolf-Rayet riches en azote (WN). Ils ont trouvé que le mécanisme κ opérant sur une bosse de l'opacité du fer peut mener à des modes instables avec des périodes de quelques heures.

Du point de vue des observations, les étoiles Wolf-Rayet candidates pour des pulsations sont peu nombreuses. Bratschi & Blecha (1996) ont cherché des périodes de pulsations dans six étoiles Wolf-Rayet dont les observations s'échelonnaient sur trois ans, mais n'en ont trouvé aucune. Une période photométrique de 3,5 heures a été mesurée pour l'étoile WR 66 à partir d'observations obtenues sur 61 nuits (Antokhin et al. 1995). Cette période est trop courte pour être attribuée à la rotation et WR 66 est donc une candidate intéressante pour des pulsations (Antokhin 1996), mais son cas a reçu peu d'attention depuis. Pour l'étoile WR 123, la période de 9,8 heures détectée à l'aide du satellite *MOST* (Lefèvre et al. 2005) est également trop courte pour la rotation étant donné le rayon relativement grand de cette étoile de type WN8. Townsend & MacDonald (2006) ont proposé que la variabilité pourrait être causée par des modes g, alors que Dorfi et al. (2006) et Glatzel (2008) ont plutôt suggéré des modes étranges dont les périodes devraient être de quelques heures vu le grand rayon de WR 123.

1.4 Présentation et justification de l'étude sur WR 46

L'étoile Wolf-Rayet WR 46 est bien connue pour sa variabilité cyclique sur une échelle de temps d'environ 7-8 heures. Les trois mécanismes présentés à la section précédente (binarité, rotation, pulsations) ont été suggérés pour expliquer sa variabilité. Chacun de ces scénarios représenterait un phénomène rarement observé pour une étoile Wolf-Rayet. La confirmation de l'un ou l'autre des mécanismes pourrait permettre de lever le voile sur un rare système WR + c, une première étoile Wolf-Rayet en rotation rapide, ou encore un nouveau membre dans un groupe très restreint d'étoiles Wolf-Rayet candidates pour montrer des pulsations.

WR 46 a fait l'objet de plusieurs études, mais aucune n'a pu offrir d'explication concluante de la variabilité cyclique à court terme de cette étoile. Récemment, certains auteurs ont mis de l'avant le scénario des pulsations, mais sans pouvoir exclure la présence d'un compagnon. Il apparaissait donc évident que des observations supplémentaires étaient nécessaires pour progresser dans notre compréhension. Ces observations se devaient de ne pas être une simple répétition des nombreuses campagnes d'observations intensives menées dans les dernières an-

nées, principalement dans le domaine visible du spectre électromagnétique. C'est dans cette optique que nous avons observé WR 46 sur plusieurs cycles avec le satellite *FUSE* (*Far Ultraviolet Spectroscopic Explorer*) qui observe dans l'ultraviolet lointain, et que nous avons récupéré des données en rayons X obtenues avec le télescope spatial *XMM-Newton* (*X-ray Multi-Mirror mission - Newton*). *FUSE* donne accès à des profils P Cygni forts. Le profil P Cygni de O VI $\lambda\lambda$1032, 1038, à cause du potentiel d'ionisation élevé de O VI, peut notamment permettre d'étudier des phénomènes énergétiques difficiles à observer autrement. Les rayons X fournissent également des informations à plus hautes énergies qui n'avaient pas été considérées auparavant pour WR 46.

Nous présentons au Chapitre 2 ces nouvelles observations de WR 46 et leur interprétation. Nous débutons par un survol historique des propriétés et de la variabilité de cette étoile. Les observations *FUSE* et *XMM-Newton* sont ensuite présentées. L'analyse de ces données suit, avec un accent particulier sur la caractérisation de la variabilité détectée dans l'ultraviolet lointain et les rayons X. Finalement, les résultats obtenus sont discutés dans le contexte de chacun des scénarios suggérés pour expliquer la variabilité cyclique à court terme de WR 46. À noter, outre la réduction des données *XMM-Newton* qui a été effectuée par deux des co-auteurs (A.M.T. Pollock et S. Carpano), le reste de l'article présenté au Chapitre 2 (réduction des données *FUSE*, analyse, interprétation, rédaction) est le fruit du travail de l'auteur principal (V. Hénault-Brunet), les co-auteurs ayant contribué à orienter la discussion par leurs commentaires et leur expertise.

Chapitre 2

New clues to the nature of the variability of the Wolf-Rayet star WR 46

V. Hénault-Brunet[1], N. St-Louis[1], S.V. Marchenko[2], A.M.T. Pollock [3], S. Carpano [4]

To be submitted to *The Astrophysical Journal*

August 2009

[1]Département de Physique, Université de Montréal, and Centre de Recherche en Astrophysique du Québec (CRAQ), C.P. 6128, Succ. Centre-Ville, Montréal, Québec H3C 3J7, Canada

[2]

[3]XMM-Newton Science Operations Center, European Space Astronomy Centre, 28080 Madrid, Spain;

[4]Research and Scientific Support Department, ESTEC/ESA, PO Box 299, 2200, AG Noordwijk, the Netherlands;

2.1 Abstract

The Wolf-Rayet star WR 46 is known to exhibit a very complex variability pattern on relatively short timescales of a few hours and also on longer timescales of months. Periodic but intermittent radial velocity shifts of optical lines as well as multiple photometric periods have been found in the past. Non-radial pulsations, rapid rotational modulation or the presence of a yet-to-be-confirmed low-mass companion have been proposed to explain the short-term behaviour. In an effort to unveil its true nature, we observed WR 46 with *FUSE* over several short-term variability cycles. We found significant variations on a timescale of about 7.5 hours in the FUV continuum, in the blue edge of the absorption trough of the O VI $\lambda\lambda$1032, 1038 doublet P Cygni profile, and in the S VI $\lambda\lambda$933, 944 P Cygni absorption profile. We also retrieved archival *XMM-Newton* data of this star. We found the X-ray light-curve to show variations on a timescale similar to the UV and FUV continuum light-curves, and the X-ray spectrum of WR 46 to be very soft with a peak below 1 keV. We discuss the different constraints on the nature of the variability that these new observations help to establish. Among the suggested scenarios, we propose that non-radial pulsations is the most likely, although we are far from a complete picture.

2.2 Introduction

The Wolf-Rayet (WR) star WR 46 (HD 104994, DI Cru) is well-known for its remarkable variability. All the suspected causes of this variability (a close binary companion, rapid rotational modulation, non-radial pulsations) represent very rarely observed phenomena for Wolf-Rayet stars and therefore the confirmation of one of these scenarios would likely provide insight into our understanding of the physics and evolution of massive stars.

Despite the fact that some scenarios have been favoured to explain its puzzling behaviour, we still lack a satisfying explanation of the underlying mechanism. Because of the detection of radial velocity variations, the presence of an unseen close binary companion has been a popular suggestion, but as we will review, this hypothesis runs into many difficulties. We are

still looking for observational evidence that would once and for all confirm or invalidate the existence of a companion. It has also been suggested that multi-frequency non-radial pulsations of a single WR star cause the observed wind variability (Veen et al. 2002c; Oliveira et al. 2004). While this last scenario appears to be at least part of the solution, more observations are needed to progress towards a clear picture of this enigmatic star. For example, additional intense monitoring campaigns with simultaneous photometry and spectroscopy, or observations in selected spectral windows (like the ultraviolet or X-rays) would certainly be useful.

It is with this aim in mind that we obtained a time-resolved series of *FUSE (Far Ultraviolet Spectroscopic Explorer)* observations and that we retrieved from the archive available *XMM-Newton (X-ray Multi-Mirror Mission - Newton Space Telescope)* observations of WR 46. *FUSE* observed in the far ultraviolet (FUV) spectral range, giving access to P Cygni profiles of resonant transitions from various species. These profiles are characteristic of dense stellar outflows and the study of their variability enables us to probe the evolution of the wind structure of WR 46 as a function of time. We were particularly interested in the high ionization potential O VI $\lambda\lambda$1032, 1038 doublet, which, along with the X-ray spectrum and light-curve from *XMM-Newton*, could provide information on energetic phenomena such as accretion onto a compact companion or wind-embedded shocks.

Before we discuss these new observational clues, we first review in §2.3 key aspects of the rich but complex observational history of WR 46. In §2.4 we describe our observations and the data reduction procedures that were carried out. In §2.5, we present the analysis performed on the data, while in §2.6 we present a discussion of the possible underlying physical mechanisms. Our conclusions can be found in §2.7.

2.3 Observational history

2.3.1 Physical properties

WR 46 is classified as WN3p in the Seventh Catalogue of Galactic Wolf-Rayet Stars (van der Hucht 2001). The “p" stands for peculiar and denotes the presence of unusually strong O VI $\lambda\lambda$3811, 3834 emission lines. Although it has long been included in catalogues of galactic Wolf-Rayet stars, the identification of WR 46 as a Wolf-Rayet star has not always been unequivocal. For example, Niemela et al. (1995) suggested it to be an evolved low mass X-ray binary system containing an accretion disk. Steiner & Diaz (1998) considered this star as a member of the V Sagittae group of stars, interpreted as the Galactic counterparts of the close binary supersoft X-ray sources (CBSSs) observed in the Magellanic Clouds and in M31, in which bright emission lines are claimed to originate in an accretion disk. As we will see, this hypothesis no longer stands.

Crowther et al. (1995), Marchenko et al. (2000), Veen et al. (2002a,c), and Oliveira et al. (2004) all argued in favor of the Wolf-Rayet nature of WR 46. The Wolf-Rayet spectrum of WR 46 is well reproduced by the Population I wind model of Crowther et al. (1995). Marchenko et al. (2000) argued against the classification of WR 46 as a “V Sagittae” star and noted that the strong stratification of the line formation zones in WR 46 resembles the stratification of a typical WR wind. The lines of high ionization in WR 46 are indeed narrowest, consistent with the interpretation that they are formed in the inner and hotter WR wind at lower expansion velocity (Herald et al. 2000). Based on the time-delays observed in the variability of different emission lines, Veen et al. (2002b) also inferred that the spectrum is formed in a stratified stellar wind with optical depth larger than one, and not in a stellar disk as proposed by Niemela et al. (1995) and Steiner & Diaz (1998). This was confirmed by Oliveira et al. (2004), who also listed several other arguments in favor of the WR scenario or against the CBSS scenario.

Crowther et al. (1995) presented a detailed study of the ultraviolet and optical spectrum of WR 46 in the context of weak-lined WN early (WNE) stars using unblanketed wind models.

Compared to CNO-equilibrium values, these authors found an unusually high oxygen abundance, three times larger than for the two other weak-lined WNE stars (WR 128 and WR 152) in their study. Since the O VI $\lambda\lambda$3811, 3834 lines are not seen in WR 3 (Hamann et al. 1995), a star with nearly identical parameters to those of WR 46, Crowther et al. (1995) argued that the high oxygen abundance in WR 46 is not due to imperfections of the model. However, Veen et al. (2002b) noted that the O VI $\lambda\lambda$3811, 3834 doublet is more susceptible to low wind-density (i.e. predicted for WN stars solely for very low wind density). These authors argued that a more proper abundance indicator is the ratio of O VI λ5290 to He II λ5411, which is in fact similar in WR 46 and WR 3. Veen et al. (2002b) therefore concluded that the oxygen abundance of WR 46 is probably not peculiar.

As mentioned above, the results of Crowther et al. (1995) support the idea that WR 46 is a Population I WR star (with a possible compact companion) rather than a low mass X-ray binary, as had been previously suggested. The line profiles are indeed well reproduced by their Population I wind model, and the derived properties for WR 46 are similar to those of other weak-lined WNE stars. These weak-lined WNE stars are as hot as the strong-lined WNE stars, but with mass-loss rates about an order of magnitude lower. As is the case for the other weak-lined WNE stars analysed by Crowther et al. (1995), WR 46 exhibits a low degree of atmospheric extension ($R_* \sim R_{\tau_R=2/3}$ and triangular emission-line profiles indicate very low wind densities). In general, weak-lined WNE stars tend to exhibit these triangular line profiles (as opposed to the more typical Gaussian lines of strong-lined WNE stars) because one can observe strongly accelerated material much closer to the stellar core.

The high luminosity found by Crowther et al. (1995) for WR 46, $\log L/L_\odot = 5.53$, is also typical of Wolf-Rayet stars. In determining the luminosity, they adopted a distance of 4.0$\pm$1.5 kpc, which is consistent with the distance of 4.0 kpc based on the membership of WR 46 to the Cru OB4.0 association as suggested by Tovmassian et al. (1996) from ultraviolet photometry. Physical parameters for WR 46 similar to those determined by Crowther et al. (1995) were found in other spectroscopic analyses, for example the ones by Hamann & Koesterke (1998)

and Hamann et al. (2006), the latter using blanketed models. This object was considered as a single Wolf-Rayet star in these studies since the spectrum does not appear to be composite.

In the present work, we adopt the results from a recent CMFGEN (Hillier & Miller 1998) blanketed wind model of WR 46 (Crowther, private communication) with the following parameters estimated from a combination of nitrogen and oxygen optical/uv line diagnostics : luminosity $\log L/L_{\odot} = 5.7$, radius $R_{\star}(\tau_R \sim 20) = 2.9\ R_{\odot}$, terminal velocity $v_{\infty} = 2450$ km s^{-1}, temperature $T_{*} = 90.21$kK, and mass-loss rate $\log\ (\dot{M}/M_{\odot}\mathrm{yr}^{-1}) = -5.4$. These parameters are again similar to those previously reported. However, instead of the value of 2450 km s^{-1} from this model, we adopt the terminal velocity of 2775 km s^{-1} measured from the saturated O VI $\lambda\lambda$1032, 1038 P Cygni absorption line (Willis et al. 2004), a resonance doublet that in principle allows to trace material further out in the wind (at lower densities, closer to the actual terminal velocity) than the non-resonance optical/uv lines used in other studies. Note that this adopted value is somewhat lower than the terminal velocity found by Prinja et al. (1990) based on the P Cygni absorption of the N V λ1238 resonance line, but Willis et al. (2004) argued that it is probably more reliable since the N V λ1238 line is blended with interstellar Lyα. From the luminosity, $\log L/L_{\odot} = 5.7$, we derive a stellar mass of 18 $M_{\odot}$ using the mass-luminosity relation of Schaerer & Maeder (1992). The adopted stellar and wind parameters of WR 46 are presented in Table 2.1.

To conclude on the general physical properties of WR 46, we note that it is a known X-ray

TAB. 2.1 – Adopted stellar and wind parameters of WR 46

Parameter	Value
R_{*}	2.9 $R_{\odot}$
T_{*}	90,210 K
M	18 $M_{\odot}$
L	0.5×10^{6} $L_{\odot}$
v_{∞}	2775 km s^{-1}
$\dot{M}$	4×10^{-6} $M_{\odot}$ yr^{-1}
D	4.0 kpc

source. The X-ray discovery of WR 46 with *Einstein* was reported by Pollock (1987). An X-ray luminosity $L_{\rm X}(0.2{-}4$ keV$) \sim 3 \times 10^{33}$ erg s^{-1} was then derived with an estimated distance of 8.7 kpc. This corresponds to $\sim 6 \times 10^{32}$ erg s^{-1} at 4 kpc if we simply scale down the luminosity with an inverse square law in distance. Later, based on *ROSAT* PSPC observations (Wessolowski et al. 1995), Crowther et al. (1995) determined the X-ray luminosity of WR 46 to be $L_{\rm X} = 5 \pm 2 \times 10^{31}$ erg s^{-1} (with D=4.0 kpc) and noted that this is typical of single WN stars (Pollock 1995). Oskinova (2005) adopted a distance to WR 46 of 4.07 kpc and found $L_{\rm X} = 3.2 \times 10^{32}$ erg s^{-1} based on *XMM-Newton* EPIC archival data. In the context of her study of a large number of X-ray observations of Wolf-Rayet stars, WR 46 appears somewhat bright for a WNE star, but agrees with the usual $L_{\rm X} - L_{\rm bol}$ -relation for single O stars where $L_{\rm X} \approx 10^{-7}\ L_{\rm bol}$ (Berghoefer et al. 1997).

2.3.2 Variability

We summarize in this section the variability of WR 46 as observed by various authors. We also briefly present the scenarios favoured to explain the short-term variability, but we delay the detailed discussion of these scenarios to §2.6.

Smith (1968) already suspected WR 46 to be variable in her photometric investigation of WR stars, but Monderen et al. (1988) were the first to officially report the photometric variability of this object. In their ∼5-hour V-filter observation of this star taken in 1986, they observed a 0.075 mag amplitude variability on a timescale of about 3 hours. A follow-up photometric campaign of several nights in February and March 1989 by van Genderen et al. (1991) revealed variability with an amplitude of 0.15 mag and a dominant period of 0.1412 d (3.39 h), but the shape of individual cycles showed a large scatter from one cycle to the other. Because of the apparent succession of deep and shallow minima (although not very regular), these authors adopted the double-wave period of 0.2824 d (6.78 h) instead. They suggested a binary nature based on the fact that the light-curve resembles that of a binary consisting of a deformed bright component (the WR star) and a smaller one. The companion was proposed to be a

low-mass star, possibly a compact companion.

A first radial velocity curve of WR 46, obtained in 1989, was presented by van Genderen et al. (1991). The radial velocity variability was later confirmed by Veen et al. (1995) and Niemela et al. (1995). The radial velocity curve presented by Veen et al. (1995) was obtained in 1991. This curve showed a period P=0.28 d (6.8 h) and a semi-amplitude K of about 100 km s^{-1}. This might have seemed to confirm the binary nature suggested from photometry. However, in their radial velocity curve obtained in 1993, Niemela et al. (1995) intriguingly found a distinct period of 0.311 d (7.46 h) with a larger semi-amplitude K of about 200 km s^{-1}.

Marchenko et al. (2000) later presented the results of an intense optical spectroscopic and photometric monitoring campaign of WR 46 carried out in 1999. This study revealed clear periodic variations in the radial velocities of the emission lines of highest ionization potential (O VI and N V) with again a slightly different period of 0.329±0.013 d (7.90±0.31 h), and an amplitude of about 100 km s^{-1}. As these lines are formed deep in the Wolf-Rayet wind, it was suggested that they are least likely to be perturbed by a companion and thus are good tracers of orbital motion. The authors considered their period compatible with the P=0.311 d (7.46 h) periodicity found by Niemela et al. (1995), although the amplitude of radial velocity variations observed in 1999 is about twice as small, similar to that of Veen et al. (1995). They also found coherent short-term variability (i.e. following the 0.329 d period) in the equivalent width of lines with lower ionization/excitation potential and in the continuum flux. The magnitude of the line profile variability was found to depend on the level of the continuum, with higher flux corresponding to a higher level of line variability.

Marchenko et al. (2000) interpreted the radial-velocity period of 0.329 d (7.90 h) as the orbital motion of a binary system containing a classical Population I Wolf-Rayet star, but also showed that the radial-velocity modulation unexpectedly disappears from time to time, thus revealing a new puzzle. This undeniable apparent ceasing of the orbital motion was found in about one out of three consecutive nights. The authors also found some indication of a similar

behaviour in their re-analysis of the 1993 spectra of Niemela et al. (1995), which they argued could explain the large scatter in the folded radial velocity curve obtained from these data. To try to understand this curious phenomenon, they investigated the possibility that the apparent intermittent ceasing of the radial velocity variations is rooted in a sudden change of the wind structure, but found no obvious spectroscopic evidence for the anticipated radical change.

In a series of three papers, Veen et al. (2002a,b,c) presented a detailed analysis of a large-scale photometric and spectroscopic data set of WR 46 obtained between 1986 and 1999. In their first paper, they presented the results of the photometric monitoring, and confirmed that the star shows cyclical variability on a timescale of hours. The shape of the light-curves they obtained is quite complex, varying from purely sinusoidal to irregular, and from an amplitude of 0.1 mag to constancy. They also found significant night-to-night variability in the mean brightness, causing a large scatter in the folded light-curves. They identified significantly different dominant single-wave frequencies of 7.08 cycles per day (P=0.1412 d=3.39 h) and 7.34 d^{-1} (P=0.1362 d=3.27 h) in two large data sets from 1989 and 1991 respectively. These frequencies were found not only in the light but also in the colour variations, with the star turning red when optically bright and blue when optically faint. Strong evidence for an additional frequency of 4.34 d^{-1} (P=0.2304 d=5.53 h) was also found in light variations of the 1989 data, but not in the colour variations of this same data set.

When folding their data using twice the dominant single-wave period (i.e. P=0.2825 d=6.78 h in 1989, P=0.2727 d=6.54 h in 1991), Veen et al. (2002a) found the folded light- and color curves to appear ellipsoidal with unequal minima, in line with what was previously suggested by van Genderen et al. (1991). This was true for both the 1989 and 1991 data sets, although the difference in the depth of the minima of the folded light-curves is hardly significant (on average $\sim$0.04$-$0.07 mag for the deep minimum and $\sim$0.03$-$0.05 mag for the shallow minimum). The radial-velocity measurements of their second paper (Veen et al. 2002b) are in better agreement with these double-wave periods, although the radial velocities often do not vary at all. The single-wave radial-velocity period determined by Marchenko et al. (2000) is also of the same

order as these double-wave periods. It is however worth noting that the radial velocity in a given night is in phase with that of the preceding nights in the data of Marchenko et al. (2000), while the data of Veen et al. (2002b) show them to be in anti-phase. In the end, because of the circumstantial evidence (radial-velocity variability and different minima), Veen et al. (2002a) suggested that the true period of the system is the double-wave period (i.e. P=0.2825 d in 1989 and P=0.2727 d in 1991). Therefore, they concluded that a significant period decrease of 14 minutes occurred between 1989 and 1991.

In addition to the short-term photometric variability discussed above, WR 46 is also known to exhibit significant long-term photometric variability. Marchenko et al. (1998) detected a long-term brightening of the star between 1989 and 1993 with the *Hipparcos* satellite, a unique case among all the Wolf-Rayet stars in the *Hipparcos* survey. The brightness was found to increase from 1989 to a maximum $\Delta H_{\rm p}$(Hipparcos photometry) $\simeq 0.25$ mag by the end of 1991. This was confirmed by Veen et al. (2002a) who found an increase in brightness of 0.12 mag between 1989 and 1991, accompanied by a slight reddening. The brightness subsequently decreased to the level of 1989 in the course of 1993 (Marchenko et al. 1998). In addition to the *Hipparcos* brightening, other long-term brightenings appear to have occurred in the course of 1997 and in 1999-2000 (Veen et al. 2002a).

Veen et al. (2002a) noted that the change of the dominant light- and colour double-wave frequency between 1989 and 1991 appears to be related to the long-term brightening. However, their 1995 data suggest that the frequency change persisted even though the brightness returned to its original level in the course of 1993. These authors also showed that the mean amplitude of the light-curve was larger in 1991 (when the star was brighter) by a factor of about 1.7, but stressed that except for the different period and larger amplitude, the variability shows the same characteristics in 1989 and 1991, indicating, according to them, a true period change.

In their second paper, (Veen et al. 2002b) presented their spectroscopic observations of WR 46 obtained simultaneously with the photometric data. They found that the radiative fluxes (the

so-called continuum-corrected equivalent widths) of the optical emission lines vary on the same time scale as the light-curves and with a comparable behaviour (i.e. their maxima an minima coincide roughly). The short-term variability of these line fluxes supports the substantial period change between 1989 and 1991. The line-flux variability however did not provide obvious support for a shorter second period as was observed in the photometric data of 1989.

The radial velocity variations (K=50−100 km s^{-1}) observed by Veen et al. (2002b) usually displayed a coherent single-wave on the timescale of the double-wave photometric period, and sometimes displayed the so-called radial velocity stand-stills revealed by Marchenko et al. (2000). They also found small but persistent time-delays in the line flux of the outer-wind lines with respect to the line flux of the inner-wind lines. The radial-velocity variations showed much larger time-delays than the line fluxes, but their behaviour appeared less consistent. These time-delays were also observed in the start of a radial-velocity stand-still, with the outer-wind lines observed to enter a stand-still much later than the inner-wind lines. Another time-delay effect was observed within a single emission line. The radial-velocity variations of the peak of the line were found to precede the radial-velocity variations of the wings of the line. As noted above, the various time-delay effects observed by these authors are consistent with the formation of the spectrum in a stratified stellar wind, with the outer layers trailing the inner ones. Veen et al. (2002b) suggested that the radial-velocity stand-stills may be related to the observed time-delay effects present in the radial-velocity data, in particular to a loss of coherency between the stellar core and the line-emitting regions when the radial-velocity time-delay becomes too large. Beside the line-flux and radial-velocity variations, the spectroscopic monitoring by Veen et al. (2002b) also revealed significant and complicated line-profile variability in the He II λ4686 line on a timescale of hours.

Because the line-flux variability of the N V λ4604, 4620 line was found to be much larger than that of its neighbouring He II λ4686 line, and because this N V line was shown to be more susceptible to changes in temperature and mass-loss rates (Crowther et al. 1995), Veen et al. (2002b) concluded that the short-term variability of the photometry and line fluxes indicates

a varying local density distribution in the wind.

In addition to the short-term spectroscopic variations just described, Veen et al. (2002b) observed long-term spectroscopic changes in WR 46. They found that the line fluxes follow the observed brightenings on a timescale of years, with larger line fluxes when the object is brightest, in harmony with the photometric behaviour going from faint to bright states. A similar correlation was previously reported between the continuum flux and the equivalent width (EW) of the He II λ5412 line (Veen et al. 1995, 1999). Veen et al. (2002b) argued that this correlation between the line flux and the photometric behaviour on the long-term timescales implies that the Wolf-Rayet itself is the cause of the brightening instead of light from a possible companion.

Veen et al. (2002b) also investigated the long-term spectroscopic behaviour of WR 46 using a series of *IUE* spectra. These spectra confirmed the variability on timescales of days to years. The last spectrum was observed at the time of the maximum brightness recorded by *Hipparcos* in 1991. Of all the *IUE* spectra of this star, this last one shows the strongest emission lines, so the trend of a high continuum flux state linked with stronger lines also appears to be true in the ultraviolet. By observing the O V λ1371 P Cygni profile, they found that its absorption trough is also deepest for this spectrum obtained during the high state. Because the edge velocity of this absorption trough did not seem to change from one spectra to the other, they assumed that the velocity law of the wind remained constant over the years, and therefore that the deeper absorption trough in 1991 is due to an increase of the mass-loss rate. This is in line with the long-term increase in the mean continuum flux and in the mean line flux, which indicates an increase of the radius of the emission forming layers, and thus suggests a higher wind density.

Based on these evidences, Veen et al. (2002b) concluded that the long-term behaviour is indicative of a varying global density of the wind. It was noted that such a correlation between brightness and mass-loss rate is in agreement with the relation found by Smith & Maeder (1998). Applying a luminosity-radius relation (Schaerer & Maeder 1992), Veen et al. (2002b)

translated the 12% brightness increased between 1989 and 1991 into a radius increase of 4%. To interpret their observations (especially the short-term variability), Veen et al. (2002c) developed a geometrical model. This model shows how the suggested photometric double-wave variability can be interpreted as a rotating ellipsoidal density distribution in the stellar wind. Veen et al. (2002c) discussed the different mechanisms that could drive the variability and give rise to this rotating ellipsoidal density distribution. They interpreted the distinct periods of the system as either multiple non-radial pulsation periods or a gradual change in the underlying clock rate. Stellar rotation of a single star was ruled inconsistent with the period change and possible radius change between 1989 and 1991, and it was discarded as a likely cause of the variability. They studied the possibility of a close binary system. Although these authors did not completely reject it, this scenario appears rather unlikely. They also investigated an interpretation in terms of non-radial multi-mode pulsations, which seems consistent with the period change and the multi-frequency behaviour. The pulsation mode $l = 1$ $|m| = 1$ was proposed as it may mimic a “binary" light- and radial-velocity curve.

The most recent in-depth observational study of WR 46 was performed by Oliveira et al. (2004). They searched for spectroscopic evidence of a possible companion star, without success. Their observations, obtained between 1996 and 2002, once again exhibit complex photometric and spectroscopic variability on short (few hours) and long (months) timescales. Photometric variations on timescales of months were observed with an amplitude of 0.45 mag, while the night-to-night light-curve shape was found to depend strongly on the level of overall brightness, which motivated the authors to separate the data in three groups: low, indermediate, and high brightness phase. As also noticed by Veen et al. (2002b), they found a significant amount of variations from night to night in the N V $\lambda\lambda$4604, 4620/He II λ4686 line ratios, with the former varying more than the latter by a factor of about 2. The He II λ4686 line showed P Cygni-like variable absorption as also reported by Marchenko et al. (2000), and the N V $\lambda\lambda$4604, 4620 lines showed a broad variable component interpreted by Oliveira et al. (2004) in terms of the continuum fluorescence from a source of variable temperature (possibly the optically thick wind with a variable optical thickness). As opposed to the line profile varia-

tions found in the case of N V $\lambda\lambda$4604, 4620 and He II λ4686, the narrow N V λ4945 line only showed radial-velocity displacements. The authors argued that this is because the N V λ4945 line is much less sensitive to changes in temperature than the N V $\lambda\lambda$4604, 4620 lines. They also found evidence for a difference in the degree of ionization of WR 46 between June 1996 and January 2002 and suggested that this is probably caused by wind density variation.

Oliveira et al. (2004) argued that multiple photometric and radial velocity periods were present in their data. The main radial velocity period they found, 0.3319 d (7.97 h), is similar to that found by Marchenko et al. (2000), although the amplitude K=58 km s^{-1} is almost twice as small. The same period was found in photometric measurements when the star is at intermediate brightness, with an average light-curve showing a double wave with two unequal minima, as previously reported. However, when the star is in its bright phase, four distinct photometric periods were suggested, but the 0.3319-day radial-velocity period was not found in the photometric data. The different photometric periods claimed range between 0.183 and 0.583 d (between 4.39 and 13.99 h), with the dominant one being 0.253 d (6.07 h). The authors did not report the periodicity when the star is at a low brightness level, possibly because the amount of data in this low phase was not sufficient. In addition to the dominant radial-velocity period of 0.3319 d, Oliveira et al. (2004) claimed that secondary radial-velocity periods (0.267 d=6.41 h, and to a lesser degree 0.233 d=5.59 h and 0.278 d=6.67 h) are present in data from 1999 (maximum brightness level). When combining these data with their measurements from 1998, the 0.3319-day period was still there, but a secondary period of 0.282 d (6.77 h) was also apparently present. They noted that the additional radial-velocity periods of 0.233 d and 0.278 d are very close to the photometric periods found in the 1989 and 1991 data by Veen et al. (2002a), and that the values of 0.267 d and 0.278 d are also close to the oscillations seen in the radial-velocity data in 1989 and 1991 by Veen et al. (2002b). Oliveira et al. (2004) argued that the star therefore keeps its frequency memory. They also suggested that the radial-velocity standstills repeating with timescales of 2$-$3 days could result from interference between the two main periods ($\simeq$0.3319 and 0.267 d). While they did not completely discard the hypothesis of Marchenko et al. (2000) that the main radial-velocity period of WR 46 ($\simeq$0.3319 d) is the

orbital period of a binary system, Oliveira et al. (2004) concluded that the existence of secondary spectroscopic periods complicates the analysis and that the true binary nature has yet to be demonstrated. They argued that the additional photometric and spectroscopic periods are likely associated to non-radial pulsations, regardless of the binary nature of the star, as was originally proposed by Veen et al. (2002c). However, we stress that, ideally, the reality of each of these various periods needs to be confirmed with a long-term and very intense dataset.

2.4 Observations and data reduction

2.4.1 *FUSE*

The *FUSE* scientific instrument has been described in detail by Moos et al. (2000). The instrument consists of four co-aligned telescopes (channels) that feed light to four Rowland spectrographs. Each channel has an off-axis parabolic mirror, a focal plane assembly (including the spectrograph apertures), a diffraction grating and a section of one of two detectors. Two mirrors and gratings are coated with silicon carbide (SiC) for optimum reflectivity from 905 to 1105 Å. The two other mirrors and gratings are coated with aluminum and a lithium fluoride (LiF) for optimum reflectivity from 1000 to 1187 Å. One SiC spectrum and one LiF spectrum are imaged onto each detector. In the end, four spectra (SiC1, SiC2, LiF1, LiF2) are imaged and split in two segments (A and B), for a total of eight spectral segments covering the spectral window from 905 to 1187 Å with substantial overlap between individual segments.

We secured *FUSE* observations of WR 46 under guest observer time (program E113, PI: N. St-Louis) in order to perform time-resolved far-UV spectroscopy over many cycles of variability of the star. In total, for the three main consecutive observations of this program (E1130103, E1130104, E1130105), the star was followed for more than 30 hours spread over a timespan of about 50 hours. A previous observation of WR 46 was presented by Willis et al. (2004) in their *FUSE* atlas of Wolf-Rayet stars, and a few other shorter observations of this star are also found in the *FUSE* archive. We retrieved all available observations of WR 46 for the analysis

presented in this work. All observations were recorded using the large aperture (LWRS, 30″ × 30″) except observation S5160101 for which the medium-resolution aperture (MDRS, 4″ × 20″) was used. All observations were obtained in time-tag (TTAG) mode, for which the arrival times of photons are recorded. The log of the *FUSE* observations is presented in Table 2.2, which gives the *FUSE* data set number, the date and time of the beginning and end of the observation, the aperture and mode used, as well as the number of exposures and the total exposure time of each observation.

TAB. 2.2 – Log of *FUSE* observations

Data set*	Start time (UT)	End time (UT)	Aperture	MODE	Number of exposures	t_{exp}(s)
P1170601	2000-04-08 03:36:26	2000-04-08 07:25:06	LWRS	TTAG	4	4891
M1121501	2000-05-25 18:43:20	2000-05-25 20:36:10	LWRS	TTAG	2	5480
S5160101	2000-05-26 18:08:36	2000-05-26 23:10:08	MDRS	TTAG	12	16910
Z9900101	2002-06-28 14:31:54	2002-06-28 15:56:39	LWRS	TTAG	2	3946
E1130101	2005-07-17 04:09:40	2005-07-17 10:26:59	LWRS	TTAG	9	10210
E1130102	2005-07-20 03:46:53	2005-07-20 08:12:58	LWRS	TTAG	6	6199
E1130103	2006-03-09 14:28:48	2006-03-09 20:23:59	LWRS	TTAG	4	9955
E1130104	2006-03-10 02:46:20	2006-03-10 19:38:25	LWRS	TTAG	11	29682
E1130105	2006-03-11 03:44:02	2006-03-11 17:06:18	LWRS	TTAG	9	28213

* The data are archived in the Multimission Archive of the Space Telescope Science Institute (MAST).

Each individual raw exposure was run through the latest version of the *FUSE* calibration pipeline, CalFUSE v3.2 (Dixon et al. 2007). The pipeline first corrects the input data for "gaing-sag", "event bursts", and positional shifts of detected photons due to various effects. Then, a correction for background light is applied and a one-dimensional spectrum is extracted. Finally, the eight channel spectra are calibrated in wavelength and flux. In order to maximize the time coverage, we did not mask the data obtained during the day-time portion of the orbit as is often performed on *FUSE* data. Geocoronal airglow emission lines are stronger for day-time data, but this did not represent a serious constraint here. The strongest airglow line, H I Lyman-β at 1026 Å, is located right in the saturated part of the absorption component of the O VI $\lambda\lambda$1032, 1038 P Cygni profile of WR 46 and therefore it does not mask any precious spectral information. The other airglow lines seen in our data were much weaker.

Since we wanted photometric exposures to later extract accurate light-curves, we modified CalFUSE output intermediate data files (IDF) to remove the time intervals where the count rate in the spectral extraction window drops relatively abruptly due to the drifting of the star out of the aperture or away from the aperture center. It is well known that the photometric accuracy of *FUSE* is influenced by various effects that cannot be fully corrected by the CalFUSE pipeline (Dixon et al. 2007). A target centered in an aperture of the guide channel (LiF 1 prior to July 2005, LiF 2 after that) can be misaligned in the apertures of the other three channels. Also, with the loss of reaction wheels (the first two in 2001), channel drifts can even temporarily move the target out of the guide-channel aperture, as happened for some exposures of WR 46. The pipeline attempts to flag times when the target is out of the aperture, but this time lost to pointing excursions is by default underestimated to avoid the rejection of good data. A careful examination and screening of the IDF allowed us to insure the photometric quality of the data. New spectra were then extracted from these IDF for each exposure separately. The individual exposure times of these spectra are typically on the order of a thousand seconds. Note that we attempted to further break down all the exposures in small pieces of a few hundred seconds, but came to the conclusion that the marginal improvement in time resolution was generally not worth the associated decrease in the signal-to-noise ratio of spectra.

Photometric data are necessary to extract light-curves, but certainly not to extract spectra and analyse spectral-line variability. Even with non-photometric data (leading to errors in the absolute flux level calibration), we can always normalize the continuum flux level of all the spectra and focus on line variability. However, in the present case, screening the data by masking the time intervals lost to pointing errors does not cause much harm. Because the count rate during the masked intervals is lower than normal and because these masked intervals usually represent a minor fraction of the exposure time (especially for the guide channel apertures), the fraction of spectral photons lost because of this screening is small. Thus, the signal-to-noise ratio of the extracted spectra is not significantly affected. In a few cases, a major fraction if not all of the exposure had to be masked and no spectrum was extracted. In

these cases, the original spectrum that was extracted previous to screening for pointing losses had a very low signal-to-noise ratio and was hardly usable anyway. There is also an advantage to making sure that we have photometric data before extracting spectra. Photometric data allow us to extract spectra with a reliable absolute flux calibration, and thus make it possible to study long-term changes in the FUV spectrum of WR 46. For all these reasons, the spectra were extracted from the same modified IDF that were used to obtain light-curves.

When possible, an instrumental artifact nicknamed the “worm" was removed from the data. This feature is caused by electron repeller grid wires that prevent light from the target from reaching the detector, resulting in a wide artificial absorption trough. It was most noticeable in the LiF1B spectral segment of the observations we retrieved. It was also sometimes seen in the LiF2A segment. To remove the LiF1B (LiF2A) worm of a given exposure while keeping intact the smaller scale spectral features of the LiF1B (LiF2A) spectrum, we multiplied the LiF1B (LiF2A) spectrum by the smoothed ratio of LiF2A (LiF1B) and LiF1B (LiF2A) spectra. This method was not always possible, as for some exposures a worm was apparent in both LiF2A and LiF1B. In these cases, the LiF1B and LiF2A spectral segments of these exposures were not considered in our analysis of spectral variability (see §2.5.2). There were also several exposures (from data sets P1170601, M1121501, and S5160101) for which significant differences were found between the LiF2A and LiF1B segments, but where the discrepancies did not appear to be caused by worms. Since we could not identify the source of the systematic errors, we did not consider the LiF1B and LiF2A spectral segments of these exposures for the analysis of spectral variability.

To first isolate spectral line profile variability from continuum variability, all spectra were scaled to a common continuum level. The spectra were also co-aligned by cross-correlating them over small spectral ranges that include narrow interstellar absorption lines. Exposure E1130104010, for which the flux appeared stable in all channels, was used as a reference for scaling and alignment. All the spectral segments from this reference exposure were previously co-aligned on the guide-channel (LiF 2) spectral segments, for which the wavelength calibra-

tion errors are minimal (Dixon et al. 2007). For each exposure, we then performed a weighted average merging of the flux data in all eight channels, with the weights inversely proportional to the square of the statistical errors. In the end, we obtained a one-dimensional, heliocentric wavelength, flux-calibrated spectrum for each exposure (except when the exposure suffered from serious misalignment of the target).

Light-curves were then obtained to investigate the FUV continuum variability. Other light-curves were also extracted to look at variable spectral-line regions (see §2.5.2) integrated over broader wavelength intervals than the typical resolution of *FUSE* spectra, but with a much better time-resolution than it would be possible by just looking at our time-series of spectra. The routine ttag_lightcurve (see Bernard Godard's IDF cookbook[5]) was used to extract light-curves from the modified IDF discussed above. We estimated 1-σ uncertainties on the data points of the light-curves by assuming Poisson statistics (i.e. $\sigma = \sqrt{N}$, where N is the number of counts).

Specifically, three different types of light-curves were produced. The first shows the variations in the FUV continuum. The spectral window used for these FUV continuum light-curves includes all wavelength intervals that do not encompass the emission lines and P Cygni profiles identified in §2.5.1, the strongest predicted airglow emission lines (see Feldman et al. 2001), the edges of the wavelength range of each spectral segment, where systematic errors in the flux are significant (Sahnow et al. 2000), and narrow interstellar absorption features. The two other types of light-curves show the variations in the O VI $\lambda\lambda$1032, 1038 and S VI $\lambda\lambda$933, 944 doublet P Cygni absorption components, the only two variable spectral regions in the *FUSE* spectrum of WR 46 (see §2.5.2.). The O VI light-curve was extracted using the wavelength region from 1019.5 to 1022.5 Å, and the S VI light-curve the wavelength regions from 924.5 to 929 Å and 934 to 939 Å.

For each extracted light-curve, the contributions from all possible spectral segments were com-

[5]http://fuse.pha.jhu.edu/analysis/idfcook/

bined. For the FUV continuum light-curve, we combined the continuum light-curves of all eight *FUSE* spectral segments since continuum variations appeared to be the same across the entire *FUSE* spectral range. For the O VI $\lambda\lambda$1032, 1038 P Cygni absorption light-curve, all the spectral segments covering the spectral range concerned (namely LiF1A, LiF2B, SiC1A, and SiC2B) were used. Similarly, spectral segments SiC1B and SiC2A, covering the absorption component of the S VI $\lambda\lambda$933, 944 P Cygni profile, were used for the third light-curve. Note that when a worm feature was present in a spectrum, the light-curve of the affected spectral segment and exposure was not used.

To combine the light-curves of individual spectral segments we first normalized their average count rate to 1 for each observation and rebinned them into time intervals of 0.2 hours, propagating Poisson's 1-σ errors accordingly. An average light-curve of all the individual spectral segments concerned, weighted using errors, was then computed. To double-check the photometric quality of the data, we made sure that the light-curves from individual channels appeared correlated before averaging them. Finally, we divided the O VI and S VI normalized light-curves by the continuum normalized light-curve to remove the effect of continuum variability on the line variability.

2.4.2 *XMM-Newton*

WR 46 was observed by *XMM-Newton* (Jansen et al. 2001) between 02:05:52 and 23:22:57 on 2002 February 8 (ObsID 0397_0109110101; 2XMM catalogue source name = 2XMM J120518.7-620310) with the EPIC and OM instruments. We retrieved the public data from this observation to complement our *FUSE* data set. The EPIC observations presented here were obtained with the pn dectector which was used in the extended full frame mode (Strüder et al. 2001) and with the medium filter to reject parasite optical/UV light from the target. The OM instrument was used in the imaging mode with the broadband ultraviolet filters UVM2 (25 images, first half of the observation) and UVW2 (30 images, second half of the observation).

Version 7.0 of the *XMM-Newton* Science Analysis System (SAS) package was used to reduce the raw data. The EPIC-pn raw data were processed using the *epproc* procedure to transform raw data to a proper event lists. We filtered the event lists according to the standard procedure for the pn detector: only events with PATTERN in the 0 to 4 range (single and double pixel events) were selected, and the XMMEA-EP criterion and a flag of zero were set, providing the most conservative screening criteria for various conditions such as events near hot pixels. The event lists were also cleaned for the bad time intervals caused by proton flares, with a standard treshold chosen so that periods with more than 1.0 counts/s for the pn detector were rejected. The EPIC-pn spectrum of WR 46 was obtained in the 0.3-10.0 keV range using the *evselect* task of the SAS package in the spectrum extraction mode. The *evselect* task was also used to extract the X-ray light-curve of WR 46 in the 0.3-10.0 keV band, as well as a 0.3-10.0 keV background light-curve used to produce a background subtracted light-curve of WR 46. For the OM data, the images produced by the OM pipeline were used directly. For each OM image, counts from WR 46 were integrated and the background was extracted. The background subtracted count rates from the 55 OM images were used to produce a UV light-curve.

2.5 Analysis

2.5.1 Time-averaged *FUSE* spectrum

From a visual inspection of the time-averaged *FUSE* spectrum of WR 46 (see Figure 2.1, top panels) and the synthetic interstellar transmission spectra for the *FUSE* range computed, for example, by Willis et al. (2004), it is clear that the spectrum of WR 46 is highly contaminated by ISM features. The column density of interstellar H_2 is perhaps as high as 10^{18} atoms/cm^2 and maybe even more. The interstellar H_2 and H-Lyman lines effectively remove a large fraction of the stellar flux shortward of 1020 Å. Despite the plethora of interstellar lines in the *FUSE* spectrum of this star, we focus in this work on the FUV stellar wind features.

WR 46 (WN3p) is the earliest WN subtype covered in the *FUSE* atlas of WR stars of Willis

et al. (2004). Unfortunately, the substantial interstellar contamination makes it very difficult to identify the expected S VI $\lambda\lambda$933.4, 944.5, C III λ977, and N III λ991 resonance lines. Willis et al. (2004) noted that the latter two are clearly not strong in emission or as P Cygni profiles, but that the S VI doublet seems to be present as a P Cygni profile. We can indeed identify, although with difficulty, the absorption troughs of this P Cygni profile around ∼925 Å and ∼935 Å. Note that this S VI resonance doublet is also observed as a P Cygni profile in the *FUSE* spectrum of the other WN3 star (HD 32109, WN3b) of the atlas of Willis et al. (2004). HD 32109 is in the LMC and suffers far less ISM contamination, which makes the identification of this spectral feature much easier.

Willis et al. (2004) also reported that the He II λ1085, P V $\lambda\lambda$1118, 1128, and possibly Fe VI λ1168 lines appear present as weak emissions or P Cygni profiles in WR 46. We note that the presence of a relatively wide absorption trough around 1060 Å which might be the absorption component of a currently unidentified weak P Cygni profile. The *FUSE* spectrum of WR 46 is dominated by a very strong saturated P Cygni profile in the O VI $\lambda\lambda$1032, 1038 resonance doublet. Given the high level of ionization potential species in the wind, Willis et al. (2004) attributed the formation of O VI in this case to normal photoionization as opposed to Auger-ionization formation in shocked wind gas. More generally, they considered the “super ions" of O VI and S VI as photoionized wind features for WN3-WN6 stars, while they are probably the result of Auger ionization in WN7-WN9 stars, and probably absent in WN10-WN11 stars.

The presence of species of high ionization potential (138 eV for O VI) in the *FUSE* spectrum of WR 46 is not surprising given the very high effective temperature of this star. It is also in agreement with what is observed in its *IUE* spectrum (Willis et al. 1986) which is dominated by N V $\lambda\lambda$1238, 1242 and O V λ1371 P Cygni profiles and He II λ1640 emission, but in which no significant N III emission is detected. *IUE* observations of WR 46 were also presented by Crowther et al. (1995) who noted that the He II λ1640, N IV λ1718, and C IV $\lambda\lambda$1548, 1550 lines are observed as pure emission features, with N IV and C IV extremely weak, while lines from higher excitation stages such as N V $\lambda\lambda$1238, 1242 and O V λ1371 are observed as

P Cygni profiles. The optical spectrum of WR 46 is also dominated by emission lines from the high-ionization species N V and O VI, and also from He II (e.g. Oliveira et al. 2004).

2.5.2 Time-series analysis of *FUSE* spectra

To statistically determine which parts of the *FUSE* spectrum of WR 46 show significant variability, we performed a temporal variance spectrum analysis (TVS; Fullerton et al. 1996). We did this separately for each *FUSE* channel, which allowed us, by comparing the results, to distinguish more easily real variable features from spurious variations. It was also easier to assess the quality of individual spectra by proceeding channel by channel. The co-addition of several *FUSE* spectral segments (with two to four segments overlapping depending on the wavelength region) introduces more variations of the continuum noise across the spectrum, which would complicate the determination of the weights in the calculation of the TVS (see below). The spectra from all observations for which we provide a summary in Table 2.2 were used in the computation of the TVS. Prior to computing the TVS of each channel, we rebinned the spectra onto a common linear wavelength scale with a 0.13 Å bin size. The TVS is given by

$$(\mathrm{TVS})_j = \frac{\sum_{i=1}^{N}(w_i/\alpha_{ij})(S_{ij}-\bar{S}_j)^2}{N-1}, \tag{2.1}$$

where j indices refer to pixels and i indices refer to spectra, such that S_{ij} is the flux at the wavelength pixel j of spectrum i. The weights of the individual spectra are given by $w_i = (\sigma_0/\sigma_{\mathrm{ic}})^2$ with $\sigma_0^2 = (1/N\sum_{i=1}^{N}\sigma_{\mathrm{ic}}^{-2})^{-1}$, where σ_{ic} is the noise in the continuum. This continuum noise was estimated by fitting a linear function to selected regions of the continuum for each channel. The wavelength correction factors are given by $\alpha_{ij} = (\sigma_{ij}/\sigma_{\mathrm{ic}})^2$, and $\bar{S}_j$ is the weighted mean spectrum. The values of σ_{ij} were taken from the flux error estimates given by CalFUSE, obviously modified according to the rebinning of the data. The effect of the w_i is to suppress the contribution of lower quality spectra ($\sigma_{\mathrm{ic}} > \sigma_0$) and to enhance the contribution of higher quality spectra ($\sigma_{\mathrm{ic}} < \sigma_0$), while maintaining their overall normalization ($\sum_{i=1}^{N} w_i = N$). The wavelength correction factors α_{ij} account for the pixel-to-pixel variations of σ_{ij} caused by the

presence of absorption ($\alpha_{ij} < 1$, smaller flux levels) or emission ($\alpha_{ij} > 1$, greater flux levels) features.

It can be shown (see Fullerton et al. 1996) that the behaviour of the TVS under the null hypothesis ("not variable") is described for each pixel j by the $\sigma_0^2\chi^2_{N-1}$ distribution. Consequently, contours of statistical significance, represented by horizontal lines, can be drawn on each TVS spectrum. If the TVS exceeds a contour computed for a sufficiently unlikely value (here we use the 1% right-tail probability of the $\sigma_0^2\chi^2_{N-1}$ distribution) and for several pixels of a line profile, then we can say that the feature is variable at a level exceeding the noise threshold permitted by the quality of the data (here more than 99% confidence).

We present in Figure 2.1 (bottom panels) the $\mathrm{TVS}^{1/2}$ spectrum for each channel. The quantity $\mathrm{TVS}^{1/2}$ scales linearly with the size of the spectral flux deviations and is therefore more practical to use than the TVS itself because it gives a direct estimate of the amplitude of the spectral variations. Note that when plotting the TVS, we masked the wavelength intervals where peaks were caused by variability in airglow emission lines. We also masked spurious peaks caused by isolated outlying data points. These were common in the wings of narrow interstellar lines, since the TVS is very sensitive to small residual wavelength misalignment in the presence of steep spectral gradients.

The dashed horizontal line plotted with the $\mathrm{TVS}^{1/2}$ spectrum of each channel indicates the $[\sigma_0^2\chi^2_{N-1}(99\%)]^{1/2}$ value for that channel. We can see from Figure 2.1 that there is significant variability in the blue edge of the O VI $\lambda\lambda$1032, 1038 P Cygni absorption components and also, with a lower level of variability, in the S VI $\lambda\lambda$933, 944 P Cygni absorption components. These lines are in fact the two strongest P Cygni profiles present in the *FUSE* spectrum of WR 46. To show the evolution of these variable features with time for all *FUSE* observations of WR 46, we present in Figure 2.2 a gray-scale plot of the differences between each individual spectrum and the reference time-averaged spectrum for the wavelength regions where significant variability was detected. In this figure, the bottom panels display each differenced profile as an intensity

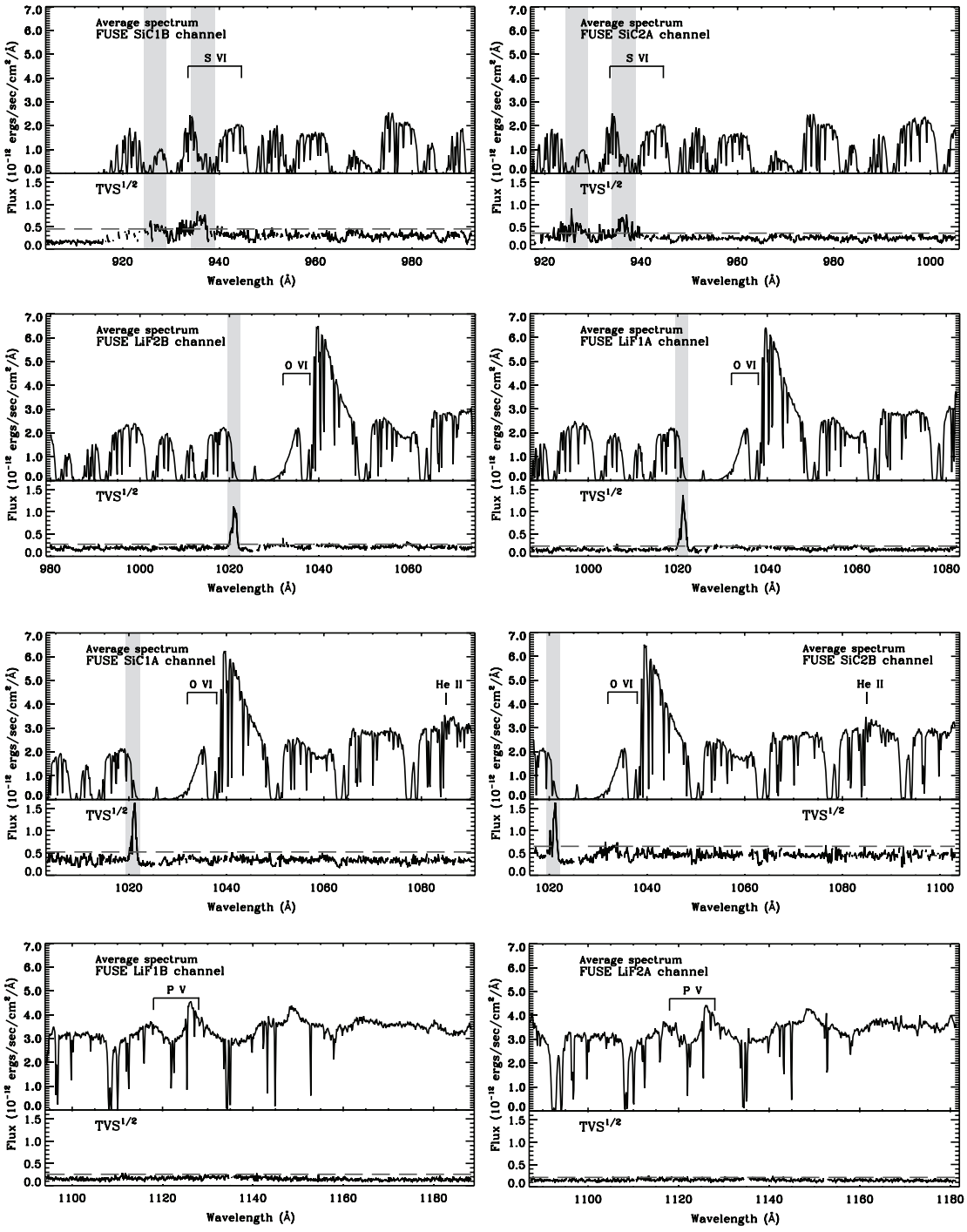

FIG. 2.1 – *Top panels:* Time-average spectrum for each *FUSE* channel. *Bottom panels:* Square-root of the temporal variance spectrum ($TVS^{1/2}$) for our time series of spectra for each channel. The dashed line indicates the 99% confidence level for variability. The wavelength intervals where spectral variations were found and for which light-curves were computed are highlighted in gray.

profile. The top panel presents the time-averaged spectrum (thick line) with the spectra from all exposures overplotted (thin lines). For each line, we also overlay a velocity scale to show the velocity of the variable feature with respect to the center of the line. To normalize the velocities, we used the terminal wind velocity $v_\infty = 2775$ km s^{-1} from Willis et al. (2004).

We can see that the variability in each component of the S VI doublet P Cygni absorption occurs mainly for velocities ranging from -0.6 v_∞ to a little faster than -v_∞, while the variability in the saturated O VI P Cygni absorption occurs in excess of -v_∞, up to approximately -1.25 v_∞. From the gray-scale plot of the consecutive observations E1130103, E1130104, and E1130105, we also see that the spectral features evolve on timescales of several hours, although the variability pattern is clearly not strictly periodic. It is indeed difficult to conclude anything about this variability pattern just by looking at the sequence of spectra. We do not clearly see displacement of spectral features in velocity space as a function of time, especially for the S VI doublet. The variations in each component of the S VI doublet absorption seem more or less correlated with each other, as expected. When the variable features are different in the two components, it is probably due to the fact that the velocity intervals severely affected by interstellar absorption are also different for the two components. Finally, by comparing the evolution of the O VI and S VI profiles, we see no obvious correlation between the variability patterns in these features.

Recall that for the above analysis, all the spectra were scaled to a common continuum level to focus on spectral-line variability. We can see from this analysis that the spectral lines do not seem to vary in strength over the years spanned by our *FUSE* observations, but it gives no information on the long-term continuum variability. It the next section (§2.5.3), we will look at the short-term continuum variability, but the light-curves (normalized for each observation individually) will not allow us to study the long-term variability. To investigate the possible long-term variability, we looked at series of spectra that were not scaled to a common continuum level. We found no evidence for significant long-term variations in the FUV continuum in our observations.

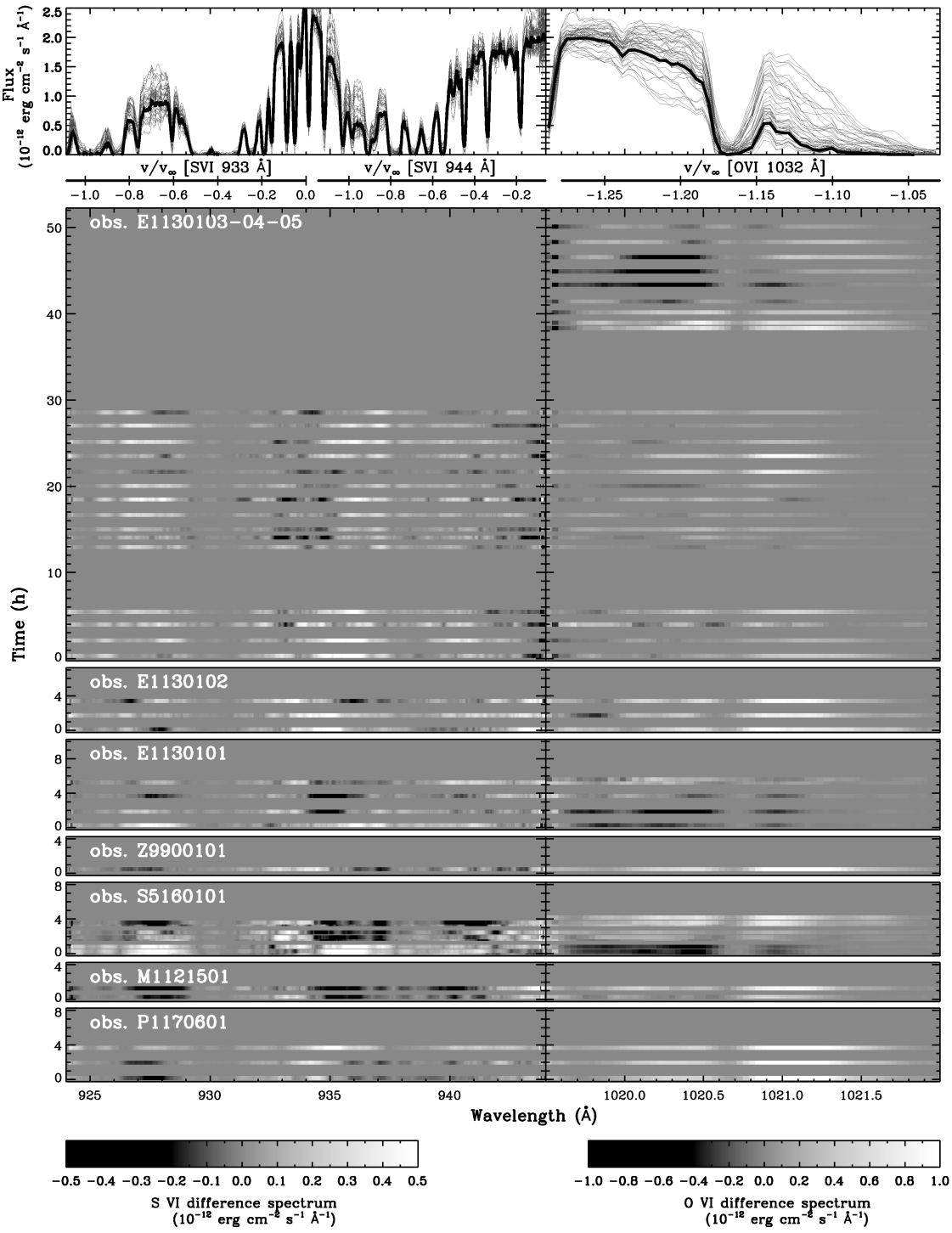

FIG. 2.2 – Gray-scale plot of the differences between individual spectra and the time-averaged spectrum (*top*, thick line) for the S VI $\lambda\lambda$933, 944 P Cygni absorption trough (*left*) and the O VI $\lambda\lambda$1032, 1038 P Cygni absorption blue edge (*right*). Time is given in hours since the beginning of each observation. The velocity scales below the top panel are given with respect to the center of the S VI λ933, S VI λ944, and O VI λ1032 lines, using the adopted $v_\infty = 2775$ km s^{-1}. The narrow absorption features are of interstellar origin. To reduce noise, smoothing factors of 15 and 5 were applied to the S VI and O VI difference spectra respectively. The real signal-to-noise of the difference spectra is therefore lower than seen here.

2.5.3 *FUSE* light-curves and period search

The *FUSE* light-curves extracted with the method described in §2.4 are presented in Figure 2.3. Times are given in hours from the beginning of each observation (from the beginning of observation E1130103 for observations E1130103, E1130104, and E1130105). As mentioned previously, these light-curves were extracted to provide a measure of the FUV continuum variability and of the integrated variability in selected spectral regions. Since the spectral variations generally appeared as broad features in the gray-scale plot of Figure 2.2, we believe that these light-curves, in which the flux across the whole variable spectral region is integrated, represent a good measure of the global line variability.

As we can see from Figure 2.3, the amplitude of the FUV continuum light-curve is typically around 5% (10% peak-to-peak), and sometimes near 9% (18% peak-to-peak). The amplitude of the O VI P Cygni absorption blue edge light-curve is typically around 20% (40% peak-to-peak), and sometimes near 40% (80% peak-to-peak). The situation of the S VI P Cygni absorption light-curve is similar to that of the O VI light-curve, although the velocity intervals over which the changes occur are different. Interestingly, the amplitude of the variability in the P Cygni absorption components for both the O VI and S VI lines is larger when the amplitude of the FUV continuum variability is also larger. We also note some similarity in the shape of the three light-curves, although they do not appear strictly correlated. We will explore possible correlation and delays between the different light-curves in §2.5.6.

To search for periodicities in the variability pattern of WR 46, we applied the fast Lomb-Scargle algorithm of Press & Rybicki (1989) to the light-curves of the consecutive observations E1130103, E1130104, and E1130105. The resulting periodograms are displayed in Figure 2.4. We also plot on each periodogram a dashed line corresponding to the 99% significance level for variability based on white noise simulations. The FUV continuum periodogram shows a significant peak at a frequency of 3.15 cycles day^{-1} (P=0.3175 d=7.62 h), and another minor peak barely exceeding the 99% significance threshold at a frequency of 2.27 d^{-1} (P=0.4405 d=10.57 h). The O VI P Cygni blue edge periodogram shows a significant peak at a frequency of 2.94 d^{-1}

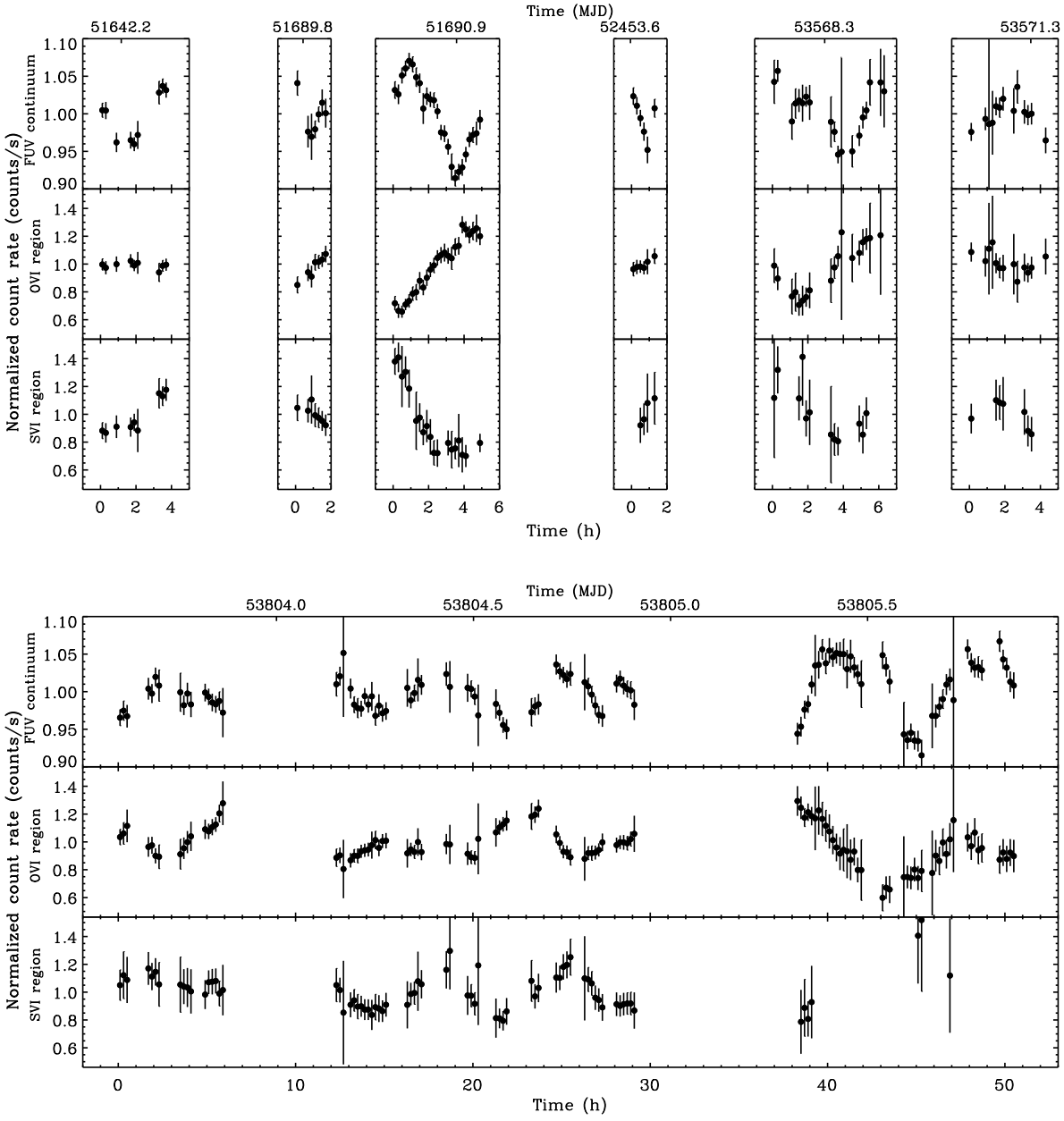

FIG. 2.3 – Light curves of all *FUSE* observations of WR 46 in spectral windows corresponding to the FUV continuum (*top panels*) and the variable regions of the O VI and S VI P Cygni profiles (*bottom two panels*).

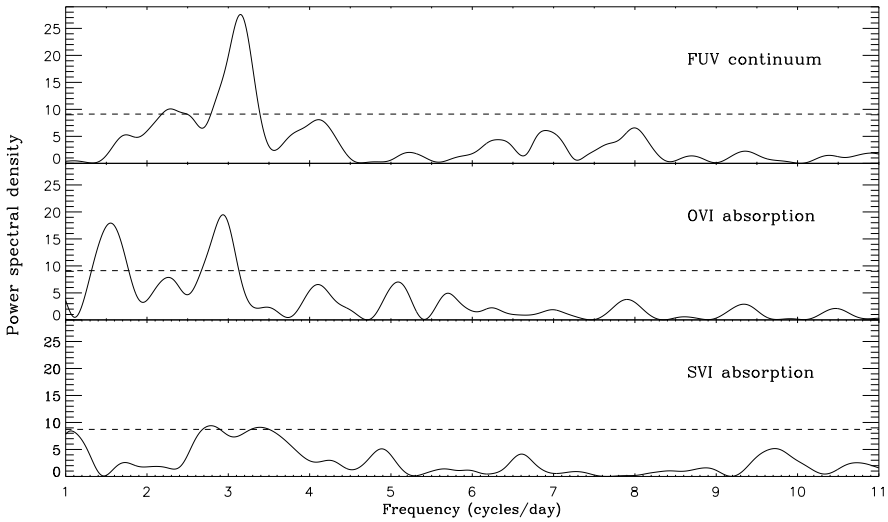

FIG. 2.4 – Lomb-Scargle periodograms for the combined light-curves of *FUSE* observations E1130103, E1130104 and E1130105, in spectral windows corresponding to the FUV continuum and the variable absorption component of the O VI and S VI P Cygni profiles. The dashed lines indicate the 99% significance level based on white noise simulations.

(P=0.3401 d=8.16 h), and a second significant peak, just slightly weaker, at a frequency of 1.55 d^{-1} (P=0.6452 d=15.48 h). This second peak might be linked to the first one since its frequency is almost 1/2 of the frequency of the main peak. The slight difference is perhaps just an effect of the limited time coverage of the data. The situation is less clear for the S VI P Cygni absorption periodogram, partly due to the poor time coverage of the S VI light-curve for observation E1130105 (during which SiC1B and SiC2A greatly suffered from pointing losses). There are two peaks around a frequency of 3 d^{-1} (P=0.33 d=8.00 h), but they just only slightly exceed the 99% significance level.

Given the large widths of the peaks in the periodograms of Figure 2.4 and the modest size of the data set from which we computed these periodograms, we will refer to the above measurements as dominant timescales and not as periods. The above results suggest that the variations in the FUV continuum and in the S VI and O VI P Cygni profiles are all consistent with a dominant timescale of about 0.33 d (∼8 h).

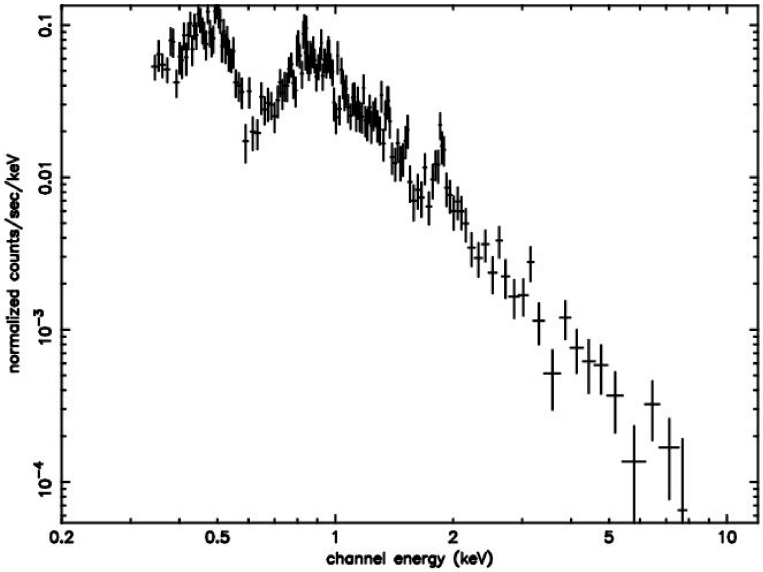

FIG. 2.5 – XMM-EPIC spectrum of WR 46.

2.5.4 *XMM-Newton* spectrum

The X-ray (EPIC) spectrum of WR 46 is presented in Figure 2.5. It is somewhat similar to the *XMM-Newton* spectrum of other nitrogen-rich Wolf-Rayet stars presented by Skinner et al. (2002b) and Ignace et al. (2003). The spectrum of WR 46 shows a prominent Si XIII (1.85 keV) emission line, as is the case for the three other WN stars with an XMM-Newton spectrum (EZ CMa, WR 110, WR 1). Mg XI (around 1.4 keV) is also possibly present in emission, as well as S XV (2.45 keV). The spectrum is soft, with apparently two distinct soft components peaking below 1 keV and a flux level at 3 keV about two orders of magnitude smaller than the flux level at 1 keV. However, some harder photons are detected and could constitute a weaker hard component.

We do not perform here a detailed quantitative analysis of the X-ray spectrum of WR 46, as this is beyond the scope of this work and detailed fits will be presented in an upcoming paper by Gosset et al. (2009). We also adopt the *XMM-Newton* X-ray luminosity in the 0.3-10 keV as determined by Oskinova (2005) (see §2.3). We believe that the general characteristics of the X-ray spectrum (the relative softness with some hard counts and the X-ray luminosity)

are very relevant to our discussion of the short-term variability of WR 46 and thus useful to consider in the present study.

2.5.5 *XMM-Newton* light-curves and period search

Figure 2.6 displays the simultaneous X-ray and UV light-curves obtained with *XMM-Newton*. Times are given in hours from the beginning of the observation. We caution that the UV photometry performed with the OM instrument used the UVM2 filter for the first half of the observation and the UVW2 filter for the second half. However, the throughput of these two filters peaks at wavelengths that are not too far part, so the first and second halves of the OM UV light-curve should probe similar regions of the stellar flux distribution. This is supported by the fact that there does not seem to be a big discontinuity in the UV light-curve when the filter changes.

We can see in Figure 2.6 that the amplitude of the X-ray light-curve is around 20% (40%

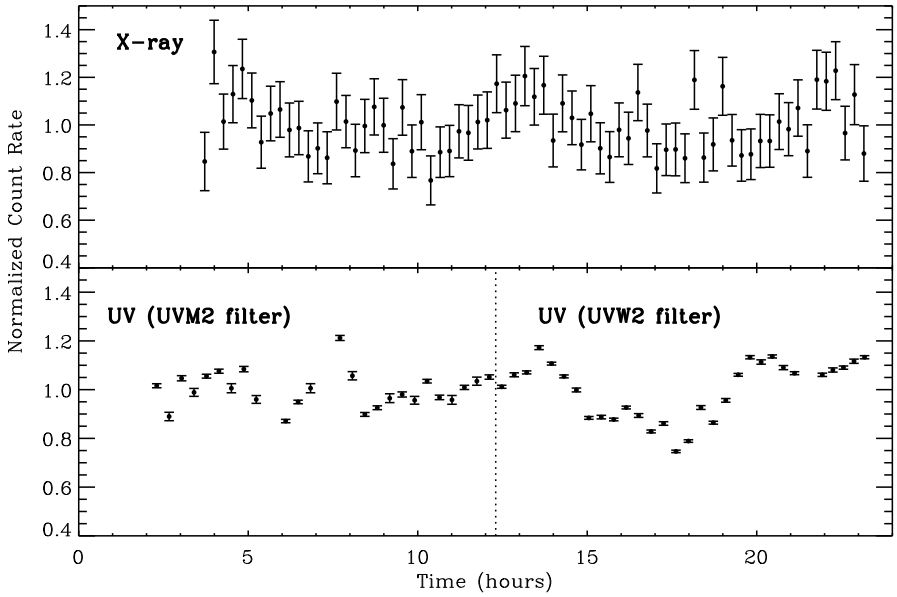

FIG. 2.6 – *Top panel*: Broadband (0.3-10 keV) XMM-EPIC X-ray light-curve of WR 46 with the mean count rate normalized to 1. *Bottom panel*: Simultaneous XMM-OM UV light-curve using the UVM2 filter for the first half of the observation and the UVW2 for the second half, with the mean count rate normalized to 1.

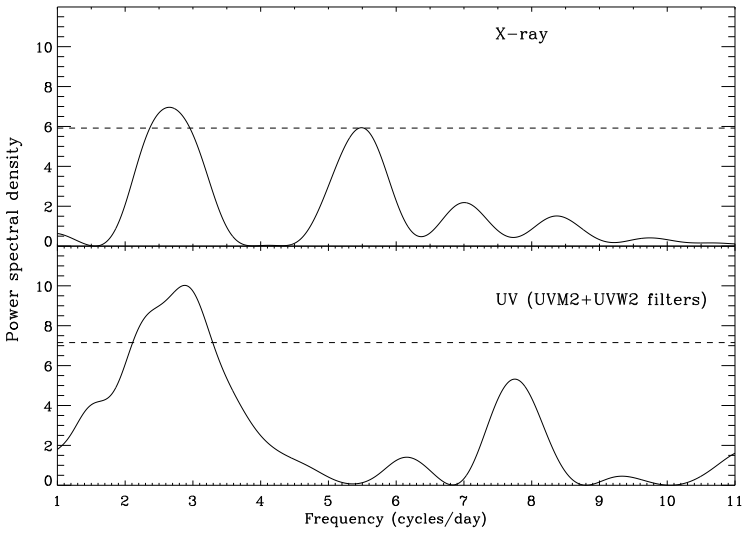

FIG. 2.7 – Lomb-Scargle periodograms for the XMM X-ray and UV light-curves of WR 46. The dashed lines indicate the 99% significance level based on white noise simulations.

peak-to-peak). The UV light-curve has quite an irregular shape and shows variations on the order of 10-15% (20-30% peak-to-peak).

We again applied the fast Lomb-Scargle algorithm (Press & Rybicki 1989) to search for periodicities in these light-curves. The resulting periodograms are displayed in Figure 2.7, with dashed lines still corresponding to the 99% significance level for variability based on white noise simulations. The UV periodogram shows a significant peak at a frequency of 2.87 d^{-1} (P=0.3484 d=8.36 h), while the X-ray periodogram shows a significant peak at a frequency of 2.66 d^{-1} (P=0.3759 d=9.02 h). Given the small number of cycles covered by these observations and the associated large widths of the peaks of the periodogram, we can only conclude that both light-curves vary on a dominant timescale close to 0.35 d. These results are not incompatible with the variability timescale observed in the FUV continuum and P Cygni absorption components.

2.5.6 Correlations and delays

Using the light-curves shown in the previous sections, we checked for possible correlations and delays between the FUV continuum and the FUV P Cygni absorption component variations,

and between the X-ray and UV variations. Such an analysis could eventually be useful to constrain a refined model of the variability of WR 46. We shifted in time the simultaneous light-curves with respect to each other and calculated the Spearman rank-order correlation coefficient (see Press et al. 1986) for different values of each shift. Before we did so, we re-binned the *XMM-Newton* X-ray and UV light-curves into common time bins. All the *FUSE* light-curves already had common time bins.

The first step in calculating the Spearman rank-order correlation coefficient is to replace the value of each x_i (the flux values of the first light-curve to correlate) by the value of its rank among all the other x_i's in the sample (i.e. 1,2,3, ..., N) sorted by increasing flux. We repeat the same procedure for the y_i's (the flux values of the second light-curve to correlate). We can then find the value of the Spearman rank-order correlation coefficient r_s, i.e. the linear correlation coefficient of the ranks

$$r_s = \frac{\sum_i (R_i - \bar{R})(S_i - \bar{S})}{\sqrt{\sum_i (R_i - \bar{R})^2}\sqrt{\sum_i (S_i - \bar{S})^2}}, \tag{2.2}$$

where R_i is the rank of x_i among the other x's, S_i is the rank of y_i among the other y's, and $\bar{R}$ and $\bar{S}$ are the averages of all the ranks of x and y respectively. The significance level of a nonzero value of r_s is then tested by computing

$$t = r_s \sqrt{\frac{N-2}{1-r_s^2}} \tag{2.3}$$

which is distributed approximately as Student's distribution with $N-2$ degrees of freedom.

We show in Figure 2.8 the results of these statistical tests. The Spearman rank-order correlation coefficient and the significance of the correlation are shown as a function of the time translation applied to the different light-curves. In the first case, we shift the X-ray light-curve by Δt and calculate the correlation with the OM UV light-curve. In the other two cases, we shift the O VI and the S VI light-curves by Δt and calculate the correlation with the FUV continuum light-curve.

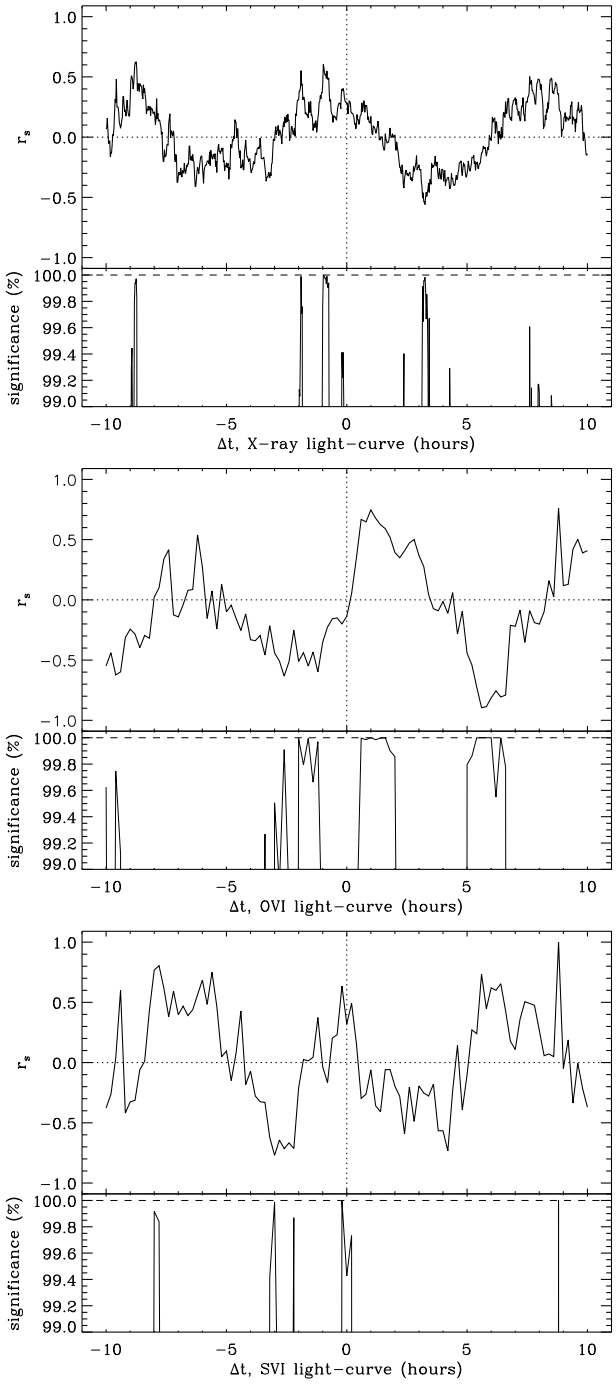

FIG. 2.8 – *Top panels*: Spearman rank-order correlation coefficient r_s as a function of the time translation applied to the light-curves. The top box shows the correlation of the shifted XMM UV light-curve with the XMM X-ray light-curve. The middle and bottom boxes show respectively the correlation of the shifted O VI and S VI *FUSE* light-curves with the *FUSE* FUV continuum light-curve. *Bottom panels*: Significance of the correlations shown on the top panels as a function of the time translation applied to the light-curves.

We see from the plots of Figure 2.8 that consecutive positive correlation peaks are roughly spaced by the dominant variability timescale of 8 hours, and the same thing is true for consecutive negative correlation (anti-correlation) peaks. We defer the interpretation of the possible correlation between the light-curves to §2.6. Concerning the delays, let us just mention the statistically significant possibilities as seen in Figure 2.8. The correlation between the X-ray and UV light-curves is very significant (>99.9%) when the X-ray light-curve is shifted by about -9 h ($r_s \simeq +0.6$), -1 h ($r_s \simeq +0.6$), or $+3$ h ($r_s \simeq -0.5$). The correlation between the FUV continuum and O VI light-curves is very significant when the O VI light-curve is shifted by about -1.5 h ($r_s \simeq -0.5$), $+1$ h ($r_s \simeq +0.7$), or $+6$ h ($r_s \simeq -0.8$). Finally, the correlation between the FUV continuum and S VI light-curves is very significant when the S VI light-curve is shifted by about -3 h ($r_s \simeq -0.7$), or not shifted ($r_s \simeq +0.5$).

2.6 Discussion

2.6.1 General considerations

2.6.1.1 FUV spectroscopic variability

The discovery of significant variability in the absorption trough of the two strongest FUV P Cygni profiles of WR 46 is not completely surprising given that ultraviolet spectroscopic variability has been found to be relatively common for Wolf-Rayet stars observed with *IUE* (St-Louis 1992). As for WR 46, the variations for the stars in the *IUE* sample were always strongest in the absorption components of major P Cygni profiles and were often found at velocities in excess of the terminal velocity. The terminal velocity of the wind is provided by the blue limit of zero residual intensity (defined as $v_{\rm black}$) in saturated P Cygni profiles (Prinja et al. 1990). On the blue side of $v_{\rm black}$, the flux gradually rises to reach the continuum at higher velocities. This “softening" of the blue edge of the absorption trough of saturated P Cygni profiles is commonly interpreted as an indication of the existence of another more chaotic velocity field superimposed upon the mean velocity profile. The variability seen in ex-

cess of the terminal velocity of the normal bulk outflow, as we found in the O VI $\lambda\lambda$1032, 1038 doublet and to some extent in the S VI $\lambda\lambda$933, 944 P Cygni profile of WR 46, is usually attributed to variable amounts of rarefied gas accelerated at velocities higher than the terminal velocity. This velocity excess is commonly taken as a measure of turbulence or shock velocity in the wind (Owocki et al. 1988), and is around $550 - 750$ km s^{-1} for WR 46 from our *FUSE* observations. The shocks can either originate from small-scale stochastic fluctuations coupled to the radiative instability intrinsic to line-driven winds (Owocki et al. 1988; Gayley & Owocki 1995, for applicability to WR stars), or originate from large-scale quasi-periodic variability induced for example by changes in the underlying star (e.g. Cranmer & Owocki 1996).

One-dimensional radiation hydrodynamics simulations of the growth of the line-driven instability along with synthetic line profile calculations show that the radiative instability can cause substantial blue-edge variability (e.g. Puls et al. 1993). However, we believe that the FUV spectroscopic variability observed in WR 46 is not primarily due to the line-driven instability because, although not strictly periodic, it appears to be modulated on a timescale of $\sim$8 h, which we would not expect from stochastic perturbations. This timescale is also close to previously reported photometric and spectroscopic periods, and consistent with the variability timescale observed in the FUV continuum, suggesting that the FUV spectroscopic variability is controlled by the same underlying quasi-periodic clock. It is also hard to see how the small-scale structures associated with line-driven instabilities would yield modulated FUV photometric variability at a level of $\sim 5 - 10\%$ and substantial variability in the P Cygni absorption components. From now on, we will therefore assume that the FUV spectroscopic variability is linked to a relatively large-scale periodic or quasi-periodic disturbance and not to stochastically appearing shocks.

Discrete Absorption Components (DACs) are a form of quasi-periodic ultraviolet spectroscopic variability commonly seen in hot stars (mainly OB stars). These features appear as absorption features superimposed on the (unsaturated) absorption part of P Cygni profiles and move from the lower blue-shift to higher blue-shift while becoming progressively narrower as they

approach an asymptotic velocity (e.g. Prinja & Howarth 1988; Massa et al. 1995; Kaper et al. 1997; Prinja et al. 2002). Note that this behavior has only been observed in one Wolf-Rayet star, WR 24 (Prinja & Smith 1992), most likely because its unsaturated UV He II P Cygni profile allows to see such features whereas it is not possible in the usually saturated P Cygni profiles of Wolf-Rayet stars. We might therefore expect to see DACs in the unsaturated S VI P Cygni profile of WR 46. When trying to compare this typical DAC behavior with our *FUSE* data of WR 46, we find that such a velocity displacement of absorption features is difficult to discern in the S VI doublet (Fig. 2.2) because of the relatively low signal-to-noise, sparse time coverage, and wealth of strong interstellar lines. While some variations might be interpreted as a displacement of relatively broad absorption features to larger negative velocities, it is impossible to identify a broad feature clearly evolving into a narrow component as it approaches terminal velocity. In some observations (e.g. S5160101), broad absorption features are even seen at or close to the terminal velocity. The variations in the absorption of the S VI unsaturated P Cygni profile of WR 46 therefore do not seem typical of DACs from what we can see from our limited data set.

It is common to assume that DACs are a manifestation of Corotating Interactions Regions (CIRs) in line-driven stellar winds, as first proposed by Mullan (1984). The CIRs are relatively large-scale spiral-shaped density and velocity perturbations that extend from the stellar surface to possibly several tens of stellar radii. With a 2D hydrodynamical model, Cranmer & Owocki (1996) simulated how azimuthal variations in surface brightness on a rotating star generate spiral CIRs in the wind. Their calculations show that CIRs can cause periodic variations in the UV wind lines that can, at least qualitatively, explain the DACs observed in hot stars. The results of these simulations show that base variations induce a wind structure with fast rarefactions that ram into slower flows. The encounter of these fast and slow flows induces a shock that compresses material into a dense shell. The interaction also induces a flat velocity plateau that is separated from the accelerating wind by a discontinuity in the velocity gradient. These structures modulate the observed stellar wind profiles as they are dragged through the line of sight by the underlying rotation of the base perturbation. The

velocity plateaus, and not the dense shells, appear to have the greatest effect on the line profile variability. The unsaturated line in the "bright spot" CIRs simulations of Cranmer & Owocki (1996) has a maximum standard deviation between roughly 0.5 v_∞ and v_∞. This is consistent with the observations of Kaper et al. (1996) who found in a sample of 10 O stars that the maximum amplitude of variability from DACs is always located at a velocity larger than half the terminal velocity. Similarly, the S VI P Cygni absorption component in our *FUSE* observations also shows maximum variability in this velocity interval.

The modeled CIRs produce definite DACs, but they can also modulate the blue edge of the absorption component of saturated P Cygni profiles on the same timescale. This is in line with observations by Kaper et al. (1996) who show that the steep blue edge of saturated UV lines varies in all cases when DACs are found in other lines. This blue-edge variability is furthermore often temporally correlated with the variability found in the absorption component of unsaturated P Cygni profiles (e.g. Henrichs et al. 1994). From a close inspection of timeseries of UV spectra, Kaper et al. (1996) suggested that blue-edge variability and DACs in fact reflect the same phenomenon. The observed similar variability timescales of the unsaturated S VI and the saturated O VI P Cygni absorption components (see Fig. 2.3 and 2.4) of WR 46 is therefore expected if its FUV spectroscopic variability is associated with CIRs.

Based on the few similarities between DACs and the FUV spectroscopic variability of WR 46, we suggest that this variability might be, in some way, related to CIRs, even though a typical DAC behavior could not be clearly identified in the unsaturated S VI line. The rotating ellipsoidal density distribution and local variations of the mass-loss rate suggested by Veen et al. (2002b,c) from their optical observations might also fit with an interpretation in terms of CIRs. It is worth noting the case of the Wolf-Rayet star EZ CMa (WR 6), for which 16 consecutive days of monitoring with *IUE* (>4 cycles) helped to link the observed UV P Cygni profile variability to CIRs, but where the variability is not really typical of the DACs commonly observed in OB stars but rather mainly found in the blue edge of the P Cygni absorption troughs.

The perturbations giving rise to CIRs are often associated to surface variations, possibly associated either with fixed magnetic structures or with non-radial pulsations (Kaper et al. 1997; de Jong et al. 2001). The recurrence and acceleration timescales of DACs (comparable to the stellar rotation period), their quasi-periodic nature, and the constancy of their pattern of variability over years suggests that stellar rotation plays a key role in the production of DACs (Prinja 1988; Henrichs et al. 1988; Massa et al. 1995; Kaper et al. 1997). Hydrodynamical simulations by Cranmer & Owocki (1996) showed that CIRs can produce DACs that evolve over timescales determined by the stellar rotation rate. However, CIRs and associated DACs are not always best explained by perturbations corotating with the stellar surface. Observations of the variability in the optical lines of HD 64760 (B0.5 Ib) led Kaufer et al. (2006) to propose a model with perturbations (spots) resulting from an interference pattern from non-radial pulsations at the base of the wind that does not corotate with the stellar surface. From the shape and evolution of the slow DACs observed in the UV lines of this star, Lobel & Blomme (2008) showed, with 3D simulations, that the CIRs must indeed originate from spots that are not locked onto the surface. For WR 46, we will see that rotational modulation of the wind by structures locked onto the surface is not a likely cause of the variability, but non-radial pulsations might be. We suggest that a hydrodynamical model exploring how CIRs caused by non-radial pulsations modulate the UV P Cygni profiles of WR 46 could provide great insight into the nature of the variability by comparison with our series of FUV spectra.

2.6.1.2 Variability originating from the photosphere?

The FUV continuum light variability on the order of $5 - 10\%$ (semi-amplitude) is not very surprising, as it is roughly the same level of variability that was observed in the optical photometry (e.g. Veen et al. 2002a). The recent model atmosphere of WR 46 by Crowther (private communication) shows that the optical depth of the stellar continuum at 1000 Å reaches a value of $\sim$1 at the very base of the wind, very close to the stellar surface, and similarly for the 5000 Å continuum. Both the FUV and optical continuum photometry are therefore dominated by the deep layers of the stellar wind which are close to the hydrostatic core.

The similar periods or timescales (∼8 h) found here or in previous studies in the optical, UV, FUV, and X-ray spectroscopic and/or photometric variability suggest that these are all related in some way. Even though they are not in phase (albeit correlated), the fact that the amplitude of variability in the S VI and O VI FUV lines is larger when the amplitude of the FUV continuum light-curve is also larger (see Fig. 2.2 and 2.3) suggests a link between the deep continuum variations and line variability further out in the wind. We thus conclude that it is possible that the variability of WR 46 originates from the photosphere of the star and propagates further out, up to the large distances where X-rays emerge. However, the causal link and phasing between the various manifestations of the variability is complex and remains to be understood.

2.6.1.3 Long-term variations vs. period changes

One last general aspect worth mentioning is the absence of significant long-term changes in FUSE spectra between 2000 and 2006 (in continuum and line strength). As a consequence, we found no evidence for a change of the mass-loss rate after 1999, unlike the change in the global mass-loss rate found by Veen et al. (2002b) in the early 90's. It is interesting to note that the variability timescales of our 2006 FUV data are similar to the photometric and spectroscopic periods found by Oliveira et al. (2004) in their data from 1998-1999. It is therefore possible that while the global mass-loss rate did not change, the dominant period of the system also stayed the same between 1998 and 2006. This is not incompatible with the suggestion by Veen et al. (2002b,c) that the long-term changes (luminosity, mass-loss rate) are linked to the period changes.

2.6.2 Rotational modulation

When the cyclical variability of a Wolf-Rayet star cannot be confidently attributed to binarity (see §2.6.3 for the case of WR 46), alternative explanations are put forward. For variations on

timescales of hours to days, one possible alternative is rotational modulation of a structured wind. A well-known example is the case of EZ CMa, for which rotational modulation has been favoured (St-Louis et al. 1995; Morel et al. 1998; Flores et al. 2007) to explain the short-term variability with a period of 3.776 days.

It is interesting to draw similarities between the UV variability reported in EZ CMa and the one we observed in WR 46. Variations were found in the absorption components of UV P Cygni profiles of EZ CMa, mainly confined to the blue absorption edge (St-Louis et al. 1993; St-Louis et al. 1995), but also in the emission component. The blue-edge variability was found in excess of the terminal velocity of the wind by as much as 900 km s^{-1}. This is similar to the variability that we found in the O VI $\lambda\lambda$1032, 1038 doublet P Cygni absorption, in excess of up to about 750 km s^{-1} of the terminal velocity of the wind. Note however that nothing like the clear sinusoidal radial-velocity excursions ($\sim$ 50-100 km s^{-1}) reported in the optical emission lines of WR 46 (Marchenko et al. 2000; Veen et al. 2002b, e.g.) was observed in EZ CMa. The reported radial-velocity changes claimed for EZ CMa are more likely the result of asymmetric flux variations than effect of orbital motion of the WR star (St-Louis et al. 1993).

In most cases, the rotation of a single WR star is not a likely cause of short-term variability with a period of a few hours because it would generally require a rotational velocity that is high relative to the break-up velocity of the star. For WR 46, assuming $R_* = 2.9\ R_\odot$, M_* =18 $M_\odot$ and a rotation period of 8 h, we get $v/v_c \approx 0.4$, where v is the rotational velocity at the equator and v_c is the critical rotational velocity of the star. The corresponding rotational velocity at the equator is $v \approx 440$ km s^{-1}, which is not impossible per se but still rather high compared to the first estimates of rotation rates of Wolf-Rayet stars by Chené & St-Louis (2008) who found rotational velocities in the range of 10-60 km s^{-1}.

Veen et al. (2002c) also argued that stellar rotation of a single Wolf-Rayet star is not a likely cause of the short-term variability of WR 46. They mentioned that the evolved nature of the WR star and its large mass-loss rate strongly disagree with a rapidly rotating single star.

They added that the bipolar structure of the wind is indicative of a bipolar magnetic field, which would argue more strongly against rapid rotation. Another of their arguments against this scenario comes from the long-term behaviour of WR 46. If rotational modulation was the source of the short-term variability, then the observed period decrease between 1989 and 1991 (Veen et al. 2002a) would imply a stellar radius decrease. However, it was found that the star brightens between 1989 and 1991, so the temperature would have to increase significantly if the radius was indeed decreasing. Because such a temperature change is not supported by the spectra (Veen et al. 2002b), Veen et al. (2002c) concluded that their observations could not be reconciled with single-star rotation, i.e. with perturbations locked onto the stellar surface and modulated by rotation. A perhaps even stronger argument against rotational modulation is the fact that the period of WR 46 is not stable. Not only is the period changing over time, but the timescales that we measured and the periods reported by Oliveira et al. (2004), when compared with previously reported periods, show that there is not even a clear general trend (e.g. a period constantly decreasing). This is clearly not consistent with rotational modulation. In comparison, EZ CMa always displays the same period of 3.766 days, even though its variability is epoch-dependant. In fact, in the case of rotational modulation, the period should always be the same or should change very little and gradually over time. The presence of multiple periods at some epochs is also difficult to explain in terms of rotational modulation. Based on the above evidence, we consider that simple perturbations corotating with the stellar surface cannot alone explain the short-term variability of WR 46.

2.6.3 Binary companion

2.6.3.1 Evolution of the period(s)

In their tentative interpretation of the period change in terms of orbital decay, Veen et al. (2002c) considered only the period change between 1989 and 1991. They noted that the period determined by Marchenko et al. (2000) is too large to be reconciled with a true change of an orbital period. They proposed that the period as detected by Marchenko et al. (2000) does not represent the orbital period, because it is based on spectroscopy. Indeed, Veen et

al. (2002b) suggested that a frequency analysis of the radial velocities may be severely affected by time-delays and stand-stills and that it may identify unreliable, mostly longer, periods than what would be found from the line-flux (which has more consistent time-delays) or the photometric analysis. Veen et al. (2002c) mention that radial-velocity studies (e.g. Veen et al. 1995; Niemela et al. 1995; Marchenko et al. 2000) may therefore identify lower-frequency alias peaks, hence artificial longer periods. They suggested that the photometry, or, possibly, the line fluxes, provide a better tool to determine the period(s) of the system than the radial velocity.

After considering conservation laws (spin and orbital angular momentum, energy) and various exchange mechanisms, Veen et al. (2002c) did not exclude that the observed period change from 1989 to 1991 represents an orbital change possibly due to the spiral-in of a companion, but they still considered such a scenario highly unlikely. Between 1989 and 1991, the change in the photometric period is 14 minutes (Veen et al. 2002a), which is extremely large for any binary system (see e.g. Veen et al. 2002c). If we then consider the significantly larger dominant photometric periods later measured by Oliveira et al. (2004), some of which are, by the way, consistent with the radial-velocity period of Marchenko et al. (2000), the interpretation of the period changes as orbital changes becomes even less plausible. Note that the timescales of the variations that we observed in the FUV (continuum and spectral lines), UV, and X-ray data are also much longer than the photometric periods of Veen et al. (2002a) from 1989 and 1991. These timescales are also close to the radial-velocity period of Marchenko et al. (2000) and to some of the periods found by Oliveira et al. (2004).

Veen et al. (2002c) stated that the obvious interpretation of the observed short-term variability (a binary) is in conflict with the observed long-term variation of WR 46. This statement is certainly amplified by the subsequent measurements of longer and multiple periods by Oliveira et al. (2004) and by the timescales that we observed in the current work. It is impossible to understand the long-term variation of the period(s) of WR 46 in terms of binarity only. There remains the possibility that a binary companion does exist, but that the observed variability

is sometimes dominated by another mechanism. If this is the case, then it is surprising that the variability always displays similar characteristics despite being controlled by different mechanisms.

2.6.3.2 Binary parameters

In the following subsections, we will assume that if WR 46 is a binary, the companion probably has a low mass, given the small amplitude of the radial-velocity curves and the fact that no spectral features have ever been identified that could be associated with a possible companion. Using lines that are considered good tracers of the orbit, Veen et al. (2002c) derived a mass function $f(M_2) = 0.012\ M_\odot$ with $K = v \sin i = 75$ km s^{-1} for the radial-velocity amplitude, while Marchenko et al. (2000) found $f(M_2) = 0.02\ M_\odot$ using $K = v \sin i = 90$ km s^{-1}. Those relatively small values for the mass function indeed point to a low-mass companion and/or a low inclination.

In our estimates of some physical quantities, we will adopt the stellar parameters from Table 2.1 for the Wolf-Rayet star and an orbital period of approximately 8 h. For simplicity, we will assume a circular orbit, i.e. that the circularization timescale is shorter than the evolutionary timescale. From Kepler's third law, we find that a low-mass companion on a circular orbit would be located at an orbital distance of 5.3 $R_\odot$, or 1.83 R_* if we adopt $R_* = 2.9\ R_\odot$. Using a simple $\beta = 1$ velocity law ($v(r) = v_\infty(1 - R_*/r)$) for the wind of the Wolf-Rayet star, we find that the velocity of the wind is about 0.45 v_∞ at the orbital separation of the companion.

2.6.3.3 X-rays and binarity

Simply from visual inspection, we can see that the X-ray spectrum of WR 46 does not show a strong hot component. If a hard component is really present, it is certainly not found at very high energies and/or it is weak compared to the dominant cool component. The X-ray spectrum of WR 46 does, in fact, present some similarities with that of the presumably single

WN star WR 1 (Ignace et al. 2003), suggesting a common mechanism for the origin of X-rays in both stars. The production of X-rays in hot-star winds is often linked to filamentary shocks distributed through the wind (Lucy & White 1980; Lucy 1982; Feldmeier et al. 1997) as a consequence of the radiatively driven instability (e.g Owocki et al. 1988; Gayley & Owocki 1995). Note however that Pollock (2007) has suggested an alternate mechanism in which the X-rays originate in the wind's terminal velocity regime in collisionless shocks controlled by magnetic fields rather than in cooling shocks. Skinner et al. (2002a,b) showed that radiative wind shock models can potentially explain the dominant cool emission component peaking near $kT_{\rm cool} \approx$0.6 keV in the WN stars EZ CMa and WR 110. The same arguments about radiative wind shocks presented by these authors could be used to explain the soft X-rays from WR 46. The X-ray spectrum of WR 46 is however somewhat in contrast with those of WR 110 and EZ CMa which appear harder. On the other hand, the hard X-ray photons detected in WR 46 might still be analog to the hot component ($kT_{\rm hot} \geq 3$ keV) that was clearly detected in EZ CMa and WR 110 in addition to the dominant cool component (Skinner et al. 2002a,b). Although one might see this as a signature of a compact binary companion for EZ CMa (the existence of such a companion has been suggested but vigorously debated) and WR 46, this interpretation is problematic in a general sense because there is no evidence at all of a compact companion to WR 110.

We can estimate the characteristic radius for the formation of X-rays in WR 46 by starting with the following equation for the optical depth (e.g. White & Long 1986)

$$\tau_x = \int_{R_x}^{\infty} \kappa_x \rho dr \tag{2.4}$$

where κ_x is the X-ray absorption cross section per unit mass at energy E_x, given by $\kappa_x = 0.6\ (10\ {\rm keV}/E_x)^{2.6}\ {\rm cm}^2\ {\rm g}^{-1}$ (Cassinelli & Olson 1979). Using the continuity equation ($\rho = \dot{M}/4\pi r^2 v(r)$) to substitute for the density in the wind and a simple $\beta = 1$ velocity law, we obtain

$$\tau_x = \frac{\kappa_x \dot{M}}{4\pi v_\infty} \int_{R_x}^{\infty} \frac{1}{r^2(1 - R_*/r)} dr = \frac{\kappa_x \dot{M}}{4\pi v_\infty} \left[\frac{\ln R_x}{R_*} - \frac{\ln (R_x - R_*)}{R_*} \right]. \tag{2.5}$$

Using the wind parameters of WR 46, $\tau_x = 1$, and solving for R_x, we find that the characteristic radius for the formation of X-rays is 1506, 250, 42 and 5.4 $R_\odot$ for energies of 0.5, 1, 2 and 5 keV respectively. Note that the above estimate assumes a spherically symmetric and monotonic velocity-law wind. The emergence radius could be smaller in clumped winds, but it is highly doubtful that the softer X-rays ($\lesssim$1 keV) emerge from the vicinity of a putative close companion, even when accounting for clumping. On the other hand, the harder X-rays could well come from a companion very deep in the wind without being too heavily absorbed. This is perhaps more easily seen by estimating the optical depth of the wind at the orbital distance of the companion. Using equation (2.5) but with $a = 5.3 R_\odot$ (the orbital distance of the companion) in place for R_x, we get the following expression for the optical depth

$$\tau_x \approx 0.17 \left(\frac{10 \text{ keV}}{E} \right)^{2.6}, \tag{2.6}$$

which yields $\tau_x \approx 411$, 68, 11 and 1 for energies of 0.5, 1, 2 and 5 keV respectively. Thus, the attenuation of harder X-rays ($\gtrsim$5 keV) from a companion should be small, and even more so in a clumped wind because τ_x would decrease due to clumping.

An optically faint neutron star companion to WR 46 would be consistent with our understanding of the evolution of massive binaries (van den Heuvel 1976). We can check whether the predicted X-ray luminosity from gravitational accretion onto a neutron star can be reconciled with the observations. The total X-ray luminosity (in ergs s^{-1}) produced by Bondi-Hoyle accretion of a stellar wind onto a degenerate object is given by (Stevens & Willis 1988)

$$L_{\rm X} \approx 2.03 \times 10^{57} \, \eta \dot{M} M_{\rm x}^2 a^{-2} v(a)^{-4} \left(1 - \frac{L_{\rm X}}{L_{\rm E}} \right)^2, \tag{2.7}$$

where η is the efficiency of the conversion of gravitational energy into X-ray emission, $\dot{M}$ is the mass-loss rate of the primary (in $M_\odot$ yr^{-1}), $M_{\rm X}$ is the mass of the secondary, $v(a)$ is the wind velocity (in km s^{-1}) at the secondary's location a (including the relative orbital velocity of the

secondary), and $L_{\rm E}$ is the Eddington luminosity (in ergs s^{-1}) given by $L_{\rm E} \approx 5.02 \times 10^{37}\ M_{\rm X}/\sigma_e$, where the electron scattering coefficient is $\sigma_e = 0.20$ for a fully ionized plasma for which the hydrogen abundance is zero. Adopting a canonical mass of $M_{\rm X} = 1.4 M_{\odot}$ for the neutron star secondary, an efficiency coefficient $\eta = 0.1$ appropriate for a neutron star (McCray 1977), and the other parameters as stated above, we obtain $L_{\rm X} \approx 1 \times 10^{37}$ ergs s^{-1}.

This expected X-ray luminosity is several orders of magnitude higher than what is observed for WR 46 ($L_X \sim 10^{32}$ ergs s^{-1}). Furthermore, an accreting neutron star would produce much harder X-rays than those we have observed, typically $E \approx 10$ keV (Rappaport & Joss 1983). Based on our above optical depth estimates, it seems unlikely that these hard X-rays would be so strongly attenuated. For EZ CMa, the predicted X-ray accretion luminosity is of order 10^{36} erg s^{-1}, about 3 orders of magnitude higher than what is observed, an argument that has been used against an accreting neutron star companion (Skinner et al. 1998). Stevens & Willis (1988) performed numerical calculations accounting for wind attenuation for a range of system parameters and predicted values of $L_x \sim 10^{35} - 10^{36}$ erg s^{-1}, still much larger than the observed value. WR 46 is a weak-lined WN star and its wind is less dense than that of EZ CMa, so the effect of wind attenuation for this star is most probably not stronger than in EZ CMa. With the 5 orders of magnitude difference between the X-ray luminosity expected from accretion onto a neutron star and the observed X-ray luminosity, it thus appears highly unlikely that WR 46 has an accreting neutron star companion. On the other hand, one can argue that if the neutron star is spinning fast enough, centrifugal inhibition of accretion occurs, thereby strongly reducing X-ray production (Stella et al. 1986; Illarionov & Sunyaev 1975). In such a case, the observed level of X-rays could possibly be reconciled with the presence of a neutron star companion, but their impact on the stellar wind should remain minimal (see §2.6.3.4), which is in contradiction with what is observed.

A black hole would also be a likely companion from an evolutionary point of view (van den Heuvel 1976). There are two possible mechanism to produce X-rays from accretion onto a black hole: spherical accretion onto a diskless black hole or disk accretion (Skinner et al. 1998). To

form a disk around a black hole companion to a Wolf-Rayet star, the Wolf-Rayet wind must be slow enough when it encounters the black hole. Illarionov & Sunyaev (1975) showed that a black hole can form an accretion disk and appear as a strong X-ray source if the orbital period P_{orb} (in hours) satisfies

$$P_{orb} \lesssim 4.8 \, \frac{M_{BH}}{v_{1000}^4 \, \delta^2} (\mathrm{h}), \tag{2.8}$$

where M_{BH} is the black hole mass in solar units, v_{1000} is the velocity of the accreted wind in units of 1000 km s^{-1} and δ is a dimensionless parameter of order unity. Using a velocity of $\sim$1500 km s^{-1} (which includes the relative orbital velocity of the companion), we find that for a period of $\sim$8 h, a disk can only form for a black-hole mass greater than $\sim$8 $M_{\odot}$. Note however that the velocity used in this estimate is based on the orbital separation calculated for a low-mass companion (relative to the 18 $M_{\odot}$ of the WR star). For a higher mass companion (e.g. on a low inclination orbit), the orbital separation would be larger, the relative velocity of the wind at the position of the companion would be increased, and the minimum mass of the black hole for a disk to form would also be larger. In any case, if a disk is present, we would expect a high X-ray luminosity. The efficiency of conversion of rest mass energy into radiation (η, see equation (2.7)) for a black hole is comparable to or greater than that for accretion onto a neutron star (Shapiro & Teukolsky 1983). The predicted accretion rate for a black hole is also larger than for a neutron star, and since most of the total radiative luminosity should emerge as X-rays (Shapiro & Teukolsky 1983), the expected X-ray luminosity should still be much too large compared to what is observed. If instead no disk is formed and accretion onto the black hole is spherical, then the X-rays produced should emerge either in the optical or as very high energy ($\geq$50 keV) X-rays and γ-rays (Shapiro & Lightman 1976). It is therefore not possible to constrain this scenario from our observations.

Three serious WR+compact candidates are now known, all of which have very different X-ray properties than WR 46. The most famous is probably the strong galactic X-ray source Cyg-X3 ($L_{\mathrm{X}} \approx 10^{38}$ erg s^{-1}, Schmutz et al. e.g. 1996, , and references therein). This system has an orbital period of 4.8 h (Parsignault et al. 1972) and is thought to consist of a Wolf-Rayet star (van

Kerkwijk et al. 1992) possibly accompanied by a black hole (Schmutz et al. 1996; Hanson et al. 2000), although this has been contested (e.g. Mitra 1998). A first extragalactic WR+compact candidate, IC 10 X-1, was detected in the starburst galaxy IC 10 (Bauer & Brandt 2004; Wang et al. 2005). It also has a high X-ray luminosity ($L_{\rm X}(0.2-10$ keV$) \sim 1.2 \times 10^{38}$ erg s^{-1}), and its period is close to 35 h (Prestwich et al. 2007). Silverman & Filippenko (2008) confirmed that this system is a WR + black hole binary, and that it possibly contains the most massive stellar-mass black hole known. Another extragalactic WR + black hole candidate, NGC 300 X-1, was identified by Carpano et al. (2007b). Its observed (absorbed) luminosity in the 0.2-10 keV band is $\sim 2 \times 10^{38}$ erg s^{-1}, and it was found to have a period close to 33 h (Carpano et al. 2007a). It is interesting to compare the *XMM-Newton* spectrum of NGC 300 X-1 (see Fig. 3 of Carpano et al. 2007b) with that of WR 46. The X-ray spectrum of NGC 300 X-1 can be modelled by a power-law with $\Gamma \sim 2.45$ with additional relatively weak line emission, notably around 0.95 keV. The relatively soft line-emission spectrum of WR 46 is in contrast with the harder blackbody or power-law spectrum expected from a compact companion.

Possible low-mass binary companions other than a neutron star or a black hole have been proposed for WR 46. One of these suggestions, a white dwarf, is obviously very peculiar from an evolutionary point of view and we will not explore it further. A normal main-sequence companion is also unusual and appears unlikely because it would imply a very large initial mass ratio, which is not favored in the present-day O + O binary statistics (Garmany et al. 1980). However, it is worth investigating based on the prediction by Vanbeveren (1998) that 3 to 5% of the Wolf-Rayet stars have an intermediate or low-mass companion. Since gravitational accretion onto a faint normal (non-degenerate) stellar companion seems unlikely (Stevens & Willis 1988), we will estimate the X-ray luminosity of a normal low-mass companion in the stellar wind of WR 46 by assuming that X-rays are produced by the WR wind shocking onto the low-mass companion. This scenario was proposed by Skinner et al. (2002a,b) to account for the hot component in the X-ray spectrum of WR 110 and EZ CMa. Following equations (5), (6), and (7) from White & Long (1986), such a companion would accrete material from the WR wind at a rate $\dot{M}_{\rm acc}$ set by its geometrical cross section:

$$\dot{M}_{\rm acc} = \dot{M}_w \frac{\pi R^2}{4\pi a^2}, \tag{2.9}$$

where $\dot{M}_w$ is the mass-loss rate of the Wolf-Rayet star, R is the radius of the companion, and a is its orbital separation. The accretion luminosity L_x is equal to the kinetic energy of the accreting material, i.e.

$$L_x = \frac{1}{2}\dot{M}_{\rm acc} v_w^2, \tag{2.10}$$

where v_w is the velocity of the wind at the position of the companion. The temperature of the X-ray emitting gas is determined by the shock velocity

$$kT_x \approx 1 \text{ keV} \left(\frac{v_w}{10^3 \text{ km s}^{-1}} \right)^2. \tag{2.11}$$

If we use a typical radius of $R = 1\ R_\odot$ for the companion, we find that $\dot{M}_{\rm acc} \approx 3.6 \times 10^{-8}\ M_\odot\ \text{yr}^{-1}$, $L_x \approx 2.5 \times 10^{34}$ erg s^{-1}, and $kT_x \approx 2.2$ keV. Note that we have included the relative velocity of the companion due to its orbital motion in v_w. The X-rays produced by such a companion would thus be relatively soft, and the estimated luminosity is probably not unreasonable if wind attenuation is taken into account. It could be present but not be detected in the X-ray spectrum because too weak or weaker than the soft X-ray component intrinsic to the WR wind. A normal low-mass companion is therefore possible based on the X-ray spectrum and luminosity. However, such soft and low-level X-rays should have a limited effect of the WR stellar wind (see §2.6.3.4).

In addition to its X-ray spectrum and luminosity, the X-ray variability of WR 46 is also interesting to consider in the context of a binary. Whatever is causing it, the X-ray variability of WR 46 at a level of about 20% on a timescale of 8-9 hours is unique. Hot stars rarely show X-ray variability on timescales of a few hours (e.g. Berghoefer et al. 1997). By comparison, day-to-day variability at levels of $\leq$30% has been observed in EZ CMa by *Einstein* (Moffat et al. 1982; White & Long 1986) and *ROSAT* (Willis & Stevens 1996), but the reality of the short-term ($\leq$1 h) variability was questioned by Willis & Stevens (1996). Also, the weak mo-

dulation with the 3.77 day optical period claimed by Moffat et al. (1982) was not confirmed by a sequence of *ROSAT* exposures (Willis & Stevens 1996). EPIC-MOS X-ray light-curves of EZ CMa and WR 110 from Skinner et al. (2002a,b) showed some fluctuations, but the authors considered that a real low-level variability is unlikely, although not totally ruled out. No evidence for X-ray variability was found in WR 1 from *ROSAT* and *XMM-Newton* observations at the 10% level or above (Ignace et al. 2003). Wessolowski & Niedzielski (1996) also reported that *ROSAT* observations of WR 1 do not provide significant evidence of variability in X-ray.

As we have seen, most of the X-ray flux of WR 46 probably originates from very large radial distances in the wind. It is therefore impossible to interpret the variability of those soft X-rays in terms of a binary located deep in the wind. Only if we dramatically overestimated the emergence radii of X-rays are could the variability of the soft X-rays be attributed to changes of the column density of gas attenuating the X-rays as the companion orbits the Wolf-Rayet star. However, in this case, the attenuation of the X-rays by the wind would be less important, and the problems with the expected X-ray luminosity outlined above would be enhanced. Even the expected X-ray luminosity of a normal companion could become a problem in this case.

To explain the ellipsoidal density distribution and local density variations inferred from their optical observations in terms of a binary, Veen et al. (2002c) noted that any disturbance (e.g. a close companion) of the physical conditions below the sonic point affects the mass-loss rate (Lamers & Cassinelli 1999). In the binary scenario, such local mass-loss rate variations caused by a companion might propagate far out in the wind and modulate the absorption of X-rays or the structure of wind shocks on the same timescale as the orbital period. However, note that the sonic point should be much closer to the stellar surface than the companion. The sound speed a is given by $a = (RT/\mu)^{1/2}$, where R is the gas constant, T is the temperature, and μ is the mean atomic weight of the particles expressed in units of $m_{\rm H}$. Assuming for simplicity $T \sim T_* \sim 90,000$ K and $\mu \simeq 2$ (pure ionized helium), we get $a \sim 19$ km s^{-1}. In a $\beta = 1$ velocity law with $v_\infty = 2775$ km s^{-1}, the sonic point would be located about 0.007 R_* away from the surface. Therefore, to affect the mass-loss rate locally, the companion would have to perturb

the physical conditions of the wind much closer to the base of the wind than its actual orbital separation, and to our knowledge there is no a simple mechanism by which this would occur other than the ionization effect of the X-rays from the companion. We will show in §2.6.3.4 that this ionization effect should be negligible for WR 46, so it seems unlikely that a binary companion generates large-scale structures in the WR wind. Thus, the above suggestion to explain the X-ray variability in terms of the effect of a companion on the local mass-loss rate is probably not valid.

2.6.3.4 The Hatchett-McCray effect

A binary X-ray source immersed in the stellar wind of its companion star can ionize a surrounding region and lead to observable variations. In particular, such a system could show variability with orbital phase in the P Cygni profile of ultraviolet resonance lines, an effect known as the Hatchett-McCray effect (Hatchett & McCray 1977), which has been observed in several high-mass X-ray binaries (HMXRBs) (e.g. van Loon et al. 2001).

Even though we have already reviewed many problems associated with the interpretation of WR 46 in terms of a binary system, it is worth verifying if the Hatchett-McCray effect could be responsible for the variability observed in the P Cygni profiles of the *FUSE* spectrum of this star. If an X-ray source was present in the wind of the Wolf-Rayet star, then there should be a region around this source in which atoms are ionized to higher stages. In this region, the fraction of O VI or S VI with respect to other ionization stages should change. Given that the ionization potential of O VI is higher than that of S VI, the number of scatterers in the region should either increase for both O VI and S VI, increase for O VI and decrease for S VI, or decrease for both O VI and S VI.

If the number of scatterers increases in the region surrounding the X-ray source, then more photons will be scattered out of the line of sight when the X-ray source is in the column between the Wolf-Rayet star and the observer (where the P Cygni absorption component forms).

If the number of scatterers increases and the X-ray source is in the part of the wind where the P Cygni emission component forms (i.e. not in the column between the Wolf-Rayet star and the observer and not eclipsed), then more photons will be scattered into the line of sight. An increased number of scatterers in the ionization region should therefore lead to an enhanced P Cygni absorption and/or emission, depending on where the ionization region is with respect to the Wolf-Rayet star and the observer. Similarly, if the number of scatterers decreases in the region surrounding the X-ray source, the P Cygni absorption and/or emission weakens. Note that it is possible for the variations in the P Cygni emission component to remain unnoticed while variations are observed in the absorption component. The region ionized by the X-ray source indeed represents a smaller fraction of the volume contributing to the emission component compared to the fraction of the volume contributing to the absorption component.

Several factors appear to go against an interpretation of the variability of the *FUSE* P Cygni profiles of WR 46 in terms of the Hatchett-McCray effect. First of all, the X-ray luminosity of WR 46 ($\sim 10^{32}$ erg s^{-1}) is very small compared to the typical X-ray luminosity of known HMXRBs showing the Hatchett-McCray effect ($\sim 10^{35}$-10^{38} erg s^{-1}) (e.g. van Loon et al. 2001). Since the size of the ionized region for a given species and ionization stage scales linearly with the X-ray luminosity of the companion and inversely with the density of the wind (Hatchett & McCray 1977), we expect this region to be very small for WR 46 which has a low X-ray luminosity and denser wind than typical O stars. The effect is obviously more difficult to observe if the ionized region is small. If it is small enough, variability in the absorption component of P Cygni profiles should be limited to the fraction of the orbit during which the companion is between the star and the observer. The fact that we see spectral variations during a major fraction of the ∼8-hour cycle appears in contradiction with the Hatchett-McCray effect of a small ionized region. We can estimate the size of such an ionized region by considering the quantity (Hatchett & McCray 1977)

$$\xi(r, r_{\rm X}) = \frac{L_{\rm X}}{n(r)\ r_{\rm X}^2} = \frac{4\pi\ L_{\rm X}\ \bar{m}}{\dot{M}}\ v(r) \left(\frac{r}{r_{\rm X}}\right)^2, \tag{2.12}$$

where $n(r)$ is the local number density of the gas, $r_{\rm X}$ is the distance from the X-ray source,

$\bar{m}$ is the average mass per ion (we assume here a pure helium atmosphere), and $L_{\rm X}$ is the intrinsic (unabsorbed) X-ray luminosity of the companion. Equation (2.12) is derived using the mass continuity equation: $\dot{M} = 4\pi r^2 \bar{m}\ n(r)\ v(r)$. The velocity as a function of r is still assumed to follow a $\beta = 1$ velocity law. In the limit $\xi \rightarrow 0$, the ionization balance of the material is unaffected by the presence of the X-ray companion and thus mainly governed by the radiation field of the Wolf-Rayet star. According to the ionization models of Kallman & McCray (1982), significant changes in ionization fraction generally only occur for values of $\log \xi > 1.6$. The variations of $\log \xi(r, r_{\rm X})$ in the orbital plane for the case of WR 46 are shown in Figure 2.9 for an assumed intrinsic X-ray luminosity of 10^{33}, 10^{34}, or 10^{35} erg s^{-1}. We can see that even in the rather unlikely case (see §2.6.3.3) where the unabsorbed X-ray luminosity

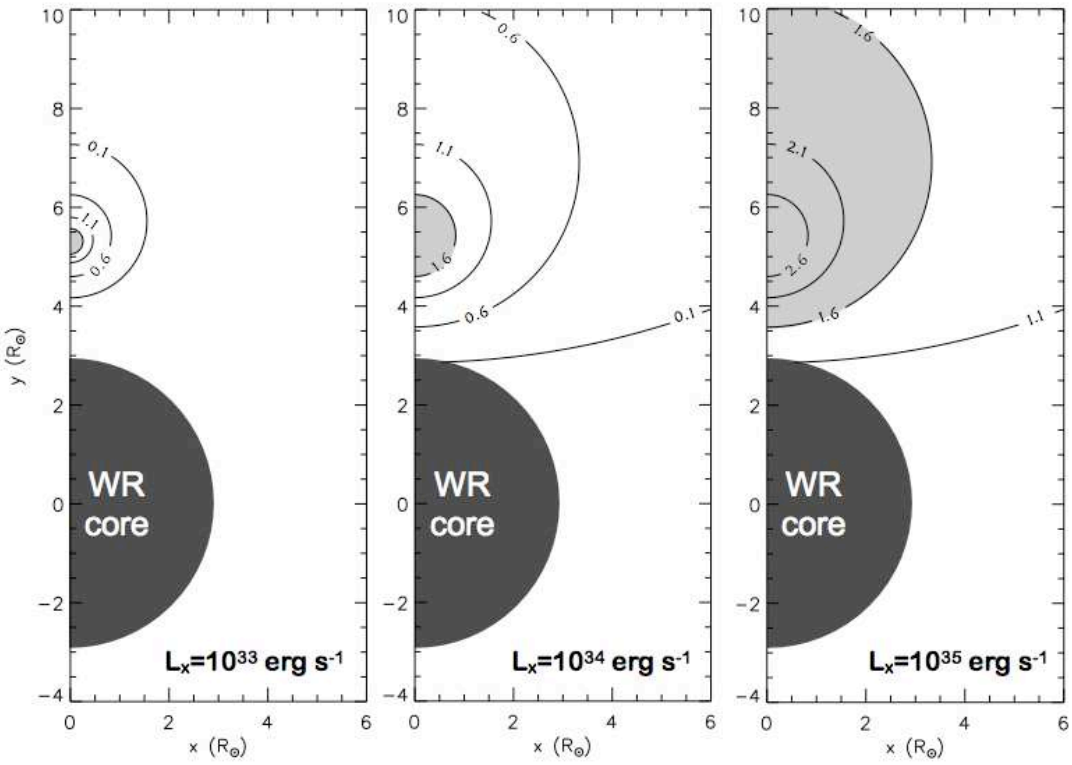

FIG. 2.9 – Contours of constant ionization parameter $\log \xi$ (in erg cm s^{-1}) for an ionizing companion located at (0, 5.3) and having an intrinsic (unabsorbed) X-ray luminosity of 10^{33}, 10^{34}, or 10^{35} erg s^{-1}. The Wolf-Rayet star is placed at the origin of the plots. The region within which $\log \xi \geq 1.6$ is indicated in light gray.

of the companion is 10^{35} erg s^{-1}, the region within which $\log \xi \geq 1.6$ is relatively small, and it is unlikely to perturb the column in front of the star for most of the orbit. Note also that equation (2.12) is valid for an optically thin gas, and that in reality the mean path length of the X-ray photons should be considerably shorter. The X-ray ionized zone is thus likely even less extended than what is shown in Figure 2.9.

An interpretation in terms of the Hatchett-McCray effect also runs into problems when looking at the possible variations in velocity space. Adopting a simple $\beta = 1$ velocity law for the wind of the Wolf-Rayet star and the same orbital parameters as above, the velocity of the wind at the position of the companion would be roughly 0.45 v_∞. Note that we ignore here the influence of the X-ray source on the velocity structure of the wind. Recall from §2.5.2 that the variability in each component of the S VI doublet P Cygni absorption occurs mainly for velocities between -0.6 v_∞ and -v_∞. Regardless of the size of the ionized region around the X-ray source, the velocities at which variability is observed in the S VI doublet do not match the velocity at the expected orbital radius of the hypothetical companion. It is difficult to interpret the variability in the O VI doublet P Cygni profile from these simple geometrical considerations because the absorption component is saturated and the variability is detected in excess of -v_∞, up to -1.25 v_∞. To see absorption in excess of the terminal velocity, the simple velocity structure of the wind must be modified, for example by shocks that cause material to flow locally at velocities higher than v_∞. We cannot constrain the location of the variability in the wind if it is in excess of v_∞. It is not excluded, however, that this variability might still be caused by the ionization effect of a companion X-ray source, even though the simple picture described above is complicated by the fact that local density variations of the shocked material might also lead to variability in the P Cygni profile absorption component. It seems reasonable to assume that if the variability in the S VI doublet is an ionization effect, then it is also true for the O VI doublet. If this is the case, then we can compare the simultaneous variations in the P Cygni profiles of both ions. We see from Figures 2.2 and 2.3 that the P Cygni absorption sometimes weakens (less scatterers) in O VI while it strengthens (more scatterers) in S VI. As noted above, this behavior is cannot be explained Hactchett-McCray effect since the ionization

potential of O VI is higher than that of S VI.

Note that there is evidence that spectral analyses overestimate the stellar radius (Moffat & Marchenko 1996), and that WR stellar radii are indeed smaller (Langer 1989; Vanbeveren 1998). With a smaller stellar radius than the one we adopted, our estimate of the velocity at the position of the companion would be larger and therefore closer to the velocities of the observed variability. However, in order to encompass the region from -0.6 v_∞ to -v_∞, the size of the ionized region would still have to be quite large, a configuration that seems highly unlikely from our above discussion. In addition, a smaller stellar radius would not solve some of the other problems that we raised. Thus, the variability that we observed in WR 46 does not seem characteristic of the Hatchett-McCray effect and is unlikely a manifestation of the ionization effect of an X-ray companion.

2.6.3.5 UV variability and binarity

A convincing interpretation of the variability of WR 46 in terms of a binary should account for the FUV continuum variability and the cyclical variability found in the absorption components of FUV P Cygni profiles.

Recall that the FUV and optical continuum are formed at the very base of the wind, near the stellar surface. The absence of core eclipses in the FUV and optical continuum light-curves (e.g. Veen et al. 2002a) suggests that the variability itself also originates from the very base of the wind. One possibility is that the companion, as it orbits the primary, induces deformations of the Wolf-Rayet star and its continuum forming layer. However, the significant cycle-to-cyle variations in the amplitude and shape of the light-curve would be difficult to explain in this context.

As for the FUV P Cygni profiles variability that we observed, we already argued that they require relatively large-scale structure variations. As we noted above, Veen et al. (2002c) sug-

gested that a close binary companion might modulate the physical conditions below the sonic point of the wind and cause local variations of the mass-loss rate, giving rise to the inferred rotating ellipsoidal density distribution. In this model, the rotating structure could possibly produce variations in the absorption components of P Cygni profiles. However, we argued in §2.6.3.3 that a companion is unlikely to induce large-scale structures in the wind. The FUV spectroscopic variability therefore appears like an additional obstacle to the interpretation of WR 46 in terms of a binary.

2.6.4 Non-radial pulsations

Marchenko et al. (2000) suggested that the intermittent and abrupt ceasing of the radial velocity variations of WR 46 might be naturally explained by a single pulsating or rotating star model. However, they rejected this hypothesis, arguing that while the whole O VI profile shifts during a 0.329-day cycle, the line changes neither its equivalent width nor its FWHM as they would expect for an emission line originating in any pulsating (or rotating) region of the inhomogeneous wind. While this argument is probably true for radial pulsations, it is not obvious that it can also be used to discard non-radial pulsations. Veen et al. (2002c) proposed a simple geometrical model in which non-radial pulsations appear to be able to cause radial-velocity shifts of the wind emission lines. As little is known about the propagation of pulsations in the stellar wind and how it affects the line profiles, we see no reason to reject the non-radial pulsation scenario. This is further motivated by the conclusions of Veen et al. (2002c) and Oliveira et al. (2004) who argued in favor of non-radial pulsations in WR 46, even though they did not completely exclude the existence of an unseen binary companion. The scenario of non-radial pulsations is indeed appealing to explain the multiple photometric periods present at a given epoch (Veen et al. 2002a). As suggested by Oliveira et al. (2004), the existence of multiple pulsation periods could provide an explanation for the ceasing of the radial-velocity variations in terms of a beat phenomenon. The different periods measured and the fact that the variations are not strictly periodic might easily be explained by the presence of multiple pulsation periods. The interference patterns between different modes could result in a com-

plex light-curve, varying both in shape and amplitude. In this context, it is also conceivable that a time-limited data set would allow to identify only one of the periods, and that another time-limited data set would show another of the periods. Note also that the variability of the optical and FUV continuum (expected to form at the very base of the wind) would find a natural explanation in the context of pulsations. It would either be caused directly by brightness variations at the stellar surface, or by velocity/density perturbations at the stellar surface deforming the continuum forming layer.

MOST (*Microvariability and Oscillations of Stars*) observations of a 9.8-h periodic signal in the light-curve of the WN 8 star WR 123 (Lefèvre et al. 2005) made it a very promising candidate for a pulsating Wolf-Rayet star. Lefèvre et al. (2005) first argued that the typical periods of strange modes, toward which Wolf-Rayet stars are known to be unstable (e.g. Glatzel et al. 1993), are too short to match the period detected with *MOST*. Later, Dorfi et al. (2006) discussed the fact that WR 123, a WN8 star, has a larger radius and consequently longer strange mode periods than standard helium star models. In their WN8 model having $R_* = 15.4\ R_\odot$, they showed that unstable radial strange modes exist with periods of the order of a half day, which appears compatible with the observations of WR 123. Townsend & MacDonald (2006) argued that because it is largely depleted of hydrogen, WR 123 may be characterized by an appreciably smaller radius than that assumed by Dorfi et al. (2006), in which case an interpretation of the 9.8-h periodic signal in terms of strange modes would not be correct. Townsend & MacDonald (2006) suggested that the variability might be caused by g modes instead. Glatzel (2008) then argued that the observed period of WR 123 may be interpreted in terms of strange mode pulsation even if the star contains no hydrogen. They showed that consecutive shock waves generated by strange mode instabilities inflate the stellar envelope considerably thus increasing the pulsation periods, and making them compatible with the period of WR 123. They added that the growth rates of the g modes considered by Townsend & MacDonald (2006) are smaller than the typical growth rates of strange modes by at least three orders of magnitude. In any case, these strange modes cannot, at least for now, explain the variability of WR 46; so far, only one-dimensional (radial) studies in spherical geometry have been performed, but

the wind asymmetry inferred from the optical variability of WR 46 (Veen et al. 2002c) would required a non-radial perturbation.

Noels & Scuflaire (1986) investigated non-radial g mode instabilities in Wolf-Rayet models, showing that such pulsations should have periods of the order of a few hours. However, the instability phase of these modes is predicted by these authors to last only about 5000 years, which makes this an unlikely cause of short-term variability for a large number of Wolf-Rayet stars. If this was the mechanism triggering the short-term variability of WR 46, it could however explain why the variability of WR 46 is so unique.

Townsend & MacDonald (2006) more recently examined the stability of $l = 1$ and $l = 2$ g modes in a pair of nitrogen-rich Wolf-Rayet stellar models. They found that a κ mechanism operating on a deep opacity bump leads to instability of modes with intermediate radial orders. In their hydrogen-depleted model, the periods of the unstable modes span $\sim 3 - 12$ h. This is interesting because this range of periods brackets the different periods that have been identified in WR 46, and also because Veen et al. (2002c) suggested a low-order non-radial pulsation mode (possibly $l = 1$) to interpret the short-term variability seen in optical data (Veen et al. 2002a,b). The stellar parameters of the 'WNE' model (i.e. hydrogen-depleted, as WR 46) used by Townsend & MacDonald (2006) in their stability analysis ($\log L_*/L_\odot = 5.62$, $M_*/M_\odot = 16.2$, $R_*/R_\odot = 2.10$) are different but still relatively close to the stellar parameters of WR 46 (see Table 2.1). Thus, self-excited g modes may be the source of the short-term cyclical variations seen in WR 46, and it would certainly be interesting to see if the results of this analysis are similar if a model with the same stellar parameters as WR 46 is used. However, it also remains to be seen what are the effects on the stability analysis of the strong radiatively driven winds of Wolf-Rayet stars. For simplicity, these dense outflows at the outer boundary of the star were neglected in the analysis of Townsend & MacDonald (2006).

Veen et al. (2002c) suggested that the lowest order sectoral mode l=1 and $|m|$=1, which results in a single bright hemisphere travelling along the equator, could produce a distorsion of

the wind of WR 46 (see their Fig. 5) and lead to a double-wave photometric period and a single-wave radial-velocity period, as observed. The bright hemisphere could distort the wind by causing an asymmetric density flow, with the "one-armed" wind appearing to rotate as the pulsational pattern travels over the stellar surface. In such a scenario, non-radial pulsations could generate spiral co-rotating interaction regions (CIRs) in the wind (e.g. Cranmer & Owocki 1996). We therefore reiterate that a CIR model with synthetic line-profile calculations tailored to WR 46 would be extremely useful when compared to our observations. We would have to see if these calculations could reproduce simultaneously the observed variability in unsaturated and saturated P Cygni profiles. Such a model should also provide an explanation for the variability of soft X-rays on the same timescale as the dominant period. A possible explanation for the variation of the X-ray emission of WR 46 in the context of pulsations is that X-rays are generated by shocks embedded in the wind, as commonly believed, but that the large-scale structure in the wind tied in with the stellar pulsations at the surface lead to quasi-periodic changes in the absorption of X-rays or in the structure of shocks which emit X-rays. We have seen that the emitting region of these soft X-rays is located very far out in the wind. Therefore, the structure induced by pulsations should also extend to very large radial distances in the wind.

The existence of a rotating structured outflow caused by non-radial pulsations in WR 46 is an attractive scenario, but much remains to be understood before concluding definitely that this is the cause of the short-term variability of this star. In particular, the long-term brightening observed from WR 46, the evolution of the period (if real), the radial-velocity stand-stills, and the phasing of the radial-velocity and light variations are certainly not trivial to explain in the context of pulsations. Veen et al. (2002c) discussed these problems and put forward some possible solutions, but these solutions are unfortunately hampered by our limited knowledge of pulsations in Wolf-Rayet stars.

2.7 Conclusion

Our new observations, in conjunction with those previously reported, can help to put very interesting constraints on the mechanism triggering the short-term variability of WR 46 (binarity, rotation, or non-radial pulsations), even though we cannot provide smoking-gun evidence in favor of either of the scenarios. We noted that the X-ray properties of WR 46 are typical of a single WN star, and are not consistent with an accreting neutron star or with disk accretion from a black hole, but they cannot be used to discard a normal low-mass companion or a spherically accreting black hole. However, in these two cases, the effects on the stellar wind would be minimal, which is in contradiction with our observations. The variability observed in FUV P Cygni profiles does not appear to be caused by the ionization effect of an X-ray companion (the Hatchett-McCray effect). We also pointed out that the fact that the period is not stable (changing with time with no particular trend, sometimes multiple) is a strong argument against rotational modulation and binarity. We cannot completely reject the existence of a companion, but if it exists it certainly does not control the period of the system at every epoch. This argument is also applicable to rotational modulation. We are therefore left with non-radial pulsations. Similar conclusions were reached by Oliveira et al. (2004) and Veen et al. (2002c). Circumstantial evidence suggests that the variability of WR 46 is rooted in photospheric perturbations, and that CIR-like structures might induce the observed P Cygni line profile and X-ray variability. We proposed that non-radial pulsations might be the source of these perturbations, although many questions raised by this scenario remain unanswered. An improved theoretical understanding of non-radial pulsations in Wolf-Rayet stars and how they propagate in the stellar wind will help to clarify this picture in the future. Meanwhile, we suggest that additional intensive and long-term monitoring campaigns of WR 46 would certainly prove useful, for example to follow the evolution of the period or the recurrence of multiple periods. If ever possible, continuous photometry (from space?) for several days or weeks would be a perfect way to test the scenario of non-radial pulsations with multiple periods.

We are thankful to Paul Crowther for providing results from his recent wind model of WR 46. V. H.-B. acknowledges support from NSERC (Canada) for a postgraduate scholarship. N. S.-L.

is also grateful to NSERC for financial assistance.

2.8 References

Bauer, F. E., & Brandt, W. N. 2004, ApJ, 601, L67

Berghoefer, T. W., Schmitt, J. H. M. M., Danner, R., & Cassinelli, J. P. 1997, A&A, 322, 167

Carpano, S., Pollock, A. M. T., Wilms, J., Ehle, M., & Schirmer, M. 2007a, A&A, 461, L9

Carpano, S., Pollock, A. M. T., Prestwich, A., Crowther, P., Wilms, J., Yungelson, L., & Ehle, M. 2007b, A&A, 466, L17

Cassinelli, J. P., & Olson, G. L. 1979, ApJ, 229, 304

Chené, A.-N., & St-Louis, N. 2008, IAU Symposium, 250, 139

Cranmer, S. R., & Owocki, S. P. 1996, ApJ, 462, 469

Crowther, P.A., Smith, L.J., & Hillier, D.J. 1995, A&A, 302, 457

Dixon, W. V., Sahnow, D. J., Barrett, P. E., Civeit, T., Dupuis, J., Fullerton, A. W., Godard, B., Hsu, J.-C., Kaiser, M. E., Kruk, J. W., Lacour, S., Lindler, D. J., Massa, D., Robinson, R. D., Romelfanger, M. L., & Sonnentrucker, P. 2007, PASP,119, 527

Dorfi, E. A., Gautschy, A., & Saio, H. 2006, A&A, 453, L35

Feldman, P. D., Sahnow, D. J., Kruk, J. W., Murphy, E. M., & Moos, H. W. 2001, J. Geophys. Res., 106, 8119

Feldmeier, A., Puls, J., & Pauldrach, A. W. A. 1997, A&A, 322, 878

Flores, A., Koenigsberger, G., Cardona, O., & de la Cruz, L. 2007, AJ, 133, 2859

Fullerton, A. W., Gies, D. R., & Bolton, C. T. 1996, ApJS, 103, 475

Garmany, C. D., Conti, P. S., & Massey, P. 1980, ApJ, 242, 1063

Gayley, K. G., & Owocki, S. P. 1995, ApJ, 446, 801

Glatzel, W., Kiriakidis, M., & Fricke, K. J. 1993, MNRAS, 262, L7

Glatzel, W. 2008, Hydrogen-Deficient Stars , 391, 307

Gosset, E., De Becker, M., Nazé, Y., Carpano, S., Rauw, G., Antokhin, I. I., Vreux, J.-M., & Pollock, A.M.T. 2009, *In preparation*

Hamann, W.-R., Koesterke, L., & Wessolowski, U. 1995, A&A, 299, 151

Hamann, W.-R., & Koesterke, L. 1998, A&A, 333, 251

Hamann, W.-R., Gräfener, G., & Liermann, A. 2006, A&A, 457, 1015

Hanson, M. M., Still, M. D., & Fender, R. P. 2000, ApJ, 541, 308

Hatchett, S., & McCray, R. 1977, ApJ, 211, 552

Henrichs, H. F., Kaper, L., & Zwarthoed, G. A. A. 1988, ESA Special Publication, 281, 145

Henrichs, H. F., Kaper, L., & Nichols, J. S. 1994, A&A, 285, 565

Herald, J. E., Schulte-Ladbeck, R. E., Eenens, P. R. J., & Morris, P. 2000, ApJS, 126, 469

Hillier, D. J., & Miller, D. L. 1998, ApJ, 496, 407

Ignace, R., Oskinova, L. M., & Brown, J. C. 2003, A&A, 408, 353

Illarionov, A. F., & Sunyaev, R. A. 1975, A&A, 39, 185

Jansen, F., et al. 2001, A&A, 365, L1

de Jong, J. A., et al. 2001, A&A, 368, 601

Kallman, T. R., & McCray, R. 1982, ApJS, 50, 263

Kaper, L., Henrichs, H. F., Nichols, J. S., Snoek, L. C., Volten, H., & Zwarthoed, G. A. A. 1996, A&AS, 116, 257

Kaper, L., et al. 1997, A&A, 327, 281

Kaufer, A., Stahl, O., Prinja, R. K., & Witherick, D. 2006, A&A, 447, 325

Lamers, H. J. G. L. M., & Cassinelli, J. P. 1999, Introduction to Stellar Winds, by Henny J. G. L. M. Lamers and Joseph P. Cassinelli, pp. 452. ISBN 0521593980. Cambridge, UK: Cambridge University Press, June 1999.

Langer, N. 1989, A&A, 210, 93

Lefèvre, L., et al. 2005, ApJ, 634, L109

Lobel, A., & Blomme, R. 2008, ApJ, 678, 408

Lucy, L. B., & White, R. L. 1980, ApJ, 241, 300

Lucy, L. B. 1982, ApJ, 255, 286

Marchenko, S. V., et al. 1998, A&A, 331, 1022

Marchenko, S. V., Arias, J., Barbá, R., Balona, L., Moffat, A. F. J., Niemela, V. S., Shara, M. M., & Sterken, C. 2000, AJ, 120, 2101

Massa, D., et al. 1995, ApJ, 452, L53

McCray, R. 1977, Highlights of Astronomy, 4, 155

Mitra, A. 1998, ApJ, 499, 385

Moffat, A. F. J., Firmani, C., McLean, I. S., & Seggewiss, W. 1982, Wolf-Rayet Stars: Observations, Physics, Evolution, 99, 577

Moffat, A. F. J., & Marchenko, S. V. 1996, A&A, 305, L29

Monderen, P., de Loore, C. W. H., van der Hucht, K. A., & van Genderen, A. M. 1988, A&A, 195, 179

Moos, H. W., et al. 2000, ApJ, 538, L1

Morel, T., St-Louis, N., Moffat, A. F. J., Cardona, O., Koenigsberger, G., & Hill, G. M. 1998, ApJ, 498, 413

Mullan, D. J. 1984, ApJ, 283, 303

Niemela, V. S., Barba, R. H., & Shara, M. M. 1995, Wolf-Rayet Stars: Binaries; Colliding Winds; Evolution, 163, 245

Noels, A., & Scuflaire, R. 1986, A&A, 161, 125

Oliveira, A. S., Steiner, J. E., & Diaz, M. P. 2004, PASP, 116, 311

Oskinova, L. M. 2005, MNRAS, 361, 679

Owocki, S. P., Castor, J. I., & Rybicki, G. B. 1988, ApJ, 335, 914

Parsignault, D. R., Gursky, H., Kellogg, E. M., et al. 1972, Nature, 239, 123

Pollock, A. M. T. 1987, ApJ, 320, 283

Pollock, A. M. T. 1995, in Proc. IAU Symp. 163, Wolf-Rayet Stars: Binaries, Colliding Winds, Evolution, ed. K. A. van der Hucht & P. M. Williams (Dordrecht: Kluwer), 429

Pollock, A. M. T. 2007, A&A, 463, 1111

Press, W. H., & Rybicki, G. B. 1989, ApJ, 338, 277

Press, W. H., Flannery, B. P., & Teukolsky, S. A. 1986, Cambridge: University Press, 1986

Prestwich, A. H., et al. 2007, ApJ, 669, L21

Prinja, R. K., & Howarth, I. D. 1988, MNRAS, 233, 123

Prinja, R. K., Massa, D., & Fullerton, A. W. 2002, A&A, 388, 587

Prinja, R. K., & Smith, L. J. 1992, A&A, 266, 377

Prinja, R. K. 1988, MNRAS, 231, 21P

Prinja, R. K., Barlow, M. J., & Howarth, I. D. 1990, ApJ, 361, 607

Puls, J., Owocki, S. P., & Fullerton, A. W. 1993, A&A, 279, 457

Rappaport, S. A., & Joss, P. C. 1983, Accretion-Driven Stellar X-ray Sources, 1

Sahnow, D. J., et al. 2000, ApJ, 538, L7

Schaerer, D., & Maeder, A. 1992, A&A, 263, 129

Schmutz, W., Geballe, T. R., & Schild, H. 1996, A&A, 311, L25

Shapiro, S. L., & Lightman, A. P. 1976, ApJ, 204, 555

Shapiro, S. L., & Teukolsky, S. A. 1983, Research supported by the National Science Foundation. New York, Wiley-Interscience, 1983, 663 p.,

Silverman, J. M., & Filippenko, A. V. 2008, ApJ, 678, L17

Skinner, S. L., Itoh, M., & Nagase, F. 1998, New Astronomy, 3, 37

Skinner, S. L., Zhekov, S. A., Güdel, M., & Schmutz, W. 2002a, ApJ, 572, 477

Skinner, S. L., Zhekov, S. A., Güdel, M., & Schmutz, W. 2002b, ApJ, 579, 764

Smith, L. F. 1968, MNRAS, 140, 409

Smith, L. F., & Maeder, A. 1998, A&A, 334, 845

Steiner, J. E., & Diaz, M. P. 1998, PASP, 110, 276

Stella, L., White, N. E., & Rosner, R. 1986, ApJ, 308, 669

Stevens, I. R., & Willis, A. J. 1988, MNRAS, 234, 783

St-Louis, N. 1992, Nonisotropic and Variable Outflows from Stars, 22, 229

St-Louis, N., Howarth, I. D., Willis, A. J., Stickland, D. J., Smith, L. J., Conti, P. S., & Garmany, C. D. 1993, A&A, 267, 447

St-Louis, N., Dalton, M. J., Marchenko, S. V., Moffat, A. F. J., & Willis, A. J. 1995, ApJ, 452, L57

Strüder, L., et al. 2001, A&A, 365, L18

Townsend, R. H. D., & MacDonald, J. 2006, MNRAS, 368, L57

Tovmassian, H. M., Navarro, S. G., & Cardona, O. 1996, AJ, 111, 306

Vanbeveren, D., Van Rensbergen, W., De Loore, C. 1998, The brightest binaries / by D. Vanbeveren, W. van Rensbergen and C. De Loore. Boston : Kluwer Academic, 1998.

van den Heuvel, E. P. J. 1976, Structure and Evolution of Close Binary Systems, 73, 35

van der Hucht, K. A. 2001, New Astron. Rev., 45, 135

van Genderen, A. M., et al. 1991, Wolf-Rayet Stars and Interrelations with Other Massive Stars in Galaxies, 143, 129

van Kerkwijk, M. H., Charles, P. A., Geballe, T. R., et al. 1992, Nature, 355, 703

van Loon, J. T., Kaper, L., & Hammerschlag-Hensberge, G. 2001, A&A, 375, 498

Veen, P. M., van Genderen, A., Verheijen, M. A. W., & van der Hucht, K. A. 1995, Wolf-Rayet Stars: Binaries; Colliding Winds; Evolution, 163, 243

Veen, P. M., van Genderen, A. M., & Jones, A. F. 1999, Wolf-Rayet Phenomena in Massive Stars and Starburst Galaxies, 193, 263

Veen, P.M., Van Genderen, A.M., van der Hucht, K.A., et al. 2002a, A&A, 385, 585

Veen, P.M., Van Genderen, A.M., Crowther, P.A., van der Hucht, K.A. 2002b, A&A, 385, 600

Veen, P.M., Van Genderen, A.M., & van der Hucht, K.A. 2002c, A&A, 385, 619

Wang, Q. D., Whitaker, K. E., & Williams, R. 2005, MNRAS, 362, 1065

Wessolowski, U., Hamann, W.-R., Koesterke, L., Hillier, D. J., & Puls, J. 1995, in Proc. IAU Symp. 163, Wolf-Rayet Stars: Binaries, Colliding Winds, Evolution, ed. K. A. van der Hucht & P. M. Williams (Dordrecht: Kluwer), 174

Wessolowski, U., & Niedzielski, A. 1996, Roentgenstrahlung from the Universe, 73

White, R. L., & Long, K. S. 1986, ApJ, 310, 832

Willis, A. J., van der Hucht, K. A., Conti, P. S., & Garmany, D. 1986, A&AS, 63, 417

Willis, A. J., & Stevens, I. R. 1996, A&A, 310, 577

Willis, A.J., et al. 2004, ApJ, 154, 651

Chapitre 3

Conclusion

Les nouvelles observations de WR 46 présentées au chapitre 2, ajoutées à celles déjà présentées par d'autres auteurs, nous permettent de poser certaines contraintes sur le mécanisme à l'origine de la variabilité cyclique à court terme de l'étoile Wolf-Rayet WR 46. Par contre, nous ne pouvons conclure avec certitude en faveur de l'un des trois scénarios proposés, soit la binarité, la rotation, ou les pulsations non-radiales. Nous avons noté que les propriétés de WR 46 dans les rayons X sont typiques d'une étoile WN simple, alors qu'elles ne sont pas cohérentes avec de l'accrétion sur une étoile à neutrons ou sur un disque autour d'un trou noir stellaire. Elles n'écartent toutefois pas la possibilité d'un compagnon de faible masse sur la séquence principale ou de l'accrétion sphérique sur un trou noir. Cependant, dans ces deux cas, les effets sur le vent stellaire seraient minimaux, ce qui est en désaccord avec nos observations. La variabilité détectée dans les profils P Cygni de l'ultraviolet lointain ne semble pas être causée par un effet d'ionisation dû à un compagnon source de rayons X (l'effet Hatchett-McCray). Nous avons noté que le fait que la période ne soit pas stable (changeante dans le temps sans tendance particulière, parfois multiple) est un argument fort contre la binarité ou les modulations associées à la rotation. Bien que nous ne puissions pas rejeter complètement l'existence d'un compagnon, il est cependant clair que ce compagnon ne contrôle pas la période du système à toutes les époques, s'il existe. Cet argument s'applique aussi aux modulations associées à la rotation. L'hypothèse des pulsations non-radiales est ainsi la plus probable.

D'après nos observations, des indices circonstanciels suggèrent que la variabilité observée dans le vent de WR 46 provient de perturbations à la photosphère de l'étoile et que des CIRs pourraient être la cause des variations observées dans les profils P Cygni et dans les rayons X. Nous avons évoqué la possibilité que des pulsations non-radiales soient la source de ces perturbations, mais ce scénario soulève encore bien des questions. Une meilleure compréhension théorique des pulsations non-radiales dans les étoiles Wolf-Rayet ainsi que de la façon dont leurs effets se propagent dans le vent stellaire aideront certainement à clarifier la situation dans le futur. Concernant la propagation des perturbations dans le vent, certains outils existent déjà et pourraient certainement fournir des réponses. Par exemple, un modèle hydrodynamique de CIRs comme celui de Cranmer & Owocki (1996) serait intéressant à tester dans un régime où la période des modulations n'est que de quelques heures, comme c'est le cas pour WR 46. Nous avons d'ailleurs commencé, dans le cadre de ce projet de maîtrise, à tester un code hydrodynamique semblable qui fournira des contraintes intéressantes à court et moyen terme. À plus long terme, d'additionnelles campagnes d'observation intensives de WR 46 seraient souhaitables, notamment pour suivre l'évolution de la période ou la récurrence de périodes multiples. Idéalement, des observations photométriques continues s'échelonnant sur plusieurs jours (depuis l'espace?) ou même semaines constitueraient le meilleur moyen de mesurer précisément une ou des périodes et de tester le scénario des pulsations non-radiales avec périodes multiples.

Bibliographie

Antokhin, I., Bertrand, J.-F., Lamontagne, R., & Moffat, A. F. J. 1994, AJ, 107, 2179

Antokhin, I. I. 1996, in LiËge International Astrophysical Colloquia, Vol. 33, LiËge International Astrophysical Colloquia, ed. J. M. Vreux, A. Detal, D. Fraipont-Caro, E. Gosset, & G. Rauw, 177

Antokhin, I. I., Bertrand, J.-F., Lamontagne, R., & Moffat, A. F. J. 1995, in IAU Symposium, Vol. 163, Wolf-Rayet Stars: Binaries; Colliding Winds; Evolution, ed. K. A. van der Hucht & P. M. Williams, 62

Bauer, F. E. & Brandt, W. N. 2004, ApJ, 601, L67

Bonnell, I. A. 2007, in Astronomical Society of the Pacific Conference Series, Vol. 367, Massive Stars in Interactive Binaries, ed. N. St-Louis & A. F. J. Moffat, 303

Bratschi, P. & Blecha, A. 1996, A&A, 313, 537

Carpano, S., Pollock, A. M. T., Prestwich, A., Crowther, P., Wilms, J., Yungelson, L., & Ehle, M. 2007a, A&A, 466, L17

Carpano, S., Pollock, A. M. T., Wilms, J., Ehle, M., & Schirmer, M. 2007b, A&A, 461, L9

Castor, J. I., Abbott, D. C., & Klein, R. I. 1975, ApJ, 195, 157

Chené, A.-N. & St-Louis, N. 2008, in IAU Symposium, Vol. 250, IAU Symposium, ed. F. Bresolin, P. A. Crowther, & J. Puls, 139–144

Cherepashchuk, A. M. & Aslanov, A. A. 1984, Ap&SS, 102, 97

Cranmer, S. R. & Owocki, S. P. 1996, ApJ, 462, 469

Crowther, P. A. 2007, ARA&A, 45, 177

de Donder, E., Vanbeveren, D., & van Bever, J. 1997, A&A, 318, 812

de Jong, J. A., Henrichs, H. F., Kaper, L., Nichols, J. S., Bjorkman, K., Bohlender, D. A., Cao, H., Gordon, K., Hill, G., Jiang, Y., Kolka, I., Morrison, N., Neff, J., O'Neal, D., Scheers, B., & Telting, J. H. 2001, A&A, 368, 601

Dessart, L. & Chesneau, O. 2002, A&A, 395, 209

Dorfi, E. A., Gautschy, A., & Saio, H. 2006, A&A, 453, L35

Feldmeier, A., Puls, J., & Pauldrach, A. W. A. 1997, A&A, 322, 878

Garmany, C. D., Conti, P. S., & Massey, P. 1980, ApJ, 242, 1063

Gayley, K. G. & Owocki, S. P. 1995, ApJ, 446, 801

Gayley, K. G., Owocki, S. P., & Cranmer, S. R. 1995, ApJ, 442, 296

Gies, D. R. & Bolton, C. T. 1986, ApJS, 61, 419

Glatzel, W. 2008, in Astronomical Society of the Pacific Conference Series, Vol. 391, Hydrogen-Deficient Stars, ed. A. Werner & T. Rauch, 307

Glatzel, W., Kiriakidis, M., & Fricke, K. J. 1993, MNRAS, 262, L7

Hamann, W.-R. & Koesterke, L. 1998, A&A, 333, 251

Hanson, M. M., Still, M. D., & Fender, R. P. 2000, ApJ, 541, 308

Hatchett, S. & McCray, R. 1977, ApJ, 211, 552

Hillier, D. J. & Miller, D. L. 1998, ApJ, 496, 407

Kaper, L., Henrichs, H. F., Fullerton, A. W., Ando, H., Bjorkman, K. S., Gies, D. R., Hirata, R., Kambe, E., McDavid, D., & Nichols, J. S. 1997, A&A, 327, 281

Kumar, C. K., Kallman, T. R., & Thomas, R. J. 1983, ApJ, 272, 219

Lamers, H. J. G. L. M., Maeder, A., Schmutz, W., & Cassinelli, J. P. 1991, ApJ, 368, 538

Lamontagne, R., Moffat, A. F. J., Drissen, L., Robert, C., & Matthews, J. M. 1996, AJ, 112, 2227

Lefèvre, L., Marchenko, S. V., Moffat, A. F. J., Chené, A. N., Smith, S. R., St-Louis, N., Matthews, J. M., Kuschnig, R., Guenther, D. B., Poteet, C. A., Rucinski, S. M., Sasselov, D., Walker, G. A. H., & Weiss, W. W. 2005, ApJ, 634, L109

Lépine, S., Moffat, A. F. J., St-Louis, N., Marchenko, S. V., Dalton, M. J., Crowther, P. A., Smith, L. J., Willis, A. J., Antokhin, I. I., & Tovmassian, G. H. 2000, AJ, 120, 3201

Lobel, A. & Blomme, R. 2008, ApJ, 678, 408

Lucy, L. B. 1982, ApJ, 255, 286

Lucy, L. B. & Abbott, D. C. 1993, ApJ, 405, 738

Lucy, L. B. & White, R. L. 1980, ApJ, 241, 300

MacFadyen, A. I. & Woosley, S. E. 1999, ApJ, 524, 262

Maeder, A. 1985, A&A, 147, 300

Maeder, A. & Schaller, G. 1991, in IAU Symposium, Vol. 143, Wolf-Rayet Stars and Interrelations with Other Massive Stars in Galaxies, ed. K. A. van der Hucht & B. Hidayat, 167

Marchenko, S. V., Moffat, A. F. J., Lamontagne, R., & Tovmassian, G. H. 1996, ApJ, 461, 386

Marchenko, S. V., Moffat, A. F. J., St-Louis, N., & Fullerton, A. W. 2006, ApJ, 639, L75

Meynet, G. & Maeder, A. 2005, A&A, 429, 581

Mitra, A. 1998, ApJ, 499, 385

Moffat, A. F. J. 1992, A&A, 253, 425

Moffat, A. F. J., Drissen, L., Lamontagne, R., & Robert, C. 1988, ApJ, 334, 1038

Moffat, A. F. J., Firmani, C., McLean, I. S., & Seggewiss, W. 1982, in IAU Symposium, Vol. 99, Wolf-Rayet Stars: Observations, Physics, Evolution, ed. C. W. H. de Loore & A. J. Willis, 577–581

Morel, T., Marchenko, S. V., Eenens, P. R. J., Moffat, A. F. J., Koenigsberger, G., Antokhin, I. I., Eversberg, T., Tovmassian, G. H., Hill, G. M., Cardona, O., & St-Louis, N. 1999, ApJ, 518, 428

Morel, T., St-Louis, N., Moffat, A. F. J., Cardona, O., Koenigsberger, G., & Hill, G. M. 1998, ApJ, 498, 413

Mullan, D. J. 1984, ApJ, 283, 303

Noels, A. & Scuflaire, R. 1986, A&A, 161, 125

Owocki, S. P., Castor, J. I., & Rybicki, G. B. 1988, ApJ, 335, 914

Parsignault, D. R., Gursky, H., Kellogg, E. M., Matilsky, T., Murray, S. S., Schreier, E., Tananbaum, H., Giacconi, R., & Brinkman, B. 1972, Nature, 239, 123

Pauldrach, A., Puls, J., & Kudritzki, R. P. 1986, A&A, 164, 86

Philp, C. J., Evans, C. R., Leonard, P. J. T., & Frail, D. A. 1996, AJ, 111, 1220

Prestwich, A. H., Kilgard, R., Crowther, P. A., Carpano, S., Pollock, A. M. T., Zezas, A., Saar, S. H., Roberts, T. P., & Ward, M. J. 2007, ApJ, 669, L21

Puls, J., Feldmeier, A., Springmann, U. W. E., Owocki, S. P., & Fullerton, A. W. 1994, Ap&SS, 221, 409

Puls, J., Owocki, S. P., & Fullerton, A. W. 1993, A&A, 279, 457

Rappaport, S. A. & Joss, P. C. 1983, in Accretion-Driven Stellar X-ray Sources, ed. W. H. G. Lewin & E. P. J. van den Heuvel, 1

Robert, C., Moffat, A. F. J., Drissen, L., Lamontagne, R., Seggewiss, W., Niemela, V. S., Cerruti, M. A., Barrett, P., Bailey, J., Garcia, J., & Tapia, S. 1992, ApJ, 397, 277

Sayer, R. W., Nice, D. J., & Kaspi, V. M. 1996, ApJ, 461, 357

Schmutz, W., Geballe, T. R., & Schild, H. 1996, A&A, 311, L25

Schulte-Ladbeck, R. E., Nordsieck, K. H., Taylor, M., Nook, M. A., Bjorkman, K. S., Magalhaes, A. M., & Anderson, C. M. 1991, ApJ, 382, 301

Schulte-Ladbeck, R. F., Nordsieck, K. H., Taylor, M., Bjorkman, K. S., Magalhaes, A. M., & Wolff, M. J. 1992, ApJ, 387, 347

Silverman, J. M. & Filippenko, A. V. 2008, ApJ, 678, L17

Springmann, U. 1994, A&A, 289, 505

St-Louis, N., Dalton, M. J., Marchenko, S. V., Moffat, A. F. J., & Willis, A. J. 1995, ApJ, 452, L57

St-Louis, N., Moffat, A. F. J., Drissen, L., Bastien, P., & Robert, C. 1988, ApJ, 330, 286

Stevens, I. R. & Willis, A. J. 1988, MNRAS, 234, 783

Townsend, R. H. D. & MacDonald, J. 2006, MNRAS, 368, L57

van den Heuvel, E. P. J. 1976, in IAU Symposium, Vol. 73, Structure and Evolution of Close Binary Systems, ed. P. Eggleton, S. Mitton, & J. Whelan, 35

van den Heuvel, E. P. J. & de Loore, C. 1973, A&A, 25, 387

van der Hucht, K. A. 2001, New Astronomy Review, 45, 135

van Genderen, A. M. & van der Hucht, K. A. 1986, A&A, 162, 109

van Kerkwijk, M. H., Charles, P. A., Geballe, T. R., King, D. L., Miley, G. K., Molnar, L. A., van den Heuvel, E. P. J., van der Klis, M., & van Paradijs, J. 1992, Nature, 355, 703

van Loon, J. T., Kaper, L., & Hammerschlag-Hensberge, G. 2001, A&A, 375, 498

Wang, Q. D., Whitaker, K. E., & Williams, R. 2005, MNRAS, 362, 1065

Wilson, O. C. 1939, PASP, 51, 55

Wolf, C. J. E. & Rayet, G. 1867, Comptes Rendues, 65, 292